Title
Oscillation and temporal processing in sensory cortex

Author
Mahncke, Henry W.

Publication Date
1998

Peer reviewed|Thesis/dissertation

Oscillations and Temporal Processing in Sensory Cortex

by

Henry W. Mahncke

DISSERTATION

Submitted in partial satisfaction of the requirements for the degree of

DOCTOR OF PHILOSOPHY

in

Neuroscience

in the

GRADUATE DIVISION

of the

UNIVERSITY OF CALIFORNIA

San Francisco

Date **University Librarian**

Degree Conferred: . . . . . .

For Mom and Dad

Acknowledgments:

The UCSF neuroscience program has been a unique place in which to develop as a scientist. The members of this program have a real desire to share, combine, and amplify their knowledge and experience, yielding a community of scholars of which I have been lucky to be a part. I thank Lou Reichardt and Michael Stryker for the effort that they have made to create an interactive and collaborative environment that has contributed greatly to my experience in graduate school.

My class has been a tremendous source of support throughout my time in graduate school. I thank Mini Kahlon for countless cups of coffee, Michael Silver for trip icons, Michele Solis for a mango at the right time, Jen Cummings for perspective, and Richard Hector for whale cells.

My thesis committee has provided useful advice to me over the years. Christoph Schreiner was very giving of technical and intellectual support as I began to study the auditory system; Allison Doupe was consistently enthusiastic and supportive throughout my graduate work; Len Kitzes gave encouragement and lent perspective to the writing of my thesis; and Steve Lisberger, chairperson of my committee, ensured that I stayed on course through the many twists and turns of graduate school.

Throughout my time at UCSF, Mike Merzenich has demonstrated that the abstractions of academic science can have a direct impact on the problems of clinical neuroscience. I would like to thank him for assembling a laboratory of

scientists whose breadth of interests constantly challenged me and for showing me that with vision and commitment one can change the world.

The UCSF neuroscience community has given me the opportunity to work with wonderful array of people, each of whom has contributed tremendously to my scientific and personal growth. Dean Buonomano pointed out that finishing my graduate work would require doing experiments. His intellectual breadth, experimental rigor, and offbeat humor provided an exemplary model of a scientist. Bev Wright showed me that human perceptual performance could indeed be quantified and was the person who actually taught me how to write a scientific paper. Her wisdom and laughter were constant comfort. Sri Nagarajan taught me something about everything from Indian folk tales to digital signal processing. Our collaboration was productive and fun, and I can only hope to one day approach his overall level of erudition. Michael Kilgard's dedication and zeal were an invaluable asset as we worked together to develop a rat auditory cortex preparation. David Poeppel showed me that good science and a good time go hand in hand. Along with David, I would like to thank the entire Magnetic Source Imaging group at UCSF, including Tim Roberts, Howard Rowley, Susanne Honma, Mary Mantle, Liz Disbrow, and Steve Stufflebeam, who have made human brain imaging a tremendous amount of fun over the past two years.

I would also like to thank other members of the ever-sprawling Merzenich lab. In particular, I thank Steve Cheung for encouraging the

surgeon in me, Peter Hickmott for home-brewed beer and experimental advice, Purvis Bedenbaugh for Perls of wisdom and Carolina pecans, Christopher DeCharms for late night conversations, David Blake for numerous scientific exchanges and whiskey shots, and Koichi Sameshima for taking elevators down and stairs up. I would also like to thank Ralph Beitel, Paul Johnston, John Houde, Nancy Byl, Bill Jenkins, Xiaoqin Wang, the members of the Schreiner lab, and my office mates for their scientific collegiality and companionship.

Most important of all are the people for whom no thanks can be sufficient: Mom and Dad; and Kimberly.

Oscillations And Temporal Processing In Sensory Cortex

Henry W. Mahncke

University of California, San Francisco

Graduate Program In Neuroscience

April 27, 1998

An important goal in neuroscience is to understand how stimuli interact across time. A wide variety of psychophysical and physiological effects indicate that stimuli surrounding a test stimulus in time can alter the perceived characteristics and neurophysiological representation of that stimulus. Degraded temporal perception is found in humans with learning disabilities, suggesting that these temporal interactions are important for normal perception.

To determine if stimulus-evoked alpha rhythms (7 - 13 Hz) could mediate interactions between sequential stimuli, magnetoencephalography was used to record evoked magnetic fields in response to brief somatosensory stimuli in awake humans. Single stimuli were found to generate oscillations in the alpha-band frequency range that lasted for 300 ms. The amplitude of the response to a second stimulus was systematically altered by its position in the oscillation evoked by the first stimulus. An inter-modal selective attention task was used to manipulate the attentional state of subjects. Alpha-band oscillations were observed in response to a stimulus in both the attended and

unattended conditions. The strength of these oscillations did not change as a function of attentional state.

To determine the anatomical source of these oscillations, click-evoked local field potentials and multi-unit spike activity were recorded throughout the depths of the primary auditory cortex of anesthetized rats. The evoked alpha band power in both of these response measures peaked in layer 5. A dissociation between the strengths of the short-latency response and the alpha-band oscillation indicated that layer five was uniquely able to generate strong alpha-band oscillations. Current source density analysis was consistent with a role for layer 5 cells with extended apical dendrites in the generation of alpha-band oscillations.

The role of the recovery of excitability following an extended stimulus in the control of responses to sequential stimuli was studied using a conditioning-probe stimulus paradigm and multi-unit recording in anesthetized rats. It was found that responses to probe stimuli exhibited a recovery of excitability characterized by increasing response amplitudes and decreasing response latencies as a function of the inter-stimulus interval. Post–stimulus excitability recovered more quickly following click trains with higher rates than those with lower rates.

Table of Contents

List Of Figures And Tables

Statement From The Research Advisor:

The magnetoencephalography discussed in Chapters 2 and 3 was conducted in collaboration with Dr. Srikantan Nagarajan, a postdoctoral fellow in the laboratory.

Michael M. Merzenich

INTRODUCTION

Chapter 1

Stimuli are perceived in the context of other stimuli. In the natural world outside of neurophysiological experiments, sensory stimuli occur surrounded by and coincident with other stimuli. A crucial task facing the brain is to use incoming sensory information to establish interpretations about what things exist in the environment. Contextual information surrounding a stimulus provides essential clues to aid this interpretation. In the spatial domain, a simple visual stimulus embedded in a field of similar stimuli appears to be part of a common texture, whereas a single different stimulus in that texture can "pop out" of the field and be easy to locate. In the temporal domain, it is simple to determine the order of a pair of auditory stimuli with slightly different frequencies. This task is be made much more difficult by adding a flanking stimulus before and after the pair. The task becomes easy again if many identical flanking stimuli are added, because the pair to be discriminated appears to "pop out" of the ongoing stream of flanking stimuli. These two examples serve to illustrate the fact the stimuli exert effects on other stimuli through both space and time.

Context dependent effects across space

Perhaps the best characterized example of stimulus interactions across space is the visual tilt illusion, in which the perceived orientation of a single test bar is shifted away from the orientation of a group of surrounding bars (Westheimer 1990). It has been hypothesized to serve as a form of lateral inhibition that accentuates the orientation differences between stimuli, assisting in the detection of stimuli against a patterned background. The tilt

illusion falls off with increasing distance between the test stimulus and the surrounding bars, suggesting that it is mediated by a topographically . mapped region of visual cortex. Physiological experiments have been performed in primary visual cortex using a test stimulus placed in the receptive field of a neuron under study and surrounding stimuli placed outside of that receptive field. It was found that although the surrounding stimuli could not drive a response in the absence of the test stimulus, their orientation could alter the orientation preference of the neuron to the test stimulus (Gilbert and Wiesel 1990). Similar experiments later revealed that the amplitude of the response to a test stimulus was also modulated by the orientation surrounding bars (Knierim and van Essen 1992).

Surround stimuli can also alter the detectability of weak stimuli (Polat and Sagi 1993; Polat and Sagi 1994). These experiments employed a contrast threshold measurement methodology, in which the subject's ability to detect a very low contrast grating stimulus was measured as a function of the proximity and orientation of nearby gratings. It was found that the presence of flanking high contrast gratings enhanced the subject's contrast sensitivity when those gratings were collinear with and shared the same orientation of the test stimulus. A recent neurophysiological study (Polat et al. 1998) revealed that these effects are evident in the responses of single neurons in the primary visual cortex of anesthetized cats. In these experiments, the contrast response function of single neurons was measured in the absence and in the presence of high contrast collinear flanking stimuli. These

flanking stimuli were positioned outside of the receptive field of the neuron under study and did not activate it in the absence of the test stimulus. Larger responses to low contrast test stimuli were found in the presence of the flanking stimuli, indicating that the physiological basis of this psychophysical effect was likely to be mediated by long-distance horizontal interactions in the primary visual cortex.

Recent work has demonstrated that the orientation of a annular surround interacts with the orientation of a grating stimulus to govern responses to that stimulus even when the annulus is outside of the classical receptive field of the neuron under study (Sillito et al. 1995; Sillito and Jones 1996). When the surround stimulus was perpendicular to the test stimulus, the response was facilitated; and when the two stimuli shared the same orientation, the response was suppressed.

These examples indicate that the spatial extent of cortical excitation produced by a sensory stimulus is not limited to the region of cortex that represents that region of visual space. This spatial spread has been directly measured using in vivo optical imaging techniques (Grinvald et al. 1994) revealing that small stimuli activated a region of cortex ten times the size of the region activated initially. It has been suggested that this spatial spread of excitation in the cortex is mediated by a population of pyramidal cells in the upper cortical layers with axons that range up to 8 mm in length. These neurons predominately link regions of the cortex that share similar stimulus

preferences and as such, are ideally situated for relaying information across long distances in the cortex.

Context dependent effects across time

Just as sensory stimuli have been demonstrated to interact across space, they interact across time. A wide variety of psychophysical and physiological effects indicate that stimuli surrounding a test stimulus in time can serve to enhance, degrade, or otherwise alter the perceived characteristics and neurophysiological representation of the test stimulus. The best studied psychophysical temporal interaction is the phenomenon of sensory "masking," in which a large amplitude "masking" stimulus can prevent the detection or discrimination of a small amplitude stimulus. It is not surprising that the simultaneous presentation of a test stimulus and masking stimulus results in the degraded perception of the test stimulus; but interestingly, masking effects extend both forward and backward in time from the masking stimulus. In the forward condition, the test stimulus is presented immediately after the offset of the masking stimulus. Despite the fact that the masking stimulus is no longer present, perception of the test stimulus is still impaired. In the backward condition, the test stimulus is presented immediately before the onset of the masking stimulus. Despite the fact that the masking stimulus has not even occurred when the test stimulus is presented, it is still able to degrade the perception of the test stimulus. Masking has been demonstrated in the visual, somatosensory, and auditory

modalities, and appears to represent a fundamental feature of sensory processing.

Temporal context defines the perception of temporal duration or interval. In this case, temporal interaction between the bounding stimuli serves to define a perceptual attribute, the interval between the two stimuli. Humans and animals are capable of discriminating intervals, indicating that they are a perceived stimulus attribute.

Another form of stimulus interaction across time is found in psychophysical studies of streaming, reviewed extensively by Bregman (Bregman). In these experiments, a subject is presented with a series of tones that alternate between two frequencies. If the frequencies are sufficiently close together, the subject perceives a single "stream" of stimuli that switches between the two frequencies. If the frequency separation is increased, the subject perceives two "streams" of intermingled stimuli, one at the higher frequency and one at the lower frequency. The rate at which the stimuli are presented also affects streaming in that faster rates require less of a frequency separation to cause the perception of two stimulus streams. This indicates that the ability of a stimulus to capture a subsequent stimulus as part of an ongoing stream is dependent on both the frequency similarity and interval between the two stimuli.

These data indicate that the temporal response to a stimulus must extend beyond the temporal extent of the stimulus itself. In the case of forward masking, the response to the masking stimulus must persist beyond the offset

of the masking stimulus to interfere with the proper response to the test stimulus. In the case of backward masking, there must a long-lasting response to the test stimulus that is required for the perception of the test stimulus that is blocked by the appearance of the response to the masking stimulus. Finally, the existence of interval perception demonstrates that that first bounding stimulus must evoke a time-varying response that the response to the second stimulus interacts with in such a way as to encode the bounded interval.

The nature of the extended response to a stimulus through time is not yet well understood. Several neurophysiological studies have been performed to begin to examine the temporal interactions of simple stimuli. Typically, these have consisted of presenting pairs of brief stimuli and measuring the response to the second stimulus as a function of the inter-stimulus interval. These experiments have been performed in the somatosensory thalamus (Janig et al. 1979) and cortex (Gardner and Costanzo 1980), where it was found that a stimulus evoked a 60 ms period of absolute inhibition followed by a slow recovery of excitability. The maximum interval used in these studies was 100 ms. Studies in the auditory system using paired pure tone stimuli in which the frequency of the first tone was varied while the second was held constant have shown that the first tone can inhibit the response to the second stimulus for periods of up to 400 ms (Calford and Semple 1995; Brosch and Schreiner 1997). These studies demonstrated that inhibition could be evoked by stimuli outside of the classical receptive field of the neurons under study. These studies provide an initial framework for

thinking about temporal interactions in sensory cortex by demonstrating that stimuli can have long-lasting temporal responses.

Contemporaneously with the discovery of the alpha rhythm, it was found that a brief sensory stimulus could elicit a repetitive discharge with a frequency in the alpha-range in thalamic and cortical structures of the anesthetized animal (Bartley and Bishop 1933). The response to a second stimulus presented during the evoked oscillation was shown to be modified by its position in the oscillation (Bishop 1933; Bartley 1936)]. If the second stimulus presented during an oscillatory trough, its response was sub-normal; and if presented during a peak, its response was normal or supra-normal. This evoked oscillation appeared to be an interesting candidate mechanism by which the brain could perform temporal computations. However, although its properties have been documented extensively in anesthetized preparations (Chang 1950; Aitkin et al. 1966; Webster and Aitkin 1971; Schoner et al. 1992; Sameshima and Merzenich 1993), no studies have shown that it is present the awake state, a necessary condition for it to be involved in temporal processing.

The current work

To begin to provide an understanding of the brain mechanisms by which sequential stimuli are ordered, integrated, and segregated, I have conducted neurophysiological studies of the responses to sequential stimuli in anesthetized rats and awake humans. The goals of this work were 1) to define the interactions between sequentially presented simple stimuli in the awake

human, 2) to determine if these interactions were characteristic of the attending state, 3) to characterize the neural basis of the interactions, and 4) to examine interactions between more complex stimuli with defined temporal structure.

In chapter 2, magnetoencephalography was used with awake humans to demonstrate that brief somatosensory stimuli evoke oscillatory activity in the alpha-band range in the extra-cranial magnetic field. The oscillation lasted for approximately three full cycles and appeared to reflect the repetitive reactivation of a local region of cortex. The effect of the evoked oscillation was to suppress the onset response to a subsequent stimulus that occurred in the oscillatory troughs. It had no effect on the amplitude of a later component of the response and no effect on the latency of either response component. The response evoked by the second stimulus was sub-linear compared to predicted combination of the ongoing oscillation with the onset response to a stimulus presented in isolation. Together, these data demonstrate that a sensory-evoked alpha-band oscillation has a strong effect on the response of the cortex to sequentially presented stimuli.

Chapter 3 demonstrates that these sensory evoked oscillations are present in both in somatosensory and auditory systems under conditions in which the human subject is engaged in a demanding psychophysical task. Previously, it had been suggested that oscillatory activity in this frequency range was characteristic of a relaxed or drowsy behavioral condition and that focused attention and behavioral arousal shifted brain activity from low to

high frequency oscillations. This work indicates that these oscillations are present and must play a role in the perceptual processing of time-varying stimuli. These experiment also demonstrate that the amplitude of these oscillations is not affected by selective attention in a task in which the subject directs their attention to either the somatosensory or auditory modality.

The cortical basis of the sensory evoked alpha-band oscillation was studied in Chapter 4 using the anesthetized rat auditory cortex as a model. A single click evoked alpha-band oscillations in the field potential and in the multi-unit activity in all cortical layers, but mostly strongly in layer 5. The calculated current sources indicated that the oscillatory activity was caused by cells in layer 5 with apical dendrites extending into the upper layers. Analysis of single trials demonstrated that low frequency (1-5 Hz) power predominated in both the pre-stimulus and post-stimulus time periods, but that it was unaffected by sensory stimulation. Alpha-band oscillations were specifically enhanced in the post-stimulus period, most strongly in layer 5. Regardless of the phase of the background oscillation at which the sensory stimulus occurred, the post-stimulus oscillation was fully phase-aligned to the sensory stimulus. In conjunction with previous work, these data suggest that a population of subcortically projecting layer 5 pyramidal cells specifically evoke an alpha-band oscillation in response to sensory stimuli. Despite large fluctuations in background activity, the alpha-band oscillation is a consistent feature of the post-stimulus response across trials.

In chapter 5, the interactions of more complex stimuli through time are examined in the anesthetized rat auditory cortex. Previous work has demonstrated that there is no oscillatory activity during the course of a stimulus that is extended in time. The timecourse of the post-stimulus recovery of excitability and subsequent oscillation was measured using a conditioning stimulus-probe stimulus methodology. Two important results were found. First, the rate of recovery was found to vary as a saturating linear function of the rate of the conditioning stimulus, with faster recovery times following higher rate stimuli. As a result, the integration time, or the time over which the probe stimulus did not generate a novel response, was a function of the temporal properties of the conditioning stimulus. Second, the rate of the stimulus did not affect the frequency of the alpha-band oscillation following the offset of the stimulus.

In conclusion, the existence of two distinct mechanisms by which sensory stimuli can affect each other through time are demonstrated. The first is an evoked alpha-band oscillation that governs the responsiveness of sensory cortex to repeated stimuli on the hundred millisecond time scale. The second is a rate sensitive temporal integration that controls the responses to sequentially presented temporally complex stimuli. These properties are hypothesized to contribute to the mechanisms by which the brain uses the temporal context of stimuli to build up a useful representation of objects in the world.

References:

Aitkin LM, Dunlop CW, and Webster WR (1966) Click-evoked response patterns of single units in the medial geniculate body of the cat. Journal of Neurophysiology 29:109-123.

Bartley SH (1936) Temporal and spatial summation of extrinsic impulses with the intrinsic activity of the cortex. Journal of Cellular and Comparative Physiology 8:41-62.

Bartley SH and Bishop GH (1933) The cortical response to stimulation of the optic nerve in the rabbit. American Journal of Physiology 103:159-172.

Bishop GH (1933) Cyclic changes in excitability of the optic pathway of the rabbit. American Journal of Physiology 103:213-224.

Bregman AS (1994) Auditory Scene Analysis: The Perceptual Organization Of Sound. Cambridge:MIT Press. 773 pp.

Brosch M and Schreiner CE (1997) Time course of forward masking tuning curves in cat primary auditory cortex. Journal of Neurophysiology 77:923-943.

Calford MB and Semple MN (1995) Monaural inhibition in cat auditory cortex. Journal of Neurophysiology 73:1876-1891.

Chang HT (1950) The repetitive discharge of corticothalamic reverberating circuit. Journal of Neurophysiology 13:235-258.

Gardner EP and Costanzo RM (1980) Temporal integration of multiple-point stimuli in primary somatosensory cortical receptive fields of alert monkeys. Journal of Neurophysiology 43:444-468.

Gilbert CD and Wiesel TN (1990) The influence of contextual stimuli on the orientation selectivity of cells in primary visual cortex of the cat. Vision Research 30:1689-1701.

Grinvald A, Lieke EE, Frostig RD, and Hildesheim R (1994) Cortical point-spread function and long-range lateral interactions revealed by real-time optical imaging of macaque monkey primary visual cortex. Journal of Neuroscience 14:2545-2568.

Janig W, Spencer WA, and Younkin SG (1979) Spatial and temporal features of afferent inhibition of thalamocortical relay cells. Journal of Neurophysiology 42:1450-1460.

Knierim JJ and van Essen DC (1992) Neuronal responses to static texture patterns in area V1 of the alert macaque monkey. Journal of Neurophysiology 67:961-980.

Polat U, Mizobe K, Pettet MW, Kasamatsu T, and Norcia AM (1998) Collinear stimuli regulate visual responses depending on cell's contrast threshold. Nature 391:580-584.

Polat U and Sagi D (1993) Lateral interactions between spatial channels: suppression and facilitation revealed by lateral masking experiments. Vision Research 33:993-999.

Polat U and Sagi D (1994) The architecture of perceptual spatial interactions. Vision Research 34:73-78.

Sameshima K and Merzenich MM (1993) Intrinsic oscillator contributions to response properties of SI cortical neurons. Society for Neuroscience Abstract.

Schoner G, Kopecz K, Spengler F, and Dinse HR (1992) Evoked oscillatory cortical responses are dynamically coupled to peripheral stimuli. Neuroreport 3:579-582.

Sillito AM, Grieve KL, Jones HE, Cudeiro J, and Davis J (1995) Visual cortical mechanisms detecting focal orientation discontinuities. Nature 378:492-496.

Sillito AM and Jones HE (1996) Context-dependent interactions and visual processing in V1. Journal of Physiology (Paris) 90:205-209.

Webster WR and Aitkin LM (1971) Evoked potential and single unit studies of neural mechanisms underlying the effects of repetitive stimulation in the auditory pathway. Electroencephalography and Clinical Neurophysiology 31:581-592.

Westheimer G (1990) Simultaneous orientation contrast for lines in the human fovea. Vision Research 30:1913-1921.

Stimulus-Evoked Low Frequency Oscillations In Human Somatosensory Cortex

Chapter 2

Abstract:

Low-frequency oscillations in the alpha band (7-13 Hz) have been observed in several regions of sensorimotor cortex in awake humans. However, the role of these oscillations in sensory processing remains unclear. Studies in anesthetized animals show that stimulus-evoked oscillations of local field potentials and multi-unit activity in this frequency range clearly modulate the responses to subsequent stimuli. The purpose of this study was (1) to characterize oscillations evoked by a somatosensory stimulus in awake humans; and (2) to define the effect of such oscillations on responses to stimuli occurring at various delays after the first stimulus.

Evoked magnetic fields were recorded from the somatosensory cortex in six human subjects that passively attended suprathreshold stimuli. Somatosensory stimuli were air-puffs (25 PSI) delivered to the distal tip of the index finger. Stimuli were presented singly and in pairs, with stimulus onset asynchronies between 70-270 ms. The frequency spectrum, amplitude, latency, and alpha-band power of the response elicited by each stimulus were calculated.

In response to a single stimulus, evoked magnetic field oscillations in the alpha-band frequency range were recorded that lasted between 200 and 400 ms. The amplitude of the response to a second stimulus depended on the position of that stimulus in time relative to the phase of the ongoing oscillation evoked by the first stimulus. The recovery function relating the amplitude of the response to a second stimulus to the stimulus onset asynchrony was

oscillatory. Linear predictor analyses demonstrate that the interaction of the response to the second stimulus with the ongoing response to the first stimulus was sub-linear. Current source dipole modeling suggests that evoked oscillations represent the repetitive reactivation of local cortical regions.

These data suggest that these oscillations may play a role in the processing of time-varying stimuli in the range of hundreds of milliseconds.

Introduction:

A wide variety of psychophysical studies have demonstrated that sensory stimuli can exert an influence on one another both backwards and forwards through time. These interactions are important for several classes of psychophysical effects. First, in all sensory modalities, a strong stimulus can degrade the ability of an human observer to detect or discriminate between weak stimuli occurring either immediately before or after the strong "masking" stimulus in time. Second, observers can use successive stimuli to delineate an interval of time. Given an inter-stimulus interval greater than a few tens of milliseconds, successive stimuli do not substantially alter each other's separate perceptual qualities, but information from each can be integrated to judge the intervening temporal interval. Third, observers are often able to integrate information from disparate sensory events across time, allowing for the detection of stimuli which are subthreshold when presented individually. Finally, sequences of auditory stimuli can be integrated into one perceptual stream or segregated in distinct perceptual streams, depending on the similarity between the individual stimuli, and/or the temporal interval between them.

These perceptual phenomena suggest that the neural responses between successive stimuli can interact in a variety of complex ways. For this interaction to occur, the neural response to the first stimulus must persist until the second stimulus occurs. One potential neural correlate of this long-lasting response is an evoked low frequency oscillation. In 1933, Bartley and

Bishop demonstrated that a short flash of light evoked a rhythmic series of after-discharges in the electrical potential of the visual cortex in the rabbit (Bartley and Bishop 1933). This oscillation occurred at a frequency of five hertz (Hz) and persisted for up to a second following the stimulus. The onset, or short latency, response to a subsequent stimulus was altered by its position in the phase of the oscillation evoked by the first stimulus, such that if the onset response occurred during a trough it was suppressed, and if it occurred during a peak it was enhanced. Thus a single stimulus set up a long-lasting sequence of excitability changes in the cortex which reliably affected the response to subsequent stimuli.

This oscillation could represent a neural basis by which stimuli affect each other through time. However, evoked oscillations in this frequency range have been studied almost exclusively in anesthetized animals. Although spontaneous rhythms in this frequency range have been extensively characterized both in awake humans and in animal models, most studies have claimed that sensory stimulation suppresses spontaneous rhythms. Narici and colleagues (Narici et al. 1987; Narici et al. 1990) have recently demonstrated that the visual cortex preferentially entrains to stimulus repetition rates in the alpha-band, suggesting that the spontaneous rhythms may modulate sensory reactivity. However, the existence of a sensory driven oscillation that operates during non-steady-state stimuli has not been established in the awake case. As a result, the role of these oscillations in sensory processing has remained unclear.

A technique that has proven useful in the analysis of oscillatory activity in the awake human brain is magnetoencephalography (MEG), wherein extra-cranial magnetic fields generated by electrical activity in the brain are measured using super-cooled quantum interference devices (SQUID's). MEG is most sensitive to current sources located on the walls of cortical sulci. Since the primary visual, auditory, and somatosensory cortices in humans are located largely or entirely on the walls of sulci, MEG is a useful method to study early sensory cortical activity. The magnetic field suffers little distortion as it passes through the skull and skin, allowing the current sources giving rise to the MEG signal to be localized. and may increase the temporal resolution of MEG by lessening the effective distance at which a source can influence a sensor, thus preventing distantly located sources from interfering with one another. The ability of MEG to resolve changes in neural activity in the millisecond time range make it ideal for the study of time-dependent oscillatory processes.

The goals in this study were twofold: first, to characterize the timecourse of the evoked magnetic response of the somatosensory cortex of awake humans to brief tactile sensory stimuli, and second to determine if and how the ongoing responses evoked by a brief stimulus could affect the response to a subsequent stimulus.

Methods:

Subjects

Six normal volunteers (five men, one woman, age range 26-35) participated in these experiments. These participants gave informed consent separately for the MEG and MRI components of the study. None of the subjects had any known neurological deficit.

Stimuli

The stimulus paradigm consisted of single or paired pulses of a diaphragm driven by an air-puff, generated by a somatosensory stimulator (Biomagnetic Technologies, Inc.). Stimuli were approximately 30 ms in duration with a peak pressure of 25 psi and were delivered to the index finger through a flexible membrane. The stimulus set consisted of ten trial conditions: one single pulse, and nine paired pulses with stimulus onset asynchronies (SOA's) between 70 ms and 270 ms in 25 ms increments. In most subjects (s2 - s6 in the text), the trial conditions were randomly interleaved. In s1 the trial conditions were presented in blocks consisting of a single SOA. Two hundred trial repetitions were applied for each stimulus condition. The inter-trial interval was between 1.5 and 3 seconds. Stimuli were controlled by a Labview (National Instruments) program. Subjects kept their eyes open and counted the stimuli in blocks of two hundred to maintain alertness. A single experiment typically lasted from 1-2 hours.

Data Acquisition

Evoked magnetic responses were recorded in a magnetically shielded room with a 37 channel magnetometer with SQUID-based first-order gradiometer sensors (Biomagnetic Technologies). Fiduciary points were marked for later co-registration with structural magnetic resonance images. The head shape was digitized to constrain subsequent dipole modeling. The sensor was positioned over the estimated location of somatosensory cortex (SI) of the hemisphere contralateral to the stimulated hand such that a dipolar response was evoked by single test stimuli. Data acquisition epochs were either 1100 ms or 2000 ms with a 1000 ms post-stimulus period and either a 100 ms (s1) or a 1000 ms (s2 - s6) pre-stimulus period referenced to the first stimulus of the trial condition. Data were acquired at a sampling rate of 1041 Hz (s1 - s4) or 520 Hz (s5 - s6) and initially filtered from 1-70 Hz with a notch filter at 60 Hz.

For each subject, high resolution volumetric magnetic resonance images (SPGR sequence, 1128 x 128 x 124 matrix, resolution ~ 1 x 1 x 1.5mm, TR = 36ms, TE = 8ms, flip = 70) were acquired using a 1.5 Tesla SIGNA magnetic resonance scanner (GE Medical Systems, Milwaukee WI).

Data Analysis

Most analyses were performed with Matlab (The Mathworks). For each subject, single trials were sorted by trial condition and channel and averaged across trial repetition. All analyses were performed on these averaged waveforms because the signal to noise ratio of single trials was too low, as is

typical for evoked potential research. Cross-channel average responses were calculated for each subject by calculating the mean of all channels with a signal to noise ratio above four. Signal to noise ratio was defined by the ratio of the mean value of the waveform in the period of 20-70 ms post-stimulus to the mean value of the pre-stimulus period.

In a good MEG recording session the current dipole is located directly under the sensor and tangential to the skull. The dipole generates concentric magnetic field lines around itself, meaning that approximately half of the sensors will record field lines coming out of the head and the other half record field lines going into the head. The sign of the recordings from these two groups of sensors will be opposite. Recorded waveforms were sign-inverted as necessary to ensure that the early response was positive going and that the n100 was negative going. This allowed the averaging of waveforms across channels and the assignation of standard nomenclature to the response peaks regardless of polarity of a given waveform.

In the time domain, the amplitude and latency of the early response to the stimulus was calculated for each waveform. The waveforms were bandpass filtered between 3-20 Hz to smooth them. Onset response amplitudes and latencies were calculated from the first positive-going post-stimulus peak of the smoothed waveform.

In the frequency domain, power spectra were estimated in the pre-stimulus and post-stimulus time periods for each unfiltered waveform using a multi-taper method with a time-bandwidth factor between 2 and 4. In the

pre-stimulus condition, the entire pre-stimulus time period was used to calculate the power spectrum. In the post-stimulus period, an epoch of 0-400 ms post-stimulus was used. This time period encompassed the duration of the oscillation (see data) without including post-oscillation noise. Alpha band power was calculated as the mean of the power spectrum of the unsmoothed waveform between 7 and 13 Hz. Peak frequency and bandwidth in the post-stimulus power spectra were calculated with by smoothing the power spectrum with a five bin wide triangular window and finding the highest peak. Bandwidth was calculated as the width between the half-peak-amplitude points surrounding the peak.

Time and frequency domain analyses were combined by estimating the time frequency evolution of the evoked response to a single stimulus using a sliding window method. The waveform was broken up into a series of overlapping windows, each 300 ms in duration with a step size of 6 ms. Adjacent windows overlapped by 294 ms. The power spectrum in each window was estimated. The time series of these power spectra formed the time frequency evolution of the evoked response. An estimate of the alpha-band power as a function of post-stimulus time was produced by summing the power across the alpha-band range of the time frequency evolution. An estimate of the pre-stimulus alpha-band power was computed using the same procedure on the pre-stimulus period waveform and averaging the power in the alpha-band range across windows. The duration of the evoked alpha-band oscillation was estimated by calculating the time point at which the alpha-

band power decreased below the 95% confidence limit of the pre-stimulus alpha-band power. This procedure worked for all subjects except s1 because the post-stimulus alpha-band power remained elevated above this criterion level throughout the post-stimulus data acquisition period. To estimate the duration of the alpha-band oscillation in s1, the amplitude of the decrease in post-stimulus alpha-band power from the time of its peak to the time at which it fell below the criterion level was calculated for the five subjects for which this was possible. This decrease was 9.77 dB. The duration of the alpha-band oscillation for s1 was estimated as the time at which the post-stimulus alpha-band power fell 9.77 dB from its peak.

The linearity of the response to two sequential stimuli was estimated by constructing a linear predictor model. A model response waveform was calculated for each two stimulus trial condition for each subject by summing the response to a single stimulus with that same response shifted in time by an amount equal to the SOA for that trial condition. Onset response amplitudes, latencies, and evoked alpha-band power were calculated from these model responses using the algorithms identical to those used on the real data.

A single equivalent current dipole model was calculated for each post-stimulus time point with standard BTI software operating on data that had been filtered between 1-20 Hz. The localization algorithm inversely (iterative least-squares minimization) computes a single dipole in a spherical volume of uniform conductivity. Example dipoles were picked by finding the time bin

in which a local correlation maximum was found that was closest in time to the desired time point. Dipole fits with rms values less than 0.8 and goodness-of-fit values less than 0.5 were discarded as being unfittable.

The fiduciary points marked during the MEG recording served as the basis for a common coordinate system for the MEG and MRI data sets. By superimposing these fiducial landmarks on the MR image of the appropriate subject, one can visualize the position of the computed point sources with reasonable anatomical accuracy.

Results:

Impulse Response

The characteristics of the evoked neuromagnetic response to brief air-puff stimuli are shown in figure 1. The waveform of the response recorded in a single magnetometer channel averaged over two hundred stimulus presentations is shown in figure 1a. The stimulus is indicated by the square pulse at 0 ms. The response was an alternating sequence of positive and negative peaks with an approximately 100 ms interval occurring between peaks of the same sign. The power spectra of pre-stimulus and post-stimulus intervals are shown in figure 1b. The upper solid line denotes the power spectrum of the post-stimulus period. The lower 95% confidence limit is denoted by the dashed line. The lower solid line denotes the power spectrum of the pre-stimulus period; the upper 95% confidence limit is denoted by the dotted line. Note that the post-stimulus power shows a clear peak in the alpha band. Figures 1c and d show similar data for a recording channel in a different subject. Several peaks of a low frequency oscillation are seen in the waveform. The post-stimulus power spectrum again exhibits a clear peak at 10 Hz.

For the purposes of this paper, the frequency range of 7-13 Hz will be defined as the alpha-band frequency range. These example waveforms were selected because they demonstrate the difference between post-stimulus alpha band power and pre-stimulus alpha-band power. In five out of six experiments, the example waveform chosen on this basis exhibited a peak

frequency in this range. The mean peak of the power spectrum was 7.8±0.4 Hz (s.e.m.) and the mean bandwidth was 12.3±0.8 Hz. The mean peak of the power spectra across all channels in all subjects was 7.3±0.15 Hz. (s.e.m.) and the mean bandwidth was 11.8±0.2 Hz.

To determine if these oscillations were prevalent across channels, we calculated the average evoked response across channels. The waveform of this average for a representative subject is shown in figure 2a. A clear oscillation is seen in the response. This impression is confirmed in the power spectrum, shown in figure 2b, which follows the same conventions as figure 1b. Figures 2c and d show similar data for a second subject.

Data from all six subjects are shown in figure 3. The bar graph shows the pre and post-stimulus power in the alpha-band range of 7-13 Hz, calculated from the cross-channel averaged waveforms. Both pre-stimulus and post-stimulus power are normalized to the total amount of post-stimulus power. The stimulus caused an increase in alpha-band power in all subjects, which was clearly significant when averaged across subjects (paired t-test, $p < 0.0001$, d.o.f. = 5, t = 8.810). In all experiments except s2, the peak of the post-stimulus power spectra lay within the alpha range. The peak in the post-stimulus power spectrum of s2 was at 6.1 Hz.

The power spectrum of the waveform is shown in a dynamic fashion in figure 4, in which a sliding window with a duration of 300 ms was used to estimate the power spectrum at each post-stimulus time point. Figure 4a shows a contour plot of the resulting data. The black line indicates the

contour at which the peak power has fallen by 10 dB. The stimulus evokes low frequency power in the range of 1-25 Hz, which persists for several hundred milliseconds. Figure 4b shows similar data for another subject. The duration of the oscillation was estimated by determining the length of time over which the alpha-band region of the post-stimulus power spectrum remained higher than the 95% confidence limits of the pre-stimulus alpha-band power. The mean duration of the oscillation across all subjects was 338±68 ms (s.e.m.). This suggests that three full cycles of the oscillation occurred following the stimulus.

To determine whether there was spatial structure to the oscillations across the sensor array, the coherence of the waveforms across channels in the alpha band was directly calculated and is shown in figure 5. The pairwise alpha-band coherence between each channel and its adjacent and doubly-adjacent neighbors in the pre-stimulus condition is shown in figure 5a. The color scale indicates the strength of the correlation, with red indicating that the two channels both have strong alpha-band power and blue indicating that one or both channels have weak alpha-band power. The post-stimulus coherence is shown in figure 5b. A region of low coherence divides the sensors into two groups. Sensory stimulation changes the spatial structure of the coherence in the alpha-band from a somewhat disorganized pattern to a clearly dipolar pattern. The projection vector of the first spatial eigenmode of the power spectra across channels in the pre-stimulus condition is shown in figure 5c. The angle of the arrow represents the phase of the spatial eigenmode

projection. There is a complex phase relationship among the channels in the pre-stimulus period. The phase relationships in the post-stimulus period are shown in figure 5d. A clear dipolar structure can be seen, in which two groups of channels exist that are out of phase by 180 degrees. Because these calculations are performed over a 300 ms post-stimulus window, the presence of the dipolar structure suggests that a single dipole may be responsible for the evoked alpha-band oscillation. This type of dipolar pattern in the post-stimulus period was seen in five out of six subjects (data not shown).

Responses To Successive Stimuli

Having determined that a brief stimulus evoked a long lasting response oscillatory response, it was hypothesized that this ongoing oscillation would modulate the response to a subsequent brief stimulus. This question was investigated by using a stimulus set consisting of a single air puff and a series of paired air-puffs separated by stimulus onset asynchronies (SOA's) of 70-270 ms. The SOA is the time between the onsets of two sequential stimuli. Example data from a single magnetometer channel are shown in figure 6a. The top-most trace shows the response to a single air-puff whose time is indicated by the square wave pulse. The p40 component of the response, a positive going deflection in the response waveform that typically occurs with a 40 ms latency, is marked with an asterisk. Lower traces show the response to paired stimuli. The asterisk on each trace marks the p40 to the second stimulus. These amplitudes are plotted as an amplitude recovery function are plotted in figure 6b. The p40 to the second stimulus is inhibited at the 70 ms

SOA, recovers during the 95 and 120 ms SOA, is very inhibited at the 145 ms SOA, recovers again to supranormal levels, and then returns to normal levels. These peaks at intervals of 95 ms and 220 ms are consistent with the hypothesis that the onset response to the second stimulus is affected by the phase of the evoked alpha band oscillation at which the second stimulus occurs.

The average amplitude recovery function for the p40 component of the response to the second stimulus across five experiments is shown in figure 7a. The post-stimulus power spectrum peak following a single click in subject s2 did not lie within the alpha range and this subject's slower intrinsic oscillation was accompanied by a slower recovery function (data not shown). Averaging oscillatory recovery functions with different periods does not lead to a better estimation of the group mean, so this subject was excluded from further analyses. The measured amplitudes were normalized for each subject by dividing the amplitude of the response to the second pulse by the amplitude of the response to the first pulse for that trial condition. The average response is clearly inhibited at short SOA's, recovers to a peak at a 120 ms SOA, and is somewhat inhibited until a 220 ms SOA at which point it has recovered fully. Analysis of variance with SOA as a repeated measure reveals a very significant effect of SOA ($p < 0.0005$, d.o.f. = 9, $F = 4.776$). The most important post-hoc comparison to establish that a non-monotonic recovery function exists is between the peak at the 120 ms SOA and the

trough at the 170 ms SOA. These two time points are significantly different (paired t-test, $p < 0.025$, d.o.f = 4, $t = 2.993$).

The average amplitude recovery function for the n100 component of the response to the second stimulus is shown in figure 7b. These amplitudes were normalized as described for figure 7a, except using the n100 component of the response to the first stimulus of each trial condition as a normalizing factor. ANOVA with SOA as a repeated measure shows no effect of SOA on the n100 amplitude ($p > 0.1$, d.o.f. = 9, $F = 1.696$). Exclusion of the outlier at the 95 ms time point still shows no statistically significant effect. This suggests that that the oscillation evoked by the first stimulus did not equally affect all components of the response to a subsequent stimuli.

The average recovery function for the latency of the p40 component of the response to the second stimulus is shown in figure 7c. The latency was measured from the onset of the stimulus to the onset of the first post-stimulus positive going peak in the response waveform. Latencies were divisively normalized to the latency of the response to the first stimulus. The average latency recovery function appears flat, and ANOVA with SOA as a repeated measure reveals no effect of SOA ($p > 0.3$, d.o.f. = 9, $F = 1.232$). The one outlier at the 195 ms time point was caused by anomalous data from a single subject, as is suggested by the large error bars at that point. This demonstrates that although SOA has a strong effect on the amplitude of the response to a second stimulus, it does not affect the time at which that response occurs.

The latency recovery function for the n100 component of the response to the second stimulus is shown in figure 7d. These amplitudes have been normalized as described for figure 7c, but using the latency of the n100 component of the response to the first stimulus of each trial condition as a normalizing factor. ANOVA with SOA as a repeated measure shows no effect of SOA on the n100 amplitude ($p > 0.65$, d.o.f. = 9, $F = 0.737$).

The average recovery function for the amount of alpha band power evoked by the second stimulus is shown in figure 7e. The amount of alpha-band power is calculated from the power spectra following the second stimuli and normalized to the alpha-band power evoked from a single stimulus. The shape of this function is similar to that of figure 7a, showing an initial depression, followed by a normal response, followed by depression, followed by a final recovery to normal levels. However, ANOVA with SOA as a repeated measure shows that this trend does not quite reach significance ($p > 0.05$, d.o.f. = 9, $F = 1.884$).

The measured response to the second stimulus is necessarily a combination of the pure response to the second stimulus and the ongoing response to the first stimulus. The linearity of this combination was quantified by comparing the measured response to a particular paired stimulus with a model response constructed by summing the response to a single stimulus and that same response shifted in time by an amount equal to the SOA of the paired stimulus. Model responses were calculated for each SOA of each subject. The amplitudes, latencies, and evoked alpha-band

powers of both the model and measured responses to the second stimulus were calculated and compared. The amplitude of the p40 component of the responses of the model waveform (red circles) and the actual waveform (green stars) is shown in figure 8a. Two-way ANOVA with SOA as a repeated measure demonstrates a significant effect of model ($p < 0.0002$, d.o.f. = 1, $F = 42.483$), SOA ($p < 0.0001$, d.o.f. = 9, $F = 4.668$), and an interaction between the two ($p < 0.0002$, d.o.f. = 9, $F = 3.170$). These effects show that the linear model does not fit the data and that this poor fit is a function of SOA. In particular, the model consistently overestimates the amplitude of the response.

The amplitude of the n100 component of the responses of the model waveform and the actual waveform is shown in figure 8b. Two-way ANOVA shows no significant effect of model ($p < 0.1$, d.o.f. = 1, $F = 3.362$), SOA ($p > 0.25$, d.o.f. = 9, $F = 1.270$), nor an interaction ($p > 0.05$, d.o.f. = 9, $F = 1.826$). These data suggest that the lack of effect of SOA on n100 amplitude is accounted for by linear interactions.

The latencies of the p40 component of the response of the model waveforms and the actual waveforms are shown in figure 8c. The predicted latency recovery function is quite flat and similar to the measured function. Two-way ANOVA reveals no effect of model ($p > 0.4$, d.o.f. = 1, $F = 0.720$), SOA ($p > 0.1$, d.o.f. = 9, $F = 1.600$) and no significant interaction ($p > 0.4$, d.o.f. = 9, $F = 1.051$), suggesting that the model fits the data confirming that there is no effect of SOA on evoked response latency.

The latencies of the n100 component of the response of the model waveforms and the actual waveforms are shown in figure 8d. Two-way ANOVA reveals no effect of model ($p > 0.9$, d.o.f. = 1, $F = 0.006$), SOA ($p > 0.2$, d.o.f = 9, $F = 1.333$) and no significant interaction ($p > 0.7$, d.o.f. = 9, $F = 0.654$).

The evoked alpha-band power of the model and measured waveforms are shown in figure 8e. Two-way ANOVA shows significant effects of model ($p < 0.05$, d.o.f. = 1, $F = 6.412$), SOA ($p < 0.0001$, d.o.f. = 9, $F = 8.195$), and an interaction between the two ($p < 0.005$, d.o.f. = 9, $F = 3.113$). The model clearly overestimates the evoked alpha-band power at every time point. This is particularly true at the time points at which the evoked alpha-band oscillation from the first stimulus is near its peak. At these time points, the evoked oscillations from both stimuli would be predicted to interfere constructively, yielding a supranormal response, as is seen in the model data.

Estimated Current Dipole Analysis

The oscillatory response characteristics of the evoked response to an air-puff stimulus have been discussed solely on the basis of the waveform of the response. This cause of the observed oscillation could be either the repetitive reactivation of a single region of cortex, or the sequential activation of stages of hierarchically organized somatosensory processing. To distinguish between these alternatives, single dipole models were calculated for the onset responses to each stimulus (mean post-stimulus latency 42±19 ms s.d.), and for the first cycle of the oscillatory response to a single stimulus (mean post-stimulus latency 142±19 ms, s.d.). The calculated locations of these single

dipoles were superimposed on structural MRI images to ensure that they were found within somatosensory cortex. An example fit of the early response to a single tap in one subject is shown in figure 9a, clearly located in the post-central gyrus. The fit of the first rebound response is shown in figure 9b, and localized to 2.5 centimeters lateral and ventral to the location of the onset response to the stimulus. To gain an estimate of the localization error, we calculated the dipole fits for the onset response to the second stimulus and compared them to the locations of the onset response of the first stimulus of the pair. The fit of the first stimulus is shown in figure 9c and the fit of the second stimulus is shown in figure 9d. The difference in the locations was 1.8 centimeters. Since it is known that the first and second stimuli of the pair engage identical regions of cortex (Sameshima and Merzenich 1993; Dinse et al. 1997), the difference in their calculated localizations is a measure of the error of the dipole fitting process. This difference is of the same order of magnitude as the difference in the locations of the onset and rebound response to a single stimulus, suggesting that the onset and rebound responses also activate the same region of cortex.

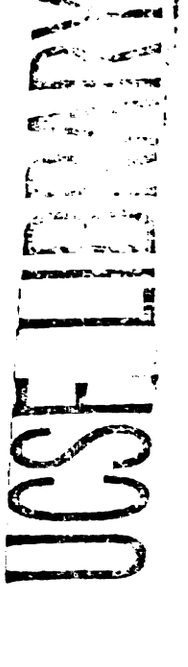

The complete distribution of localizations for the onset response to the first stimulus, to the rebound following the first stimulus, and to all second stimuli where good fits were achieved in one subject is shown in figure 10. Two stimulus conditions (195 ms and 220 ms SOA) did not yield sufficiently good localizations to be included (see methods). The responses to the second stimuli are clustered around the location of the response to the first stimulus

with a difference of 2.3±1.0 cm (s.d.). For each subject, the distance from the localization of the first stimulus to the localization of the rebound was calculated and compared to the mean distance from the localization of the first stimulus to the second stimuli. No consistent pattern in the localizations of the responses to the second stimuli of the different trials conditions was seen across subjects (data not shown). The distribution of the ratio of these two values across four subjects was not significantly different than one (mean = 1.33±0.71, s.d., paired t-test, $p > 0.2$ d.o.f. = 3, $t = 0.932$), consistent with known animal data demonstrating that the rebound response and onset response activated a similar region of cortex (Sameshima and Merzenich 1993; Dinse, et al. 1997).

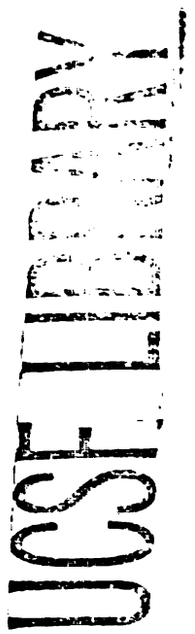

Discussion:

The goals of this study were 1) to characterize the temporal properties of the evoked magnetic field impulse response to a brief stimulus, and 2) to determine how these temporal properties altered the responses to subsequent stimuli. Two important results were demonstrated. First, a brief somatosensory stimulus evokes an alpha-band oscillation in the extracranially recorded magnetic potential above somatosensory cortex in alert humans. This oscillation appears to reflect the repetitive reactivation of a region of somatosensory cortex.

Second, this evoked oscillation causes the amplitude of the p40 component of the response to a subsequent stimulus to be modulated as a function of the phase of the oscillation at which the second response occurs. The two-pulse data demonstrate that the amplitude recovery function following a stimulus is non-monotonic, and exhibits a sub-normal response minimum at the 170 ms SOA. No evidence for enhanced responsiveness during the oscillatory peaks was found. No effect was seen on the amplitude of the n100 component of the response. Linear predictor analysis demonstrated that the evoked response to the second stimulus was generally inhibited relative to the predicted value at most time points.

No effect of SOA on the latency of the response to the second stimulus was seen. This suggests that the afferent input activates the cortex at the same latency regardless of the phase of the excitability cycle of the cortex, but that the afferent input is differentially able to drive the cortex depending on that

phase. Interestingly, this implies that the temporal interval represented by the stimuli is accurately represented by the interval between the responses to those stimuli, even though the response amplitudes may change.

Two interpretations could explain the weak effect of SOA on evoked alpha-band power. The first is that a ceiling effects exists for alpha-band power in the cortex, and that a single stimulus generates the maximum amount of alpha-band power that the cortex is capable of generating. The second stimulus can not add alpha-band power to the ongoing oscillation due to this ceiling effect. A second interpretation is that the second stimulus resets the ongoing oscillation. When the second stimulus occurs, the phase of the oscillation changes but the total power does not. The analysis of single MEG trials could distinguish between these alternatives by allowing the calculation of the change in the phase of any pre-stimulus oscillation as a result of sensory stimulation.

Previous EEG/MEG somatosensory impulse responses

The standard somatosensory evoked potential, as described by Goff *et. al.* (Goff et al. 1977), using EEG recording, shows a series of positive going peaks at 100 ms, 190 ms, 300 ms, and 420 ms post-stimulus. This "after-discharge," as they referred to it, was also seen in similar evoked potential studies in the auditory (Goff, et al. 1977) and visual (Allison et al. 1977) systems and was hypothesized to be caused by mechanisms similar to those that caused spontaneous alpha-band activity. No MEG studies to date have examined evoked alpha-band oscillations, although gamma-band oscillations

have been extensively studied (Ribary et al. 1991; Joliot et al. 1994). Most MEG studies of somatosensory evoked fields have typically correlated response peaks with activity in different somatosensory cortical regions. To our knowledge, this is the first analysis of the evoked somatosensory magnetic response in the frequency domain.

Previous two-pulse experiments

Several earlier studies have attempted to determine if the evoked response from brief stimulus alters the response to subsequent stimuli. Gastaut and Cigánek (Cigánek 1964) used paired flashes of light to study recovery of excitability of the visual cortex using EEG recording. They found that the evoked response to the second flash was modulated by its position in time following the first stimulus, with maximal responses seen at 100 ms and 200 ms and a subnormal region centered at 150 ms. These data are consistent with the hypothesis that the first stimulus evokes an alpha-band oscillation of cortical potential that alters the response to the second stimulus. Studies in the visual cortex using animal models have demonstrated that a single flash of light can evoke an after-discharge with a alpha-band frequency, termed a photically evoked after-discharge (Kimura 1962). This visually evoked oscillation alters the response to subsequent test flashes (Brankack and Klingberg 1982).

A previous study using EEG recording and paired electrical stimulation of the median nerve found no evidence for an oscillatory recovery function (Allison 1962). The difference between this result and the current

work is likely to be methodological, particularly the nature of the stimulus and the nature of the signal being recorded with electrical versus magnetic measurements, because other aspects of the experimental design, including the behavioral state of the subjects, appears to be identical.

A recent series of experiments using MEG from Loveless and Hari (Loveless et al. 1989) have employed a two-stimulus paradigm to examine stimulus interactions across time in the auditory system. They have found an enhancement of the n100 component of the response to the second of two 50 ms duration tones when the tones were separated by an SOA of between 70 ms and 230 ms, but no effect on the p40. They suggested that this effect could be related to the psychophysical effects of loudness enhancement (Loveless and Hari 1993) and temporal integration (Loveless et al. 1996). This enhancement effect is not apparent in the current data set, and in fact, no effect of SOA on n100 amplitude or latency was found. This difference is likely to be due to the different sensory systems studied. In particular, if the n100 enhancement seen by Loveless and Hari is related to the suggested psychophysical effects, the enhancement may be specific to the auditory system. Given that the temporal features of the ensembles of stimuli presented to the auditory and somatosensory systems are likely to be quite different, it would not be surprising to find learned or built-in differences in the temporal response properties of these sensory systems.

Result from this current work are consistent with those of Narici and colleagues (Narici et al. 1991), who have found that repetitive visual or

somatosensory stimulation causes a strong phase-locking of the evoked response. If the frequency of the stimulation is at the peak frequency of the measured spontaneous alpha-band activity, spontaneous rhythmic activity persists for up to one second after stimulus offset. If the frequency of the stimulation is slightly decreased or increased, no after-discharge is seen following stimulus offset. Scalp distributions of the post-stimulus oscillations were very similar to those of the spontaneous oscillations, suggesting that they had the same cortical generators (Narici and Romani 1989; Narici, et al. 1990). These data suggest the existence of a cortical oscillator that is responsive to stimuli and capable of being entrained with a preferred frequency in the alpha range. One difference between the studies of Narici and colleagues and the current study is that they found two somatosensory oscillators, with preferred frequencies of 6 and 12 Hz (Narici and Romani 1989; Narici, et al. 1990), whereas the average oscillatory frequency found in this study was 7.8 Hz. Nonetheless, it is likely that similar mechanisms are responsible for both sensory evoked alpha-band oscillations.

Relationship between MEG and EEG recording

The current generators responsible for the magnetic fields measured with MEG are likely to be the same as those responsible for the electric fields measured with electroencephalography (EEG). To generate an appreciable extra-cranial field of either sort, a large number neurons must be organized in parallel such that the electromagnetic fields they generate reinforce one another. The apical dendrites of cortical pyramidal cells are a candidate for

such a system because they are all oriented perpendicularly to the surface of the cortex. Both MEG and EEG recording are sensitive to changes in neural activity on the millisecond time scale, making them suitable for the examination of the rhythmic potentials in this study.

MEG and EEG recording are sensitive to different sources of activity in the cortex. As current moves along apical dendrites, perpendicular to the cortical surface, a electric field is induced along this axis. A corresponding magnetic field is induced concentrically around this axis. To be detected by a conventional MEG sensor outside the head, these magnetic field lines must be perpendicular to the surface of the head. When the current source is parallel to the surface of the head, as is the case for a current source on the wall of a cortical sulcus, the magnetic field lines are optimally oriented for extra-cranial detection. When the current source is perpendicular to the surface of the head, as is the case for a current source on the surface of a cortical gyrus, the magnetic field lines are oriented parallel to the surface of the head and are invisible to conventional MEG sensors.

A very different situation exists in EEG recording. As current flows between regions of a cell, corresponding extracellular volume currents must occur in the opposite direction. These currents can be measured by scalp electrodes after they pass through the cortical tissue, pia, dura, skull, and scalp but do not in themselves give rise to a detectable extra-cranial magnetic field perpendicular to the scalp. EEG recording is relatively insensitive to the orientation of the intracellular currents that give rise to these volume

currents because the volume currents spread widely throughout the surrounding tissue.

A second important difference between these two techniques is caused by the fact that electric signals and magnetic signals permeate the brain and skull differently. The volume currents measured by EEG recording encounter a high resistance barrier at the skull which attenuate the signal. Anisotropies at this barrier and in the other tissues cause the volume currents to distort and flow away from their original sources. The magnetic field measured by MEG recording is essentially unaltered by passage through biological barriers. The cortical tissue, pia, dura, skull and skin are transparent the magnetic field in the sub 1 kHz frequency range. These facts cause an EEG electrode to have a larger "seeing volume" than an equivalently located MEG sensor, meaning that a given cortical current source will be detected at a further distance with an EEG electrode than with an MEG sensor.

These two differences have several consequences: 1) identically located EEG electrodes and MEG sensors will report different signals in response to the same neural events because they are sensitive to different current sources and because they average over different volumes. 2) The equivalent current dipole fits based on EEG and MEG data will differ for the same reasons. 3) The temporal resolution of MEG data is potentially better than EEG data because of the smaller seeing volume. Each type of recording averages activity over its seeing volume. If the timecourse of activation of the active units in a given

volume is not identical, temporal smearing in the recorded activity will occur, decreasing the effective temporal resolution of the data.

Given these differences between the data derived from MEG and EEG recording, it is not surprising to find differences in the results of the various studies discussed above. Given the goals of the current study, which were to record sensory responses in local regions of primary somatosensory cortex, MEG was the more useful technique because of its sensitivity to current sources on the walls of sulci, its small seeing volume, and its high temporal resolution.

Is *it really an oscillation?*

The techniques used in this study to analyze the oscillatory properties of the evoked response have been model-free in the sense that they do not depend on what the cortical sources of the magnetic field signal are. However, to assign a functional interpretation to these data a hypothesis must be made about the brain states that these oscillations reflect. There are two distinct models for the source of these extra-cranially recorded oscillations. The first is that the oscillation reflects the repetitive reactivation of a particular cortical area. In this case, the oscillation would be an accurate reflection of the changes in electrical potential that a particular region of cortex underwent as a result of sensory stimulation. The second model is that each peak of the oscillation is the result of the activation of a new stage of cortical processing. In this case, the oscillation would not reflect the activity of any single cortical site, but instead, would reflect the staggered sequence of activation of several regions

of cortex. Distinguishing these models using extra-cranially recorded data is quite difficult. Two approaches have been used to infer the similarity of cortical sources for different peaks. The first is the scalp topography of the peaks. In a particularly careful EEG study of the somatosensory evoked potential, Goff *et. al.* (Goff, et al. 1977) found that a stimulus evoked a series of waves with peaks at 100 ms intervals. The timing of these peaks suggests that they are the EEG manifestation of an alpha-band oscillation. The scalp distributions of these peaks were somewhat different from each other and from the scalp distribution of the initial response. Data of this sort has been used to suggest that different cortical regions generate these different peaks. However, these data do not exclude an ongoing oscillatory response at the cortical site that generates the short latency response. The differences in scalp distributions could reflect the contribution of additional dipoles to the ongoing response rather than the shift in position of a single dipole.

The second approach to inferring the similarity of cortical sources for different peaks of the evoked response is the differing susceptibility of the peaks to cognitive and task demands. In particular, the amplitude of the P2 peak, occurring at approximately 200 ms post-stimulus, has been reported to be sensitive to the attentional requirements of the task, implying that the generator of the P2 is distinct from that of earlier components of the evoked response. However, if part of the P2 peak is generated by a rebound oscillation in the cortical site that generates the onset response, the attentional modulation could be due to changes in the efficacy by which that cortical

region is reactivated. Modern studies have generally concluded that this attentional modulation is actually a negative shift of the entire evoked response over a several hundred millisecond period, further suggesting that the differential sensitivity to attention of evoked components before and after the onset of this shift and does not imply a change in the location of their cortical generators.

Two results from this paper suggest that the evoked magnetic field oscillation reflects the repetitive reactivation of a single cortical region. First, the first positive rebound peak, at a latency of approximately 150 ms post-stimulus, localizes to a similar region of cortex as the initial onset transient. Although the calculated dipole localization of the rebound does not precisely overlap with that of the onset response, it typically lies within the scatter of points defined by the calculated dipole localizations of the responses to the second stimuli in the two stimulus conditions. Studies in animals have demonstrated that the onset response to the second stimulus activates exactly the same of cortex as the response to the first (Sameshima and Merzenich 1993; Dinse, et al. 1997). Thus, the difference between the localizations reflects the error of the dipole fitting technique under the noisy conditions of the immediately post-stimulus period. Second, sensory stimulation causes the phase relationships between sensor channels to assume a dipolar structure in which two groups of channels are found, 180 degrees out of phase with each other. Since these phases are calculated over a 400 ms post-stimulus window, the phase relationships suggest that the oscillation maintains a dipolar

structure over this period of time. Together, these data suggests that the extra-cranial magnetic field oscillation does reflect an oscillatory reactivation of a single cortical site.

Previous work on alpha-band oscillations

Substantial data exists from earlier studies in anesthetized animals to confirm that a local region of cortex is capable of oscillatory activity in the alpha band following sensory stimulation. A repetitive response of the cortex to sensory stimulation was first observed by Bartley and Bishop (Bartley and Bishop 1933) who found that stimulation of the optic nerve was followed by several cycles of a 5 Hz oscillation in the surface potential of the visual cortex. The finding of repetitive responses to sensory stimulation was repeated in the somatosensory (Adrian 1941) and auditory (Bremer 1943; Bremer 1949) cortices. Modern studies have replicated these results using intracortically recorded local field potentials (LFP) and single and multi-unit activity. In particular, it has been shown that a brief somatosensory stimulus evokes a long-lasting alpha-band oscillation in the somatosensory cortex of both rat (Schoner et al. 1992; Sameshima and Merzenich 1993) and monkey (Sameshima and Merzenich 1993). This oscillation persisted for up to one second and altered the response to a subsequent stimulus in a phase-dependent manner (Kopecz et al. 1993; Sameshima and Merzenich 1993). Multi-site recording revealed the evoked oscillation to be synchronous across the activated cortex (Sameshima and Merzenich 1993), suggesting that it could give rise to a strong extra-cranial field. These data conclusively demonstrate

that sensory cortex generates an in-place alpha-band oscillation in response to sensory stimulation, supporting the hypothesis that the oscillations witnessed in the current work reflect a repetitive reactivation of a local cortical region.

These evoked oscillations were considered to be the counterpart of the spontaneous alpha rhythm, discovered by Berger in humans in 1929. This rhythm was subsequently studied by Adrian (Adrian and Matthews 1934; Adrian and Yamagiwa 1935), who found that its source was in the occipital lobe and that it was only present when the visual cortex was unstimulated. It was considered to be the endogenous rhythm of the unstimulated brain, and its disappearance during vision was attributed to either desynchronization or inhibition. The same rhythm has subsequently been found with MEG recording (Cohen 1968; Cohen 1972). A similar alpha-band spontaneous rhythm has been found over the somatomotor cortex with EEG (Gastaut et al. 1954) and MEG (Tiihonen et al. 1989). Called the mu rhythm, it is suppressed by movement. Over the auditory cortex, an alpha-band oscillation that is suppressed during auditory stimulation has been characterized with MEG (Tiihonen et al. 1991) and is termed the tau rhythm.

It appears that each region of sensory cortex generates spontaneous alpha-band oscillations. Most reports find that this rhythm is suppressed during engagement of the particular region of cortex, either by sensory stimulation or by working memory tasks. This suppression, frequently called "alpha blocking," is in apparent conflict with the data presented in this paper, in which sensory stimulation evokes an alpha-band oscillation. There are two

major differences in these experiments that explain this apparent discrepancy. In alpha-blocking experiments, the stimuli used are usually several hundred milliseconds in duration, and the analysis consists of estimating the power spectra of single trials before and during the stimulation. In the current experiments, the stimuli were under 30 ms in duration, and the analysis consisted of averaging trials together, then estimating the power spectra before and after the brief stimulus. These differences suggest a general model of alpha-band cortical dynamics in which spontaneous oscillations are reset by brief stimuli, yielding a post-stimulus oscillation that is phase-locked to the stimulus. If extended stimuli suppress these oscillations, this situation would yield single trials in which spontaneous oscillations were suppressed by extended stimuli. Averaging trials together would cause the pre-stimulus oscillations to average to zero because they would occur in random phase relative to the stimulus. Post-stimulus oscillations would still be seen in the average because they would be phase-locked to the stimulus.

This hypothesis suggests that the duration of the post-stimulus oscillations seen in the averaged responses may reflect the degree to which the single trials have identical frequencies. Any trial-to-trial jitter in these values would cause the oscillation in the average response to have a briefer duration than the oscillations in the single trials because the later cycles of the oscillations in the single-trials would be increasingly out of phase across trials and would average to zero. Data from intra-cortically evoked field potentials in the anesthetized rat show substantial trial-to-trial variability in the

oscillatory frequency (Sameshima and Merzenich 1993), supporting this hypothesis.

Cellular basis

Although the relative roles of the thalamus (Morison and Dempsey 1943) and cortex (Chang 1950) in generating these rhythms have been extensively debated, it is now clear that both the thalamus and the cortex are independently capable of producing rhythmic oscillations in this frequency range. McCormick and colleagues (von Krosigk et al. 1993; Bal et al. 1995) have shown that the cellular basis of the spontaneous spindle rhythms seen in thalamic slices lies in an interplay between thalamocortical relay cells and the local inhibitory neurons of the corresponding reticular nucleus. This interaction could form the basis of the repetitive response as well. Silva *et. al.* (Silva et al. 1991) have shown that the cellular basis of the spontaneous alpha-band oscillation found in cortical slices lies in the ability of a network of layer V pyramidal cells to generate a rhythm in this frequency range. They proposed that this could be the cellular basis of the alpha rhythm.

Spindle/alpha interaction

The relationship between the spindle oscillation and the alpha rhythm remains unclear. Most authors have associated spindling activity with slow wave sleep and drowsiness and the alpha rhythm with relaxed, unstimulated, wakefullness. However, several studies have found the presence of spontaneous spindle-like oscillations in unit activity in awake rats, especially in a behavioral state described as "quiet attentiveness," found immediately

before the rat begins exploration. It seems unlikely that the thalamus and the cortex can each generate rhythms centered at 10 Hz that are completely functionally independent, but this issue needs more study to be resolved fully.

General model based on our data and previous data

The data presented in this paper, in combination with the similarities of the evoked magnetic field potential to the intra-cortically recorded local field potentials and multi-unit activities, suggests that a brief somatosensory stimulus evokes repetitive activity within a single region of somatosensory cortex. This oscillation could be due to an evoked thalamic spindle, an evoked cortical alpha rhythm, or some combination of the two. The subjects involved in the current experiment were relaxed and attending to the stimulus, suggesting that the oscillations seen were an alpha rhythm rather than a spindle; however, it is difficult to make this assignation over the short period of time that the oscillations persisted.

Behavioral correlates of alpha activity

Since the repetitive response was discovered, people have hypothesized various roles it might play in perception. Shortly after the discovery of the alpha rhythm, Bartley demonstrated that the function relating the rate of a series of flashes to their apparent brightness peaked at 10 Hz, a phenomenon he suggested was due to driving the visual cortex at its preferred frequency. The first efforts to find a psychophysical correlate in the fluctuations of the alpha rhythm came from the studies of Lansing (Lansing 1957),

Callaway (Callaway and Yeager 1960; Callaway 1962) and Dustman (Dustman and Beck 1965). These authors found that the reaction time to a flash of light depended on the phase of the ongoing spontaneous occipital alpha rhythm at which the flash occurred. The mean difference in reaction time between the responses to the flash at the fastest and slowest phase of the alpha rhythm were approximately 10 ms. Harter and White demonstrated that when repetitive flashes of light were flashed at a rate higher than the flicker fusion frequency, the number of perceived flashes of light was equal to the number of cycles of an alpha-band oscillation that the stimulus evoked (Harter and White 1967). More recently, Varela has identified the alpha rhythm as setting a temporal frame in the visual system, such that the perceived simultaneity of two flashes could be altered by phase of the alpha rhythm at which they were presented (Varela et al. 1981; Gho and Varela 1988).

A second group of behavioral correlates of alpha-band activity exists in motor systems. In the late 19th century, it was noticed that humans exhibited a spontaneous finger tremor in the 10 Hz range. After the alpha rhythm was discovered, Jasper demonstrated that a resting tremor with an identical frequency was found in the resting finger of awake humans (Jasper and Andrews 1938). The spontaneous discharge of the motor cortex outputs through the pyramidal system has been correlated with alpha band activity in the motor cortex, suggesting that spontaneous rhythmic activity in the motor cortex causes tremors in the muscle. Kibbler (Kibbler et al. 1949) was the first to suggest that this activity might gate motor output, such that motor actions

were more likely to commence at a specific phase of the alpha rhythm. This suggestion was continued by Gaarder (Gaarder et al. 1966) who found that fixation saccades were phase locked to the alpha rhythm.

What the data imply

The combination of the physiological data demonstrated in this paper and the psychophysical data discussed earlier suggest that a onset of a sensory stimulus triggers a rhythmic sequence of changes of cortical excitability that may have important consequences for the response to sequential stimuli. Future studies will further explore the temporal evolution of the response to stimuli and the effect that this has on perception and behavior.

Figure 1: Example responses of single magnetometer channels to air-puffs delivered to the contralateral index finger. A,C: Response waveforms. A and C are two different subjects. Responses are averaged over 200 trials repetitions. Dashed trace represents stimulus. B,D: Response power spectra. B and D are the estimated power spectra of traces shown in A and C respectively. Pre-stimulus estimate is in red, post-stimulus estimate is in blue. Dashed lines are the 95% confidence limits. For clarity, only the lower limit is shown for the post-stimulus case and only the upper limit is shown for the pre-stimulus case.

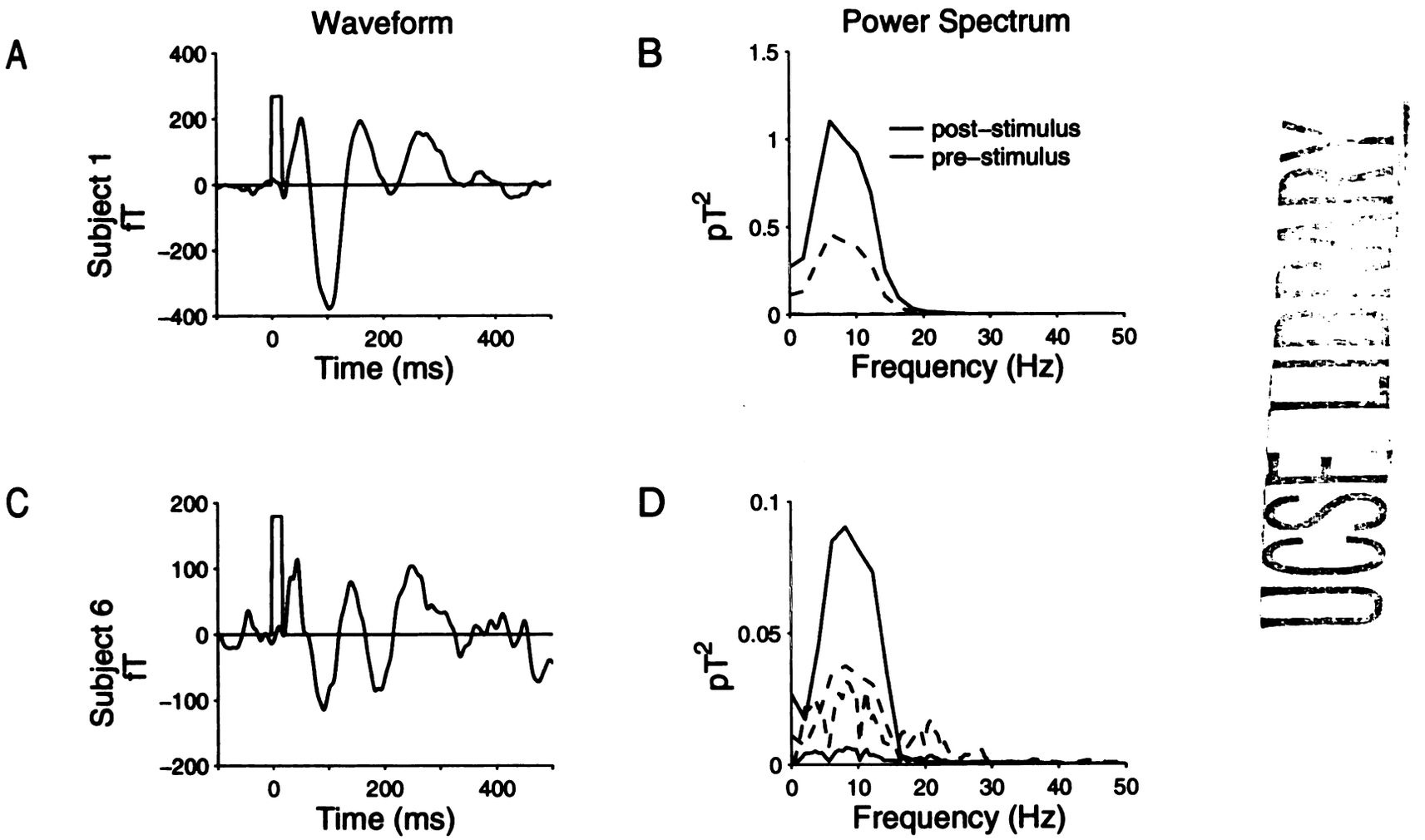

Figure 2: Example cross sensor average waveforms. Averages waveforms were calculated from channels with sufficiently high signal/noise ratios A: A,C Response waveforms. Same subjects as Figure 1. B,D: Response power spectra. Same conventions as figure 1.

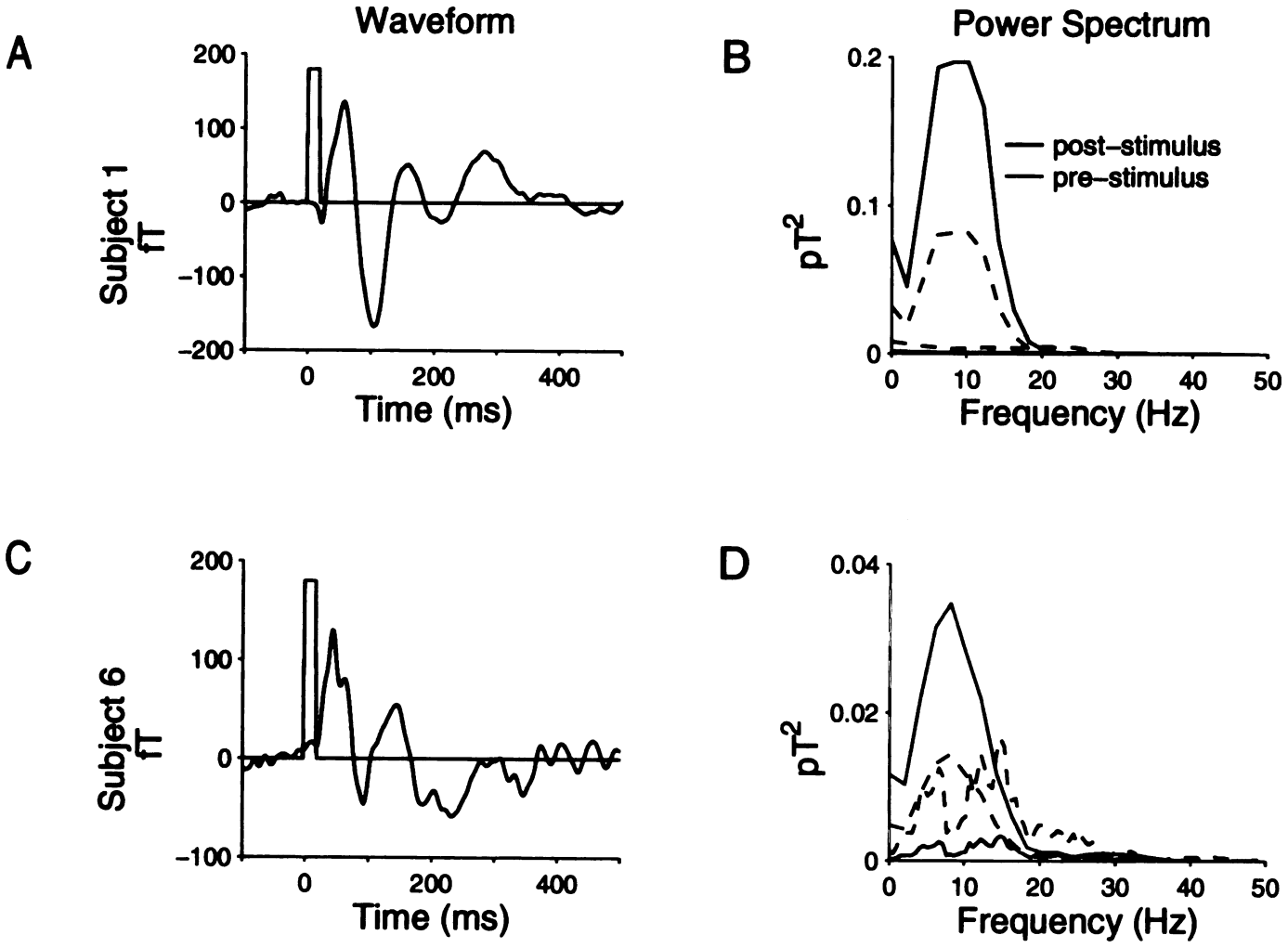
A
Waveform
Subject 1
fT
200
100
0
-100
-200
0
200
400
Time (ms)
B
Power Spectrum
0.2
0.1
0
pT2
post-stimulus
pre-stimulus
0
10
20
30
40
50
Frequency (Hz)
C
Subject 6
fT
200
100
0
-100
0
200
400
Time (ms)
D
0.04
0.02
0
pT2
0
10
20
30
40
50
Frequency (Hz)

Figure 3: Summary of evoked alpha-band power for all six subjects. Pre-stimulus power is the left-most bar of each pair and in some cases is too small to be seen on this scale. Post-stimulus power is the right-most bar of each pair. Pre and post stimulus alpha band powers are normalized to total post-stimulus power on a subject by subject basis. Error bars are s.e.m. There is significantly more alpha-band power in the post-stimulus period than the pre-stimulus period (paired t-test, $p < 0.0001$, d.o.f. = 5, $t = 8.810$).

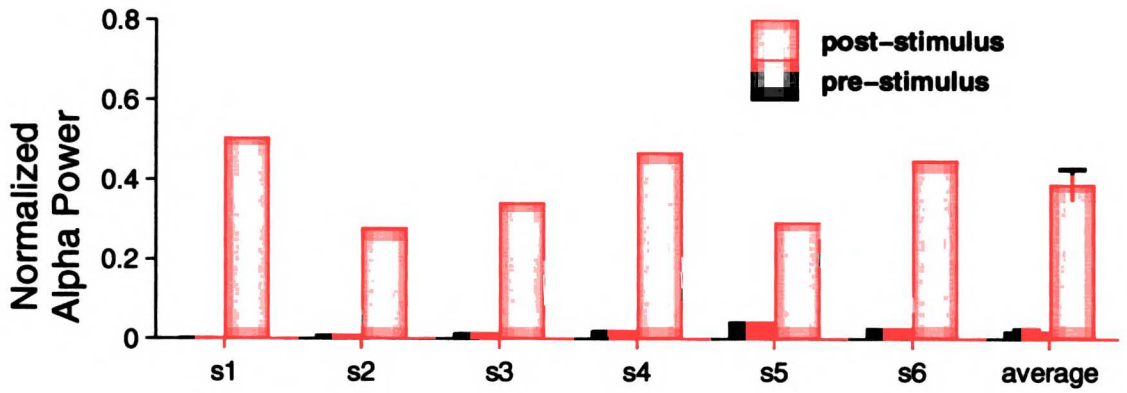
Normalized Alpha Power
0.8
0.6
0.4
0.2
0
post-stimulus
pre-stimulus
s1
s2
s3
s4
s5
s6
average

Figure 4: Example time frequency analyses. A: The power spectrum was estimated for each post-stimulus time bin with a sliding window 300 ms in duration that was advanced six ms per step. The contour plot interpolates the calculated spectra. The black line represents the contour that is a 10dB decrease in amplitude from the peak power point. The stimulus occurs at time = 0 ms. B: A second example subject.

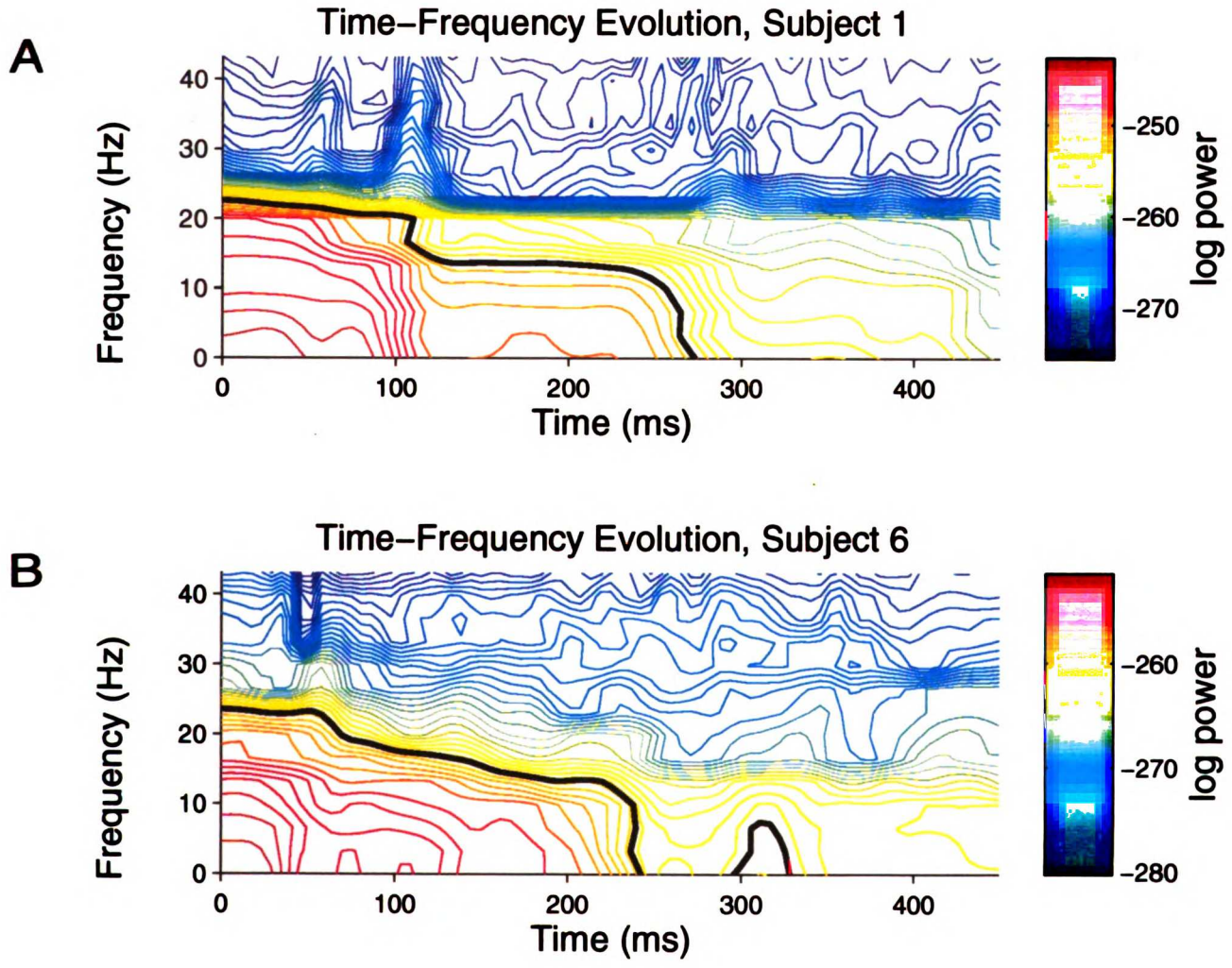
A
Time–Frequency Evolution, Subject 1
Frequency (Hz)
0
10
20
30
40
0
100
200
300
400
Time (ms)
−250
−260
−270
log power
B
Time–Frequency Evolution, Subject 6
Frequency (Hz)
0
10
20
30
40
0
100
200
300
400
Time (ms)
−260
−270
−280
log power

Figure 5: Cross channel coherence. A: Pre-stimulus coherence between adjacent and doubly-adjacent sensor channels. B: Post-stimulus coherence. C: Projection vector of the first spatial eigenmode of the power spectra across channels in the pre-stimulus condition. The angle of the arrow represents the relative phase of the alpha-band power for each sensor. D: Projection vector of the first spatial eigenmode of the power spectra across channels in the post-stimulus condition. Arrows pointing in opposite directions indicate channels that are 180 degrees out of phase.

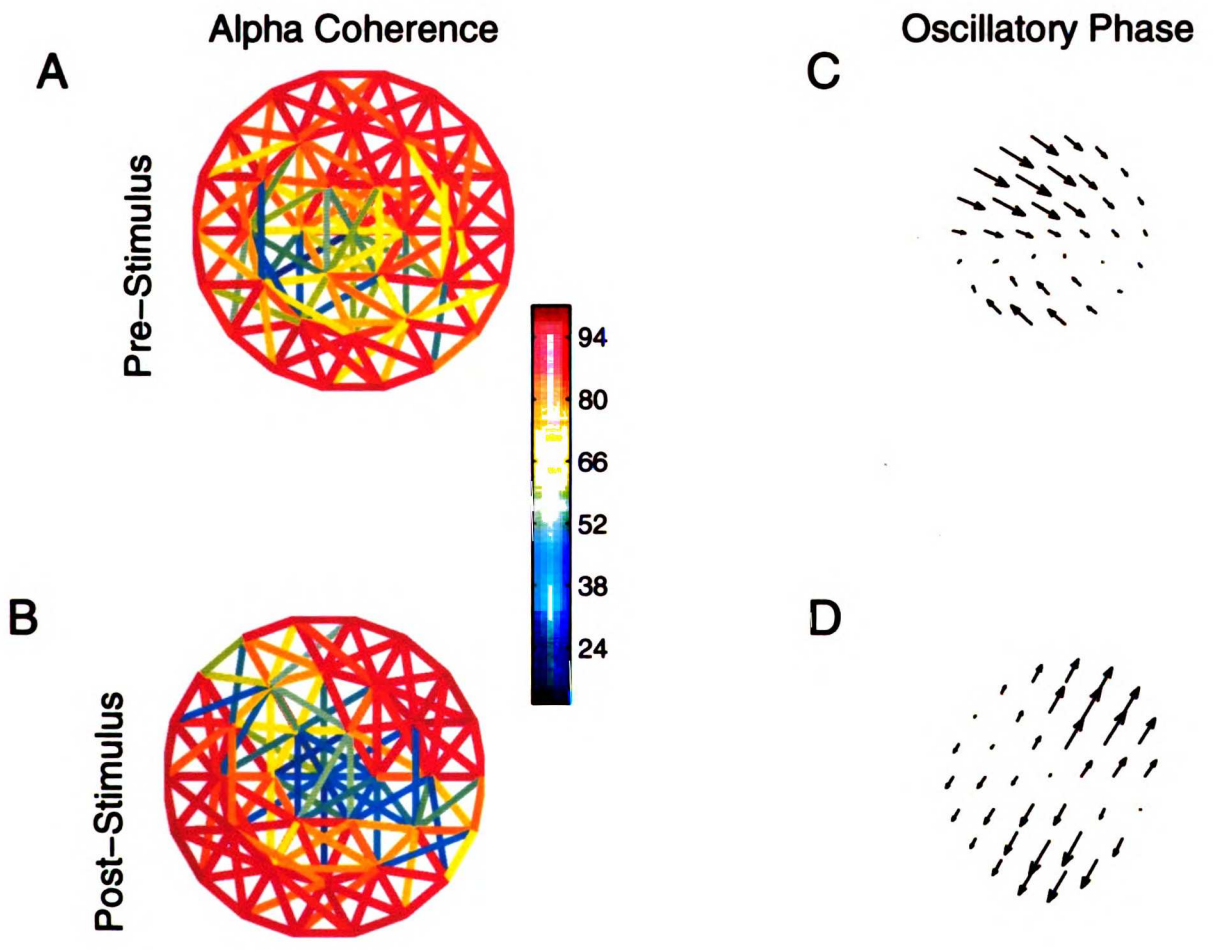
Alpha Coherence
A
Pre–Stimulus
B
Post–Stimulus
94
80
66
52
38
24
Oscillatory Phase
C
D

Figure 6: Example two pulse data. A: Example response waveforms to two-pulse stimuli. Blue traces indicate stimuli. From top to bottom, traces show increasing stimulus onset asynchronies (SOA's) ranging from a single click to 270 ms. Response waveforms are shown in green. Response amplitudes are calculated from the first positive going peak in the response waveform following the second stimulus (first pulse in single click condition) and are shown as redstars. B: Summary of response amplitude to second stimulus as a function of SOA. Zero SOA shows the control response to a single stimulus.

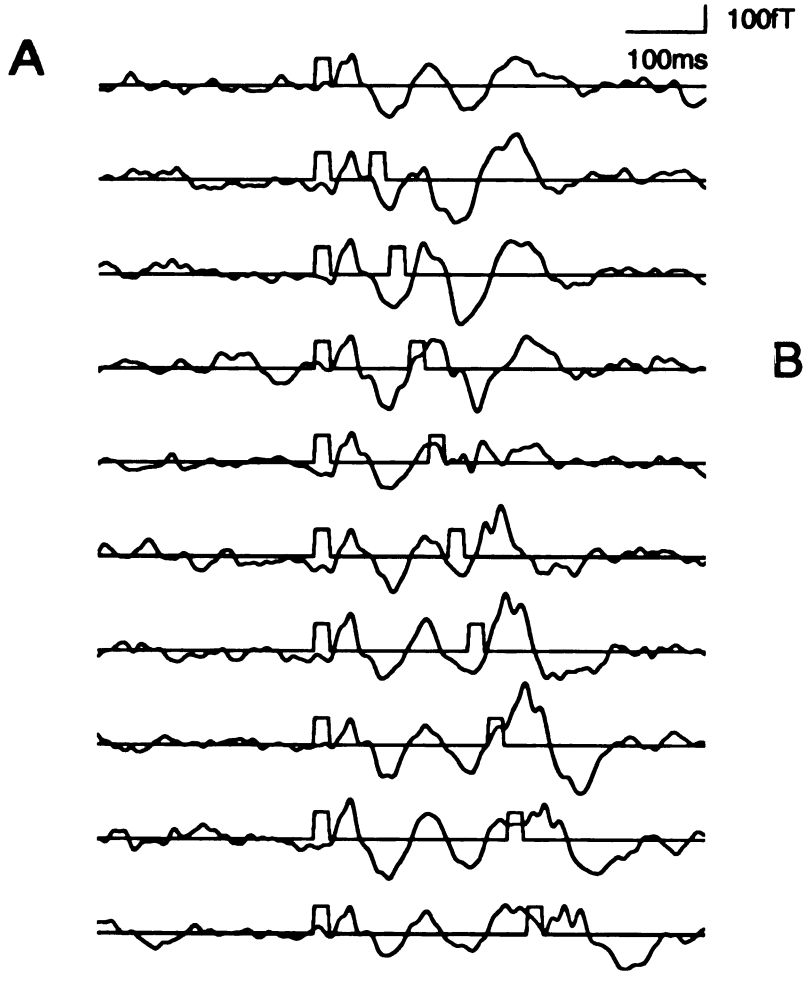
A
100fT
100ms

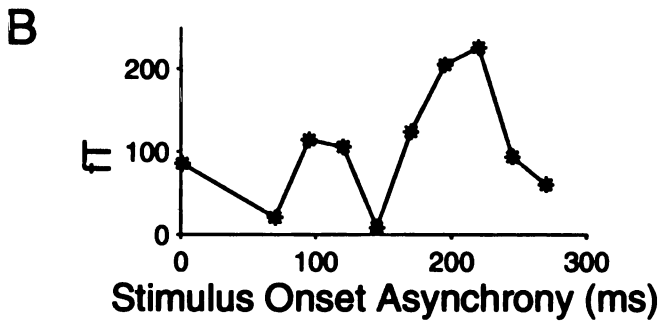
B
200
100
0
fT
0
100
200
300
Stimulus Onset Asynchrony (ms)

Figure 7: Summary of two pulse data. The data averages are across five subjects. Subject s2 was excluded because the post-stimulus power spectrum peak following a single click did not lie within the alpha range. A: Average p40 amplitude recovery function. For each subject, the response amplitude to each second stimulus is normalized by the response amplitude to the first stimulus in that trial condition. Recovery functions are then averaged across subject. Zero SOA shows control response to a single stimulus, which is equal to one and has no error by definition. Error bars are standard error. ANOVA shows a significant effect of SOA ($p < 0.0005$, d.o.f. = 9, $F = 4.776$). A paired t-test shows that the trough at 170 ms is significantly lower than the peak at 120 ms (paired t-test, $p < 0.025$, d.o.f = 4, $t = 2.993$). B :Average n100 amplitude recovery function. ANOVA shows no significant effect of SOA ($p > 0.1$, d.o.f. = 9, $F = 1.696$) C:~Average latency recovery function across the six subjects. Latency is measured as time to the first positive going peak following the second stimulus (first stimulus in single stimulus condition). Latencies are normalized on a condition by condition basis as described for amplitudes. The outlier at an SOA of 200 ms is caused by an outlier in a single subject. ANOVA shows no effect of SOA ($p > 0.3$, d.o.f. = 9, $F = 1.232$). D : Average n100 latency recovery function. ANOVA shows no significant effect of SOA ($p > 0.65$, d.o.f. = 9, $F = 0.737$). E: Average alpha-band power recovery function across the six subjects. Alpha-band power is calculated from the post-second stimulus power spectra and normalized on a condition by condition basis as

described for amplitudes ANOVA shows no effect of SOA ($p > 0.05$, d.o.f. = 9, $F = 1.884$).

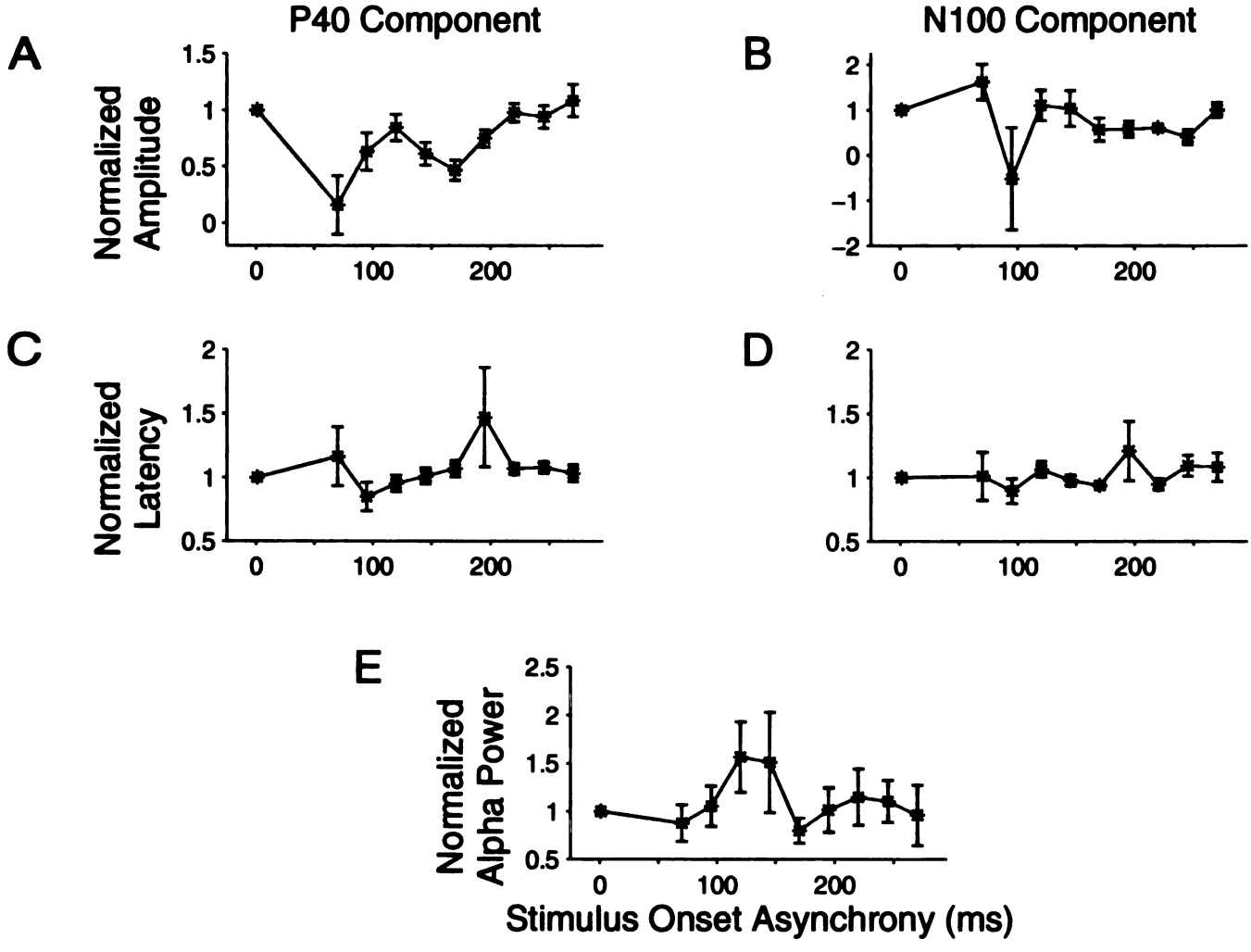
A
P40 Component
Normalized Amplitude
1.5
1
0.5
0
0
100
200
B
N100 Component
2
1
0
−1
−2
0
100
200
C
Normalized Latency
2
1.5
1
0.5
0
100
200
D
2
1.5
1
0.5
0
100
200
E
Normalized Alpha Power
2.5
2
1.5
1
0.5
0
100
200
Stimulus Onset Asynchrony (ms)

Figure 8: Summary of two pulse and linear predictor data. The data averages and linear predictor averages are across five subjects. Subject s2 was excluded because the post-stimulus power spectrum peak following a single click did not lie within the alpha range. A Model (green circles) and actual p40 (red stars) amplitude recovery functions. Response amplitudes are calculated for model and actual waveforms and normalized as described in figure 7. Two-way ANOVA shows significant effects of model ($p < 0.0002$, d.o.f. = 1, $F = 42.483$), SOA ($p < 0.0001$, d.o.f. = 9, $F = 4.668$), and an interaction between the two ($p < 0.0002$, d.o.f. = 9, $F = 3.170$). B : Model and actual n100 amplitude recovery functions. Two-way ANOVA shows a no significant effect of model ($p < 0.1$, d.o.f. = 1, $F = 3.362$), SOA ($p > 0.25$, d.o.f. = 9, $F = 1.270$), nor an interaction ($p > 0.05$, d.o.f. = 9, $F = 1.826$) (see text for details). C: Model and actual p40 latency recovery functions. Two-way ANOVA show no effect of model ($p > 0.4$, d.o.f. = 1, $F = 0.720$), SOA ($p > 0.1$, d.o.f. = 9, $F = 1.600$) or interaction ($p > 0.4$, d.o.f. = 9, $F = 1.051$). D : Model and actual n100 latency recovery functions. Two-way ANOVA reveals no effect of model ($p > 0.9$, d.o.f. = 1, $F = 0.006$), SOA ($p > 0.2$, d.o.f = 9, $F = 1.333$) and no significant interaction ($p > 0.7$, d.o.f. = 9, $F = 0.654$). E: Model and actual evoked alpha-band power recovery functions. Two-way ANOVA shows significant effects of model ($p < 0.05$, d.o.f. = 1, $F = 6.412$), SOA ($p < 0.0001$, d.o.f. = 9, $F = 8.195$), and an interaction between the two ($p < 0.005$, d.o.f. = 9, $F = 3.113$).

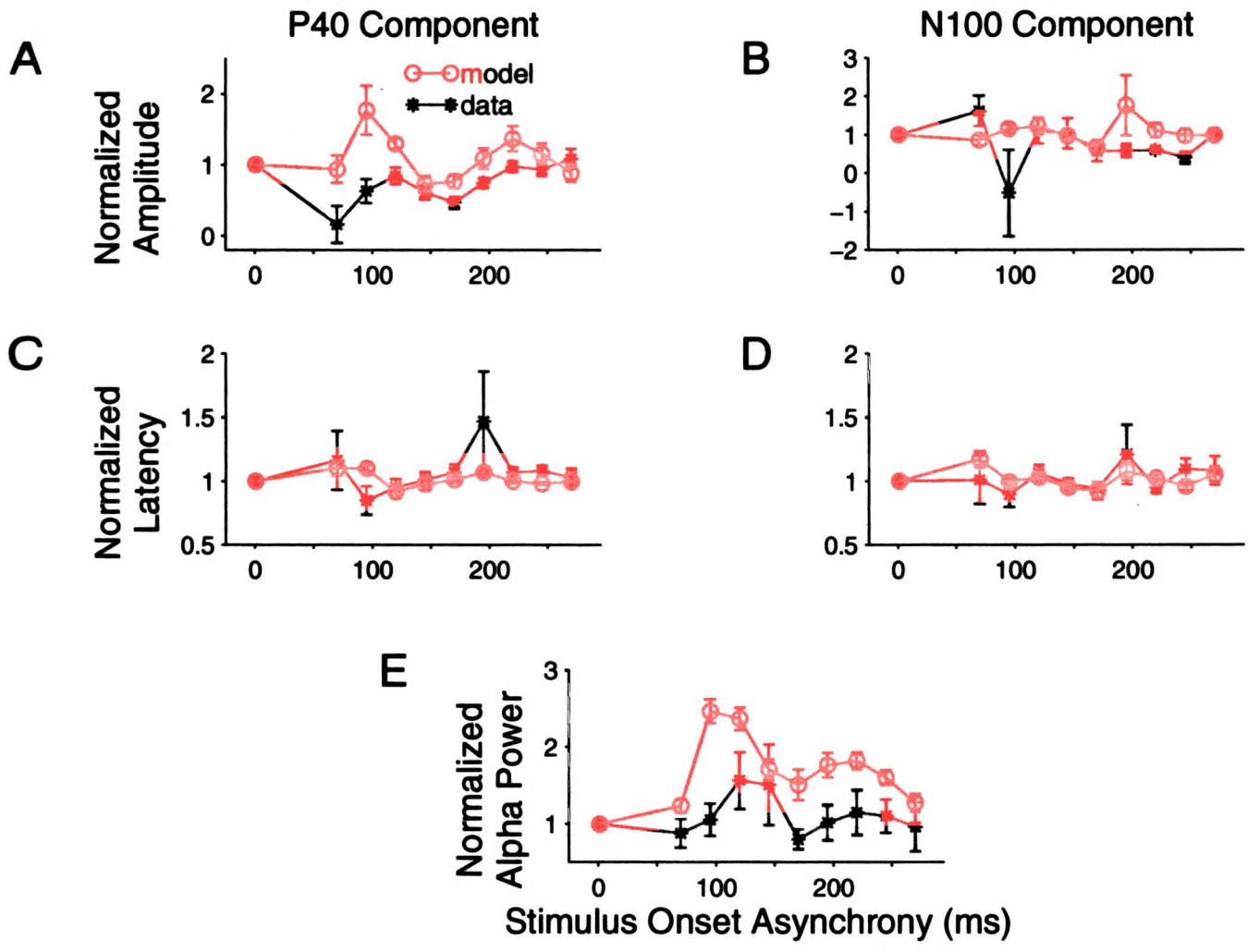
A
P40 Component
model
data
Normalized Amplitude
B
N100 Component
C
Normalized Latency
D
E
Normalized Alpha Power
Stimulus Onset Asynchrony (ms)

Figure 9: Estimated current dipole source localizations. A: Dipole source localization for onset response to first stimulus (fit at 42ms post-stimulus). B: Dipole source localization for rebound response to first stimulus (fit at 144ms post-stimulus). This is 2.5 cm from the source in A. C: Dipole source localization for onset response to first stimulus of 270 ms SOA condition (fit at 39 ms post-stimulus). D: Dipole source localization for onset response to second stimulus of 270 ms SOA condition (fit at 29 ms post-stimulus). This is 1.8 cm from the source in C.

A

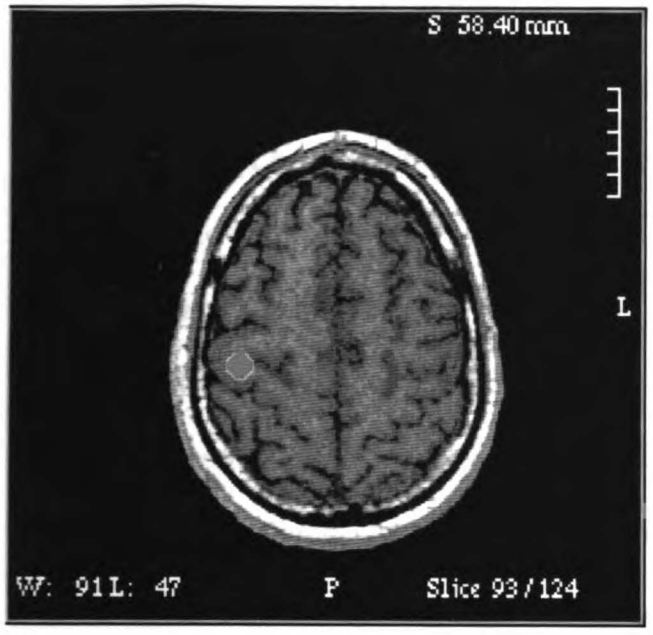

B

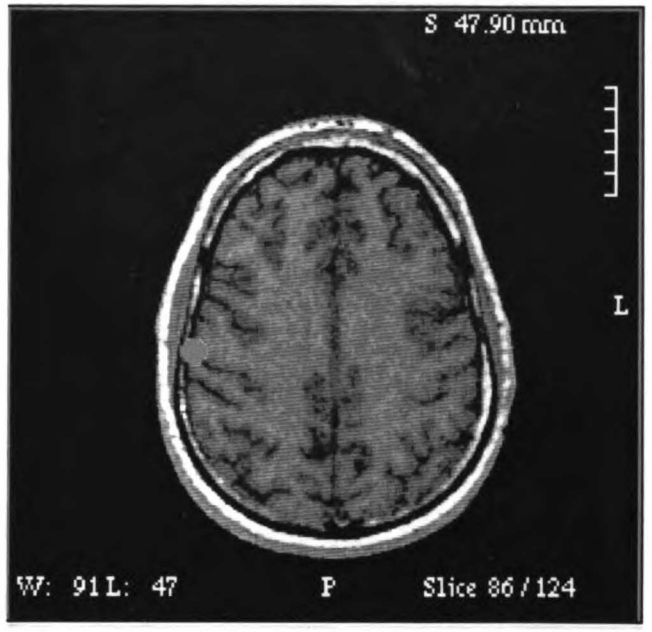

C

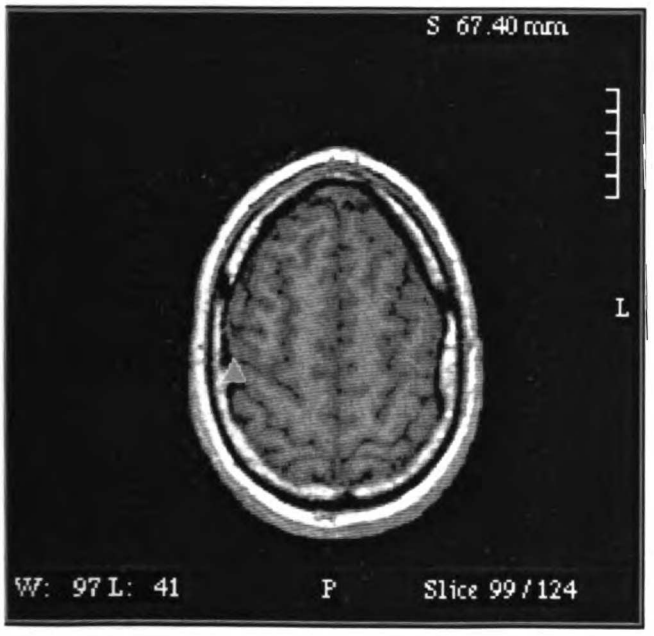

D

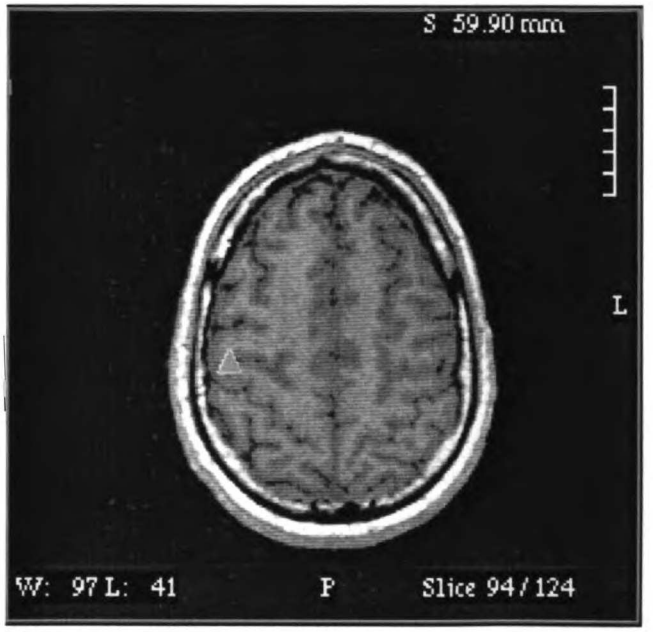

Figure 10: Example dipole fits for one subject. Graphical representation of dipole source localizations for single stimulus, single stimulus rebound, and two stimulus conditions. Localization of single stimulus response is shown in blue. Localization of rebound response is shown in green. Localization of second stimulus responses shown in red, with SOA condition in text. Axes are standard MSI coordinates. The y axis is left/right, the x axis is front/back, and the z axis is ventral/dorsal. Y = 0 defines the midline. The distance between the fit locations of the first response and the rebound response is 2.5 cm. The mean distance between the fit locations of the response to the first stimulus and the responses to the second stimuli is 2.3±1.0 cm (s.d.)

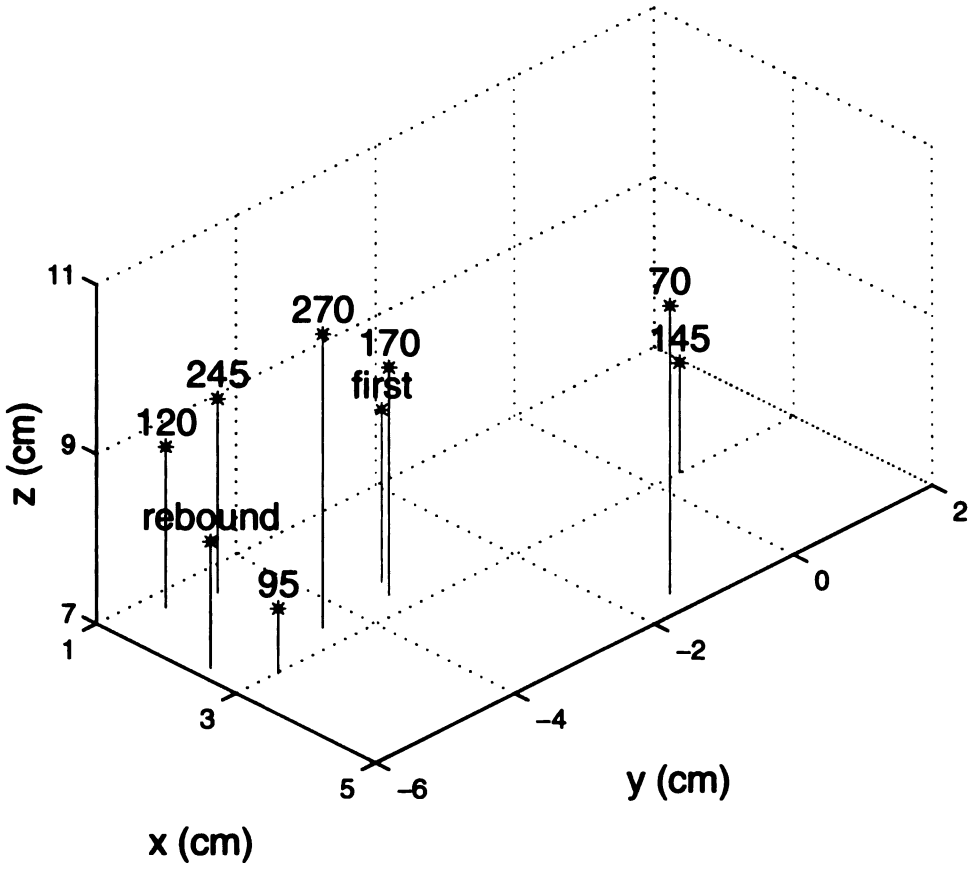
11
9
7
z (cm)
70
145
270
170
first
245
120
rebound
95
2
0
−2
−4
−6
y (cm)
1
3
5
x (cm)

References:

Adrian ED (1941) Afferent discharges to the cerebral cortex from peripheral sense organs. Journal of Physiology 100:159-191.

Adrian ED and Matthews BHC (1934) The Berger rhythm: potential changes from the occipital lobes in man. Brain 57:355-385.

Adrian EH and Yamagiwa K (1935) The origin of the Berger rhythm. Brain 58:323-351.

Allison T (1962) Recovery functions of somatosensory evoked responses in man. Electroencephalography and Clinical Neurophysiology 14:331-343.

Allison T, Matsumiya Y, Goff GD, and Goff WR (1977) The scalp topography of human visual evoked potentials. Electroencephalography and Clinical Neurophysiology 42:185-197.

Bal T, von Krosigk M, and McCormick DA (1995) Role of the ferret perigeniculate nucleus in the generation of synchronized oscillations in vitro. Journal of Physiology (London) 483:665-685.

Bartley SH and Bishop GH (1933) The cortical response to stimulation of the optic nerve in the rabbit. American Journal of Physiology 103:159-172.

Brankack J and Klingberg F (1982) Visual post-stimulus excitability changes in freely moving rats indicated by amplitude and peak time of evoked potentials. Acta Biologica et Medica Germanica 41:801-809.

Bremer F (1943) Etude oscillographique des responses sensorielles de l'aire acoustique corticale chez le chat. Archives International Physiology 53:53-103.

Bremer F (1949) Consideration sur l'origine et la nature des "ondes" cerebrales. Electroencephalography and Clinical Neurophysiology 1:177-193.

Callaway E (1962) Factors influencing the relationshi between alpha activity an visual reaction time. Electroencephalography and Clinical Neurophysiology 14:674-682.

Callaway E and Yeager CL (1960) Relationship between reaction time and electroencephalographic alpha phase. Science 132:1765-1766.

Chang HT (1950) The repetitive discharge of corticothalamic reverberating circuit. Journal of Neurophysiology 13:235-258.

Cigánek l (1964) Excitability cycle of the visual cortex in man. Annals of the New York Academy of Sciences 112:241-253.

Cohen D (1968) Magnetoencephalography: Evidence of magnetic fields produced by alpha-rhythm currents. Science 161:784-786.

Cohen D (1972) Magnetoencephalography: Detection of the brain's electrical activity with a superconducting magnetometer. Science 175:664-666.

Dinse HR, Kruger K, Akhavan AC, Spengler F, Schoner G, and Schreiner CE (1997) Low-frequency oscillations of visual, auditory and somatosensory cortical neurons evoked by sensory stimulation. International Journal of Psychophysiology 26:205-227.

Dustman RE and Beck EC (1965) Phase of alpha brain waves, reaction time and visually evoked potentials. Electroencephalography and Clinical Neurophysiology 18:433-440.

Gaarder K, Koresko R, and Kropfl W (1966) The phasic relation of a component of alpha rhythm to fixation saccadic eye movements. Electroencephalography and Clinical Neurophysiology 21:544-551.

Gastaut H, Dongier M, and Courtois G (1954) On the significance of 'wicket rhythms' ('rythmes en arceau') in psychosomatic medicine. Electroencephalography and Clinical Neurophysiology 6:687-695.

Gho M and Varela FJ (1988) A quantitative assessment of the dependency of the visual temporal frame upon the cortical rhythm. Journal of Physiology (Paris) 83:95-101.

Goff GD, Matsumiya Y, Allison T, and Goff WR (1977) The scalp topography of human somatosensory and auditory evoked potentials. Electroencephalography and Clinical Neurophysiology 42:57-76.

Harter MR and White CT (1967) Perceived number and evoked cortical potentials. Science 156:406-408.

Jasper HH and Andrews HL (1938) Brain potentials and voluntary muscle activity in man. Journal of Neurophysiology 1:87-100.

Joliot M, Ribary U, and Llinas R (1994) Human oscillatory brain activity near 40 Hz coexists with cognitive temporal binding. Proceedings of the National Academy of Sciences (USA) 91:11748-11751.

Kibbler GO, Boreham JL, and Richter D (1949) Relation of the alpha rhythm of the brain to psychomotor phenomena. Nature 164:371.

Kimura D (1962) Multiple response of visual cortex of the rat to photic stimulation. Electroencephalography and Clinical Neurophysiology 14:115-122.

Kopecz K, Schoner G, Spengler F, and Dinse HR (1993) Dynamic properties of cortical evoked (10 Hz) oscillations: theory and experiment. Biological Cybernetics 69:463-473.

Lansing RW (1957) Relation of brain and tremor rhythms to visual reaction time. Electroencephalography and Clinical Neurophysiology 9:497-504.

Loveless N, Hari R, Hamalainen M, and Tiihonen J (1989) Evoked responses of human auditory cortex may be enhanced by preceding stimuli. Electroencephalography and Clinical Neurophysiology 74:217-227.

Loveless N, Levanen S, Jousmaki V, Sams M, and Hari R (1996) Temporal integration in auditory sensory memory: neuromagnetic evidence. Electroencephalography and Clinical Neurophysiology 100:220-228.

Loveless NE and Hari R (1993) Auditory evoked fields covary with perceptual grouping. Biological Psychology 35:1-15.

Morison RS and Dempsey EW (1943) Mechanism of thalamocortical augmentation and repetition. American Journal of Physiology 138:297-308.

Narici L, Liberati D, Cerutti S, and Santoni A (1991) Analysis of the neuromagnetic data on the frequency responsivity of the human brain: a progress report. Clinical, Physical, and Physiological Measures 12 Suppl A:43-47.

Narici L, Pizzella V, Romani GL, Torrioli G, Traversa R, and Rossini PM (1990) Evoked alpha- and mu-rhythm in humans: a neuromagnetic study. Brain Research 520:222-231.

Narici L and Romani GL (1989) Neuromagnetic investigation of synchronized spontaneous activity. Brain Topography 2:19-30.

Narici L, Romani GL, Salustri C, Pizzella V, Torrioli G, and Modena I (1987) Neuromagnetic characterization of the cortical response to median nerve stimulation in the steady state paradigm. International Journal of Neuroscience 32:837-843.

Ribary U, Ioannides AA, Singh KD, Hasson R, Bolton JP, Lado F, Mogilner A, and Llinas R (1991) Magnetic field tomography of coherent thalamocortical 40-Hz oscillations in humans. Proceedings of the National Academy of Sciences (USA) 88:11037-11041.

Sameshima K and Merzenich MM (1993) Intrinsic oscillator contributions to response properties of SI cortical neurons. Society for Neuroscience Abstract.

Schoner G, Kopecz K, Spengler F, and Dinse HR (1992) Evoked oscillatory cortical responses are dynamically coupled to peripheral stimuli. Neuroreport 3:579-582.

Silva LR, Amitai Y, and Connors BW (1991) Intrinsic oscillations of neocortex generated by layer 5 pyramidal neurons. Science 251:432-435.

Tiihonen J, Hari R, Kajola M, Karhu J, Ahlfors S, and Tissari S (1991) Magnetoencephalographic 10-Hz rhythm from the human auditory cortex. Neuroscience Letters 129:303-305.

Tiihonen J, Kajola M, and Hari R (1989) Magnetic mu rhythm in man. Neuroscience 32:793-800.

Varela FJ, Toro A, John ER, and Schwartz EL (1981) Perceptual framing and cortical alpha rhythm. Neuropsychologia 19:675-686.

von Krosigk M, Bal T, and McCormick DA (1993) Cellular mechanisms of a synchronized oscillation in the thalamus. Science 261:361-364.

Stimulus-Evoked Alpha-Band Cortical Oscillations Occur In Humans During Psychophysically Demanding Task Performance

Chapter 3

Abstract:

Several types of oscillatory activity are evident in the spontaneous EEG and MEG records of awake humans. The role that they play in perception has remained unclear. The purpose of this study was (1) to characterize the oscillations evoked by single somatosensory or auditory stimuli in awake humans under conditions of demanding psychophysical performance and (2) to determine the effect of attention and inattention on such oscillations.

Two behavioral paradigms were used to manipulate the attentional state of subjects. The first, called the "inter-modal selective attention task," was designed to allow the measurement of evoked magnetic field impulse responses to individual somatosensory and auditory stimuli under conditions in which the subject was either attending to somatosensory stimuli or attending to auditory stimuli. In a given block of trials, subjects performed a difficult sensory discrimination on stimuli in one modality while ignoring stimuli in the second modality. The second behavioral paradigm, called the "vigilance task," was designed to allow the measurement of evoked magnetic field impulse responses to individual auditory stimuli under conditions in which the subject was either attending to the auditory stimuli or was not engaged in any task. In one block of trials, the subjects performed a difficult sensory discrimination on auditory stimuli. In the second block of trials, subjects were asked to ignore a similar series of auditory stimuli.

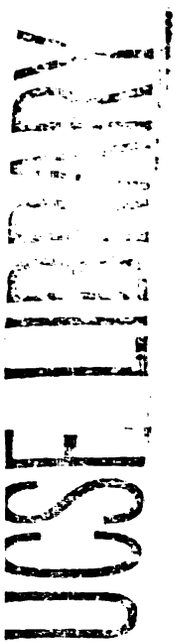

Evoked magnetic response fields (ERF's) were recorded from the somatosensory and auditory cortices in eight human subjects. Somatosensory stimuli were air-puffs (25 PSI) delivered to the distal tip of the index finger. Auditory stimuli were 1 kHz tone pips 15 ms in duration with 5 ms onset and offset ramps. The power spectrum of the ERF and the amplitude and latency of the n100 component of the ERF were calculated for each stimulus condition.

In response to a single stimulus in either modality during both the attended and unattended conditions, strong ERF oscillations in the alpha-band frequency range (7 - 13 Hz) were observed. The strength of these oscillations did not change as a function of attentional state in either of these psychophysical tasks. The amplitude of the n100 component of the ERF recorded over the right hemisphere during the vigilance experiment was sensitive to the attentional state of the subject; however no effect of attention was seen in the other hemisphere or in the inter-modal selective attention task.

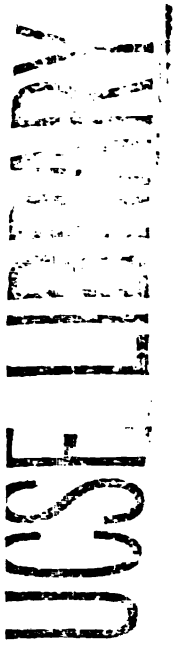

These data demonstrate that the cortex generates stimulus evoked alpha-band oscillations during psychophysically demanding behavioral states. This result suggests that the cortex must have specific mechanisms to deal with the effects that these evoked oscillations have upon sequentially presented stimuli. The fact the evoked oscillation is not altered by attention in the inter-modal selective attention task suggests that response suppression or enhancement is not required for task performance.

Introduction:

Electroencephalographic (EEG) recording has been used for years to gain insight into the brain mechanisms underlying human perception (Regan 1989). Changes in the basic appearance of the EEG reflect changes in cortical dynamics (Nunez 1995). One of the most dramatic changes occurring in the EEG accompanies the shift from the quiet sleeping state, which is characterized by large amplitude, low frequency oscillations, to the waking state, which is characterized by small amplitude, high frequency oscillations (Steriade and Llinas 1988; Steriade and McCarlet 1990). These physiological differences cause differential responsiveness of the cortex to incoming sensory stimuli. When slow wave activity is prevalent, during quiet sleep, sensory stimuli are not reliably transmitted to the cortex, whereas when fast activity is present, during the waking state and REM sleep, sensory stimuli can be transmitted to the cortex (Steriade and Llinas 1988).

This simple picture becomes significantly more complex when the sleeping and waking states are examined more closely. Just as sleep is characterized by a number of different stages, each with its own characteristic EEG signature (Barlow 1993), it is likely that the waking state can be similarly subdivided into different regimes with different EEG characteristics and potentially different sensitivities to sensory stimuli. Two rhythms have been described in the awake state, potentially delineating two behavioral states. The first is the alpha rhythm, a spontaneous oscillation with a frequency of about 10 Hz found independently over visual, auditory, and somatomotor

cortex (Salmelin and Hari 1994) These oscillations are prevalent in several different behavioral states, including relaxation, drowsiness, and anticipation. A second prominent waking EEG state is that of desynchronization, which has recently been reinterpreted to reflect low amplitude, high frequency oscillations (Steriade et al. 1996). This rhythm has been reported to be found during attentive states (Rougeul et al. 1979; Murthy and Fetz 1996).

The question of which of these rhythms is active while a subject performs perceptual task, and how that rhythm relates to task performance has not been fully addressed to date. It has been suggested that large low frequency oscillations could enhance stimulus detection, because a stimulus would provoke a strong response, and could degrade stimulus discrimination, because different stimuli would all tend to produce similar responses. Conversely, smaller high frequency oscillations could be well suited for stimulus discrimination, because they could represent small changes in a stimulus accurately, but be inappropriate for stimulus detection, because the amplitude of the response would be small (Guido et al. 1995). In any event, a more complete understanding of brain states that are active during sensory discrimination should provide insight into the mechanisms by which the sensory cortex solves these tasks.

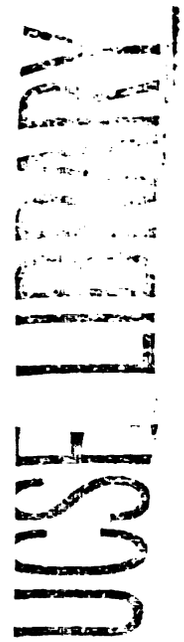

It has previously been shown that the event-related magnetic field (ERF) in response to a brief somatosensory stimulus in the awake human could be characterized as an alpha-band oscillation lasting approximately 300 ms (Mahncke 1998). This oscillation affects the response to subsequent

stimuli, such that stimuli that occur in the troughs of the oscillation evoke proportionally lower responses. Subjects were awake and were asked to count the stimuli; however, their attentional state was not specifically controlled beyond these verbal instructions. Thus the stimulus-evoked oscillations seen in this study might not reflect cortical dynamics during other behavioral states; e.g. during the performance of demanding psychophysical tasks.

The goals of this study were twofold. The first was to determine if alpha-band oscillations could be evoked by sensory stimulation when a subject was behaviorally aroused and performing a difficult psychophysical task. The second goal was to determine if the evoked response was affected by the attentional state of the subject. To answer these questions, a combination of psychophysics and magnetoencephalography (MEG) was used in order to manipulate the attentional state of human subjects while recording ERF's.

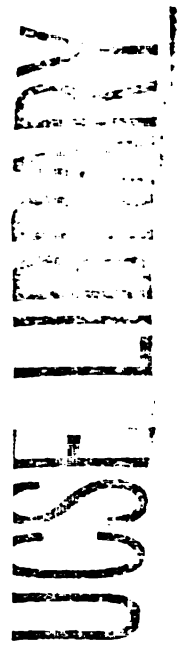

Methods:

Subjects

Nine normal volunteers (seven men, two women, mean age xx) participated in these experiments. These participants gave informed consent separately for the MEG and MRI components of the study. None of the subjects had any known neurological deficit.

Stimuli

Two behavioral paradigms were used. The first was designed to allow the measurement of event related magnetic field (ERF) responses to individual somatosensory and auditory stimuli under conditions in which the subject was selectively attending to either the somatosensory or auditory stimuli while both were being delivered. This task is illustrated schematically in figure 1. Subjects were presented with two observation periods, each of which contained a pair of brief suprathreshold auditory and somatosensory stimuli for each trial of a two alternative forced choice procedure. In a given block of trials, subjects attended to stimuli in one modality, and ignored stimuli in the other. One stimulus pair in each modality always had a stimulus onset asynchrony (SOA) of 300 ms. This pair was called the standard stimulus. The other stimulus pair in each modality had an SOA longer than 300 ms. This pair was called the target stimulus. The target SOA's were longer than the standard SOA by an amount Δt that was always positive. The Δt's used were 8 ms, 16 ms, 32 ms, 64 ms, and 128 ms. Subjects indicated which pair of stimuli within the attended modality was separated by a longer interval. The

observation periods had an SOA of 1000 ms. The observation period containing the target stimulus was randomly chosen at the start of each trial, and was uncorrelated across sensory modalities. The time of onset of the stimulus series was randomly jittered across sensory modalities by 200 ms, ensuring that stimuli from the two sensory modalities rarely coincided. Subjects pressed one of two buttons to indicate their response after all of the stimuli in a trial were presented. Thresholds were calculated as the point at which the psychometric function crossed the 79% correct level. This level was chosen to facilitate comparisons with previous data sets, in which the threshold was estimated using a three down/one up adaptive procedure, in which the task is made more difficult after three consecutive correct trial responses and is made less difficult after a single incorrect trial response. This procedure converged to a difficulty level at which the subject is correct in 79% of the trials.

Each block of stimuli contained two hundred trial repetitions, which included exactly forty repetitions of each of the five Δt values. Four blocks of stimuli were presented. The subject attended one sensory modality in blocks one and three and the other in blocks two and four. Between blocks, subjects performed twenty-five practice trials in the sensory modality to which they would attend in the next block, to ensure that their attention was fully on the new modality.

The second behavioral paradigm was designed to allow the measurement of evoked magnetic field impulse responses to individual auditory stimuli

under conditions in which the subject was either attending to the auditory stimuli, or was not engaged in a behavioral task. Two behavioral conditions were used. In the first, the subjects performed an amplitude discrimination task, illustrated schematically in figure 2. Subjects were presented with two observation periods, each of which contained a single suprathreshold auditory stimulus, for each trial of a two alternative forced choice procedure. One stimulus always had an amplitude of 60 dB and was called the "standard stimulus." The other stimulus had an amplitude larger than 60 dB and was called the "target stimulus." The target amplitudes were larger than the standard amplitude by an amount Δa, which was always positive. The Δa was adaptively changed after each trial, following a 3 down/1 up procedure, with a step size of 0.5 dB. Subjects indicated which stimulus was louder. The observation periods had an SOA of 1000 ms. The observation period containing the target stimulus was randomly chosen at the start of each trial. Subjects pressed one of two buttons to indicate their response after all stimuli in a trial were presented. In the second behavioral condition, subjects were instructed to ignore a series of 60 dB auditory stimuli.

Each block of stimuli contained two hundred trial repetitions. Three blocks of stimuli were presented. The first and third consisted of the unattended condition. The second block consisted of the amplitude discrimination experiment.

Somatosensory stimuli were air-puffs that of approximately 30 ms in duration with a peak pressure of 25 psi, generated by a somatosensory

stimulator (Biomagnetic Technologies, Inc.). Stimuli were delivered to the right index finger through a flexible membrane. Auditory stimuli were 1 kHz pure tone pips, 15ms in total duration with 5ms ramps at each end, generated by an Audiomedia II card in a Macintosh computer. All stimuli were controlled by a Labview (National Instruments) program. Subjects kept their eyes closed and used the left (unstimulated) hand to respond. A single experiment typically lasted from one to two hours.

Data Acquisition

ERF's were recorded in a magnetically shielded room with two 37 channel magnetometers with SQUID-based first-order gradiometer sensors. (Biomagnetic Technologies). Fiduciary points were marked for later co-registration with structural magnetic resonance images and the head shape was digitized to constrain subsequent dipole modeling. In the inter-modal selective attention experiment, one sensor was positioned over the estimated location of somatosensory cortex of the left hemisphere such that a dipolar response was seen to single air-puffs. The other sensor was positioned over the estimated location of auditory cortex of the right hemisphere such that a dipolar response was seen to single tone pips. Data acquisition epochs were 4000 ms in total duration with a 1000 ms pre-stimulus period, referred to the onset of the first somatosensory stimulus.

In the vigilance experiment, one sensor was placed over the estimated position of the left auditory cortex and the other over the estimated position of the right auditory cortex. Test auditory stimuli were used to ensure that a

dipolar response was seen in each sensor. Data acquisition epochs were 2000ms in total duration, with a 1000 ms pre-stimulus period. In both experiments, data were acquired at a sampling rate of 267 Hz and initially filtered from 1-70 Hz with a notch filter at 60 Hz.

For several subjects, high resolution volumetric magnetic resonance images (SPGR sequence, 1128 x 128 x 124 matrix, resolution ~ 1 x 1 x 1.5mm, TR = 36ms, TE = 8ms, flip = 70) were acquired using a 1.5 Tesla SIGNA magnetic resonance scanner (GE Medical Systems, Milwaukee WI).

Data Analysis

Most analyses were performed with Matlab (The Mathworks). ERF's for a given stimulus condition were extracted by aligning single trials to the onset of the stimulus and averaging across trials. For the inter-modal selective attention experiment, eight stimulus conditions were defined by a 2x2x2 matrix consisting of the two attentional conditions, the two sensory modalities, and the two stimuli defining the interval. For example, the attending, somatosensory, first stimulus impulse response was calculated from the two blocks of stimuli in which the subject attended to the somatosensory stimuli, averaging the responses of the first stimulus of each pair across observation periods, Δt's, and trials. The non-attending, auditory, second stimulus response was calculated from the two blocks of stimuli in which the subject attended the somatosensory stimuli, averaging the responses of the second stimuli of each pair across observation periods, Δt's,

and trials. This procedure yielded averages consisting of eight hundred single trials for each attending and non-attending impulse response data set.

For the vigilance experiment, magnetic field impulse responses were calculated for the unattended stimuli by simply averaging the single trials recorded in the condition. Each trial of these blocks contained one stimulus, yielding a total of four hundred presented in the unattended condition. Impulse responses for the attended condition were averaged across trial and across both the standard and target stimuli, ignoring the small differences in amplitude between these stimuli. Each trial of this block contained one of two stimuli, yielding a total of four hundred stimuli presented in the attended condition.

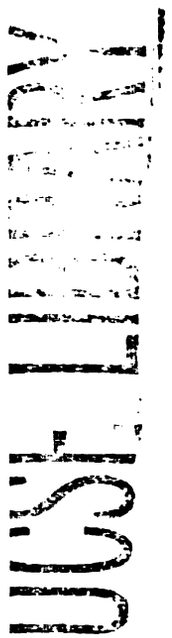

Two types of analyses were performed. In the time domain, the amplitude and latency of the n100 component of the ERF was calculated for each impulse response waveform. To accomplish this, impulse response waveforms were bandpass filtered between 3-20 Hz to smooth them. The waveforms were sign-inverted as necessary to ensure that the n100 was negative going. The amplitudes and latencies of the n100 were calculated from the first negative-going post-stimulus peak of the smoothed waveform with a latency greater than 50 ms.

In the frequency domain, power spectra were estimated in the pre-stimulus and post-stimulus time periods for each impulse response using a multi-taper method with a time-bandwidth factor between 2 and 4. In the pre-stimulus condition, the entire pre-stimulus time period was used to calculate

the power spectrum. In the post-stimulus period, a time period of 0-300 ms post-stimulus was used to avoid contamination by the second stimulus of the interval pairs in the inter-modal selective attention condition. Alpha band power was calculated as the mean of the power spectrum of the unsmoothed waveform between 7 and 13 Hz.

A single equivalent current dipole model was calculated for each post-stimulus time points with standard BTI software operating on data that had been filtered between 1-20 Hz. The localization algorithm (iterative least-squares minimization) inversely computes a single dipole in a spherical volume of uniform conductivity. The fiduciary points marked during the MEG recording served as the basis for a common coordinate system for the MEG and MRI data sets. By superimposing these fiducial landmarks on the MR image of the appropriate subject, one can visualize the position of the computed point sources with reasonable anatomical accuracy.

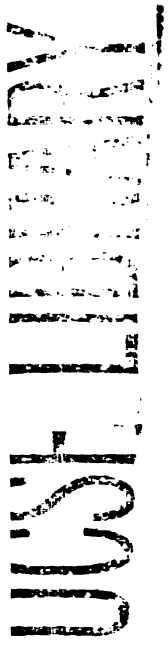

Results:

Psychophysics of selective attention

The first psychophysical task was designed with the goal of delivering brief somatosensory and auditory stimuli under conditions of controlled attentional state. In this task, subjects were presented with two observation periods, each of which contained a pair of brief suprathreshold auditory and somatosensory stimuli, for each trial of a two alternative forced choice procedure. In a given block of trials, subjects attended to stimuli in one modality, and ignored stimuli in the other. Subjects indicated which pair of stimuli within the attended modality was separated by a longer interval. When combined with MEG, this procedure allowed the calculation of the ERF's of the auditory and somatosensory cortices to attended and unattended stimuli. In this task, called the "inter-modal selective attention task," the subject's attention during the unattended case was specifically diverted to another demanding sensory task.

A typical psychometric function measured with this technique is shown in figure 3a. These data were taken from one block of trials in which the subject attended to the somatosensory stimuli and ignored the auditory stimuli. The red line shows the percent of correct interval discriminations the subject made as a function of Δt. The threshold was defined as the point at which this function crossed the 79% correct level, which in this case was 51 ms. The green line shows the percent correct calculated for the same block of trials as if the subject were attending to the auditory system. This psychometric function

was calculated from the subject's responses as if the subject were responding to the unattended stimuli. If stimuli from the unattended modality did not influence the subject's response, this function should be flat and each point should be near 50%, which is chance performance at this task. If stimuli from the unattended modality did influence the subject's response, which might be predicted to occur particularly during trials in which the unattended stimuli had a large Δt and were easy to discriminate, this function should slope upwards to a value higher than 50%. As can be seen in figure 3a, the unattended psychometric function is flat, and each value is near 50%. A second example, from a different subject, is shown in figure 3b. Note that since the intervals presented to the two sensory modalities were chosen independently and randomly, the data points for a given interval are not taken from the same trials. Together, these psychometric functions demonstrate that subjects performed the attended task well and that the responses did not reflect the presence or specific values of the unattended stimuli. This suggests that subjects were selectively attending to one stimulus modality as instructed. In all subjects, the psychometric function for the attended stimuli crossed the 79% correct threshold and the psychometric function for the unattended stimuli was flat and near 50%.

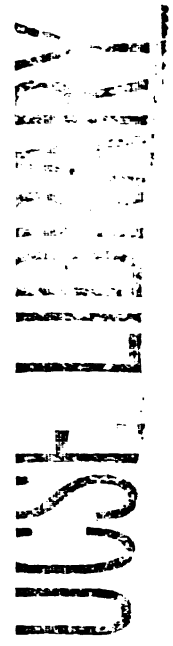

The average somatosensory interval discrimination threshold was 54±19 ms (s.d.), which is a Weber fraction of 0.18 at a base interval of 300 ms. The average auditory interval discrimination threshold was 39±10 ms (s.d.), a Weber fraction of 0.13. These thresholds compare well to those obtained in

previous studies (Wright et al. 1997; Nagarajan et al. 1998). These high performance levels again indicate that the presence of unattended stimuli does not significantly alter performance on the attended task.

Magnetic field impulse responses during selective attention

Example ERF's from the somatosensory and auditory cortices during the attended and unattended conditions are shown in figure 4. The waveforms of the somatosensory ERF's recorded from a single MEG sensor to the first stimulus of the interval pair in the attended and unattended conditions in a representative subject are shown in figure 4a. The blue pulse denotes the time of the stimulus. The red trace indicates the ERF obtained in the attended condition; the green trace indicates the ERF obtained in the unattended condition. In both conditions there was a strong oscillatory response with a frequency of approximately 10 Hz. The waveforms from the two behavioral conditions appear to be very similar. The waveforms of the somatosensory impulse responses from the same MEG sensor to the second stimulus of the interval pair are shown in figure 4b. There is considerably more pre-stimulus activity than in 4a because the evoked response to the first stimulus occurs in the pre-stimulus time period of the second stimulus. An oscillatory response following the stimulus is evident, again with a frequency of approximately 10 Hz. Again, there is no clear difference between the responses to the attended and unattended stimuli.

The waveforms of the auditory impulse responses to the first stimulus of the interval pair in the attended and unattended conditions in a representative

subject are shown in figure 4c. A strong post-stimulus alpha-band oscillation is seen in both conditions. The waveforms of the auditory impulse responses to the second stimulus of the interval pair are shown in figure 4d. In this example, the waveform recorded during the attended condition appears to have a stronger oscillatory response than that recorded during the unattended condition.

To quantify the oscillatory characteristics of the ERF's, power spectra were estimated in the pre-stimulus and post-stimulus time periods for the strongest responding channel of each subject. Alpha-band power was calculated as the mean of the power spectrum in the 7 - 13 Hz band. Each calculated alpha-band power was normalized to the total power in the evoked response, allowing these power measurements to be averaged across subjects without giving undue weight to those subjects from whom the strongest recordings were made. These data are shown in figure 5a for the attended and unattended conditions of the responses to the first and second stimuli of the intervals in the somatosensory modality. The normalized ordinate represents the fraction of total post-stimulus power in the alpha-band for each stimulus condition. The data are grouped into responses to the first stimulus on the left and responses to the second stimulus on the right. For each stimulus type, four bars are shown. The green bars represent the response to the stimulus in the unattended condition, with the pre-stimulus condition on the left (dark green) and the post-stimulus condition on the right (light green). The red bars represent the response to the stimulus in the attended condition, with the

pre-stimulus condition on the left (dark red) and the post-stimulus condition on the right (light red). Alpha-band power is high in the post-stimulus time period in all conditions. Alpha-band power is low in the pre-stimulus time period for the first stimulus, but high in the pre-stimulus condition for the second stimulus, because the pre-stimulus time period for the second stimulus includes the post-stimulus time period for the first stimulus in which there are large oscillations. Corresponding data are shown for the auditory modality in figure 5b.

Analysis of variance (ANOVA) with sensory modality as a between-factors measure and attentional state, stimulus number, and pre/post stimulus time as repeated measures showed significant effects of both pre/post stimulus time ($p < 0.0005$, d.o.f. = 8, $F = 43.375$), stimulus number ($p < 0.005$, d.o.f. = 8, $F = 16.922$), and an interaction between these two factors ($p < 0.005$, d.o.f. = 8, $F = 20.636$) on alpha-band power. This analysis demonstrates two results. First, stimuli evoke alpha-band power. This is particularly clear in the case of the first stimulus in either sensory modality. Second, the amount of stimulus-evoked alpha-band power over background depended on the stimulus number. This is evident in comparing the relative heights of the bars representing pre-stimulus and post-stimulus power in the first stimulus to those in the second stimulus. No significant effects of sensory modality ($p > 0.5$, d.o.f. = 8, $F = 0.427$) or attentional state ($p > 0.3$, d.o.f. = 8, $F = 1.029$) were found.

Many studies of intra-modal selective attention in the auditory system have revealed a negative difference potential that enhances the amplitude of the n100 component of the evoked response to an attended stimulus. To determine if this effect was present in the current study, the amplitude and the latency of the n100 component of each impulse response was calculated and averaged across subjects. The amplitudes of the n100 component of the response to somatosensory stimuli are shown in figure 6a. The responses to the first and second stimulus of the interval pair are shown for each subject. Unattended responses are marked with a star and attended responses are marked with a circle. A line connects the unattended and attended response for each individual subject to make across subject trends more clear. The n100 amplitudes to auditory stimuli are shown in figure 6b. The n100 latencies to somatosensory and auditory stimuli are shown in figures 6c and 6d respectively.

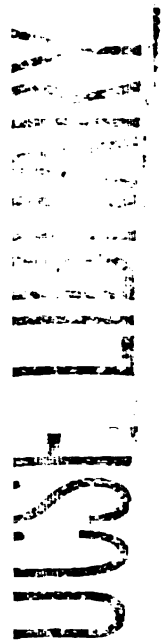

ANOVA with sensory modality as a between factors measure and attentional state and stimulus number as repeated measures shows a significant effect of stimulus number on n100 amplitude ($p < 0.001$, d.o.f. = 8, $F = 25.86$), demonstrating that the second stimulus evokes a smaller n100 than the first. No significant effect of sensory modality ($p > 0.75$, d.o.f = 8, $F = 0.087$) or attentional state ($p > 0.45$, d.o.f = 8, $F = 0.565$) was found. A similar ANOVA on the latency data shows no significant effect of sensory modality ($p > 0.5$, d.o.f. = 8, $F = 0.387$), attentional state ($p > 0.2$, d.o.f. = 8, $F = 1.582$), or stimulus number ($p > 0.75$, d.o.f. = 8, $F = 0.74$) on n100 latency.

Psychophysics and magnetic field impulse responses during vigilance changes

In the second group of experiments, a more general vigilance paradigm was used in the second set of experiments. In this task, two distinct behavioral conditions were used. In the attended condition, the subjects performed an amplitude discrimination task. Subjects were presented with two observation periods, each of which contained a single suprathreshold auditory stimulus, for each trial of a two alternative forced choice procedure. Subjects indicated which stimulus was louder. In the unattended condition, subjects were instructed to ignore a series of auditory stimuli. During the unattended case in this task the subjects' attention was not under specific sensory control. The average amplitude discrimination threshold was 1.47±0.63 dB (s.d.), or a Weber fraction of 0.02 over a standard amplitude of 60 dB. This high level of performance suggests that the subjects attended the stimuli.

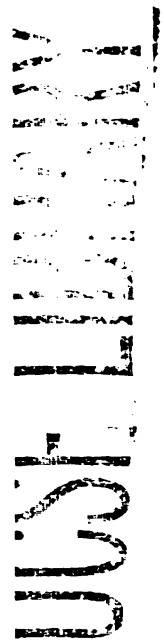

Representative ERF waveforms from one channel from the right hemisphere of one subject in the attended and unattended conditions are shown in figure 7a. The blue pulse denotes the time of the stimulus. The red trace indicates the ERF obtained in the attended condition and the green trace indicates the ERF obtained in the unattended condition. The attended condition exhibits larger n100 and p150 components than the unattended condition. Analysis is restricted to the n100 response component to facilitate comparison with established EEG literature.

Group data regarding the alpha-band power evoked by the stimulus in the attended and unattended conditions is shown in figure 7b. The data are

grouped into responses to the left hemisphere on the left and responses to the right hemisphere on the right. For each hemisphere, four bars are shown. The green bars represent the response to the stimulus in the unattended condition, with the pre-stimulus condition on the left (dark green) and the post-stimulus condition on the right (light green). The red bars represent the response to the stimulus in the attended condition, with the pre-stimulus condition on the left (dark red) and the post-stimulus condition on the right (light red). Error bars are standard errors. ANOVA with hemisphere as a between factors measure and attentional state and pre/post stimulus time as repeated measures shows a significant effect of pre/post stimulus time ($p < 0.0001$, d.o.f. = 10, $F = 2593.814$) on alpha-band power. No significant effects of hemisphere ($p > 0.75$, d.o.f. = 10, $F = 0.98$) or attentional state ($p > 0.25$, d.o.f. = 10, $F = 1.242$) were found.

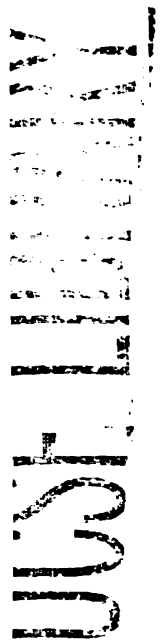

The amplitudes of the n100 component of the response are shown in figure 7c. The responses in the left and right hemispheres are shown for each subject. Unattended responses are marked with a star and attended responses are marked with a circle. A line connects the unattended and attended response for each individual subject to make across subject trends more clear. ANOVA with hemisphere as a between factors measure and attentional state as a repeated measure showed no significant effect of hemisphere ($p > 0.1$, d.o.f. = 10, $F = 3.175$) or attentional state ($p > 0.2$, d.o.f. = 10, $F = 1.499$). However, inspection of the raw data revealed that in the right hemisphere of every subject, the amplitude of n100 was larger in the attended case then in

the unattended case. A paired t-test revealed this effect to be significant ($p < 0.025$). No such effect was seen in the left hemisphere.

The latencies of the n100 component of the response are shown in figure 7d. Similar analysis showed no significant effect of hemisphere ($p > 0.45$, d.o.f. = 10, F = 0.478) or attentional state ($p > 0.1$, d.o.f. = 10, F = 3.165).

Discussion:

There were two goals in this study. The first was to determine whether alpha-band oscillations could be evoked by sensory stimulation under conditions in which subjects were performing demanding psychophysical tasks. Previous reports using EEG recording have claimed that the spontaneous alpha rhythm was found under conditions of quiet wakefulness and that arousal desynchronized the EEG, shifting the power spectrum from low frequency alpha-band power to high frequency gamma-band power (Steriade et al. 1993). The results of the current study demonstrate that evoked alpha-band oscillations accompany sensory stimulation even under conditions of high arousal and focused attention.

The second goal of the study was to determine whether or not and how attention affects measures of the stimulus-evoked magnetic field. Two distinct behavioral paradigms were used to manipulate attentional state. In the first, an inter-modal selective attention task, stimuli were presented in the somatosensory and auditory modalities simultaneously and on a block-by-block basis, with the subject selectively attending one modality and ignoring the other. The subject performed a demanding psychophysical task in both the attended and unattended behavioral conditions for each modality. Thus the difference between the conditions precisely isolated inter-modal selective attention because the stimuli, behavioral task, and general vigilance were exactly the same in the two conditions.

In the second behavioral paradigm, a vigilance task, blocks of trials in which all stimuli were simply ignored were compared to blocks of trials in which a perceptual discrimination was made about the stimuli. Several differences existed between the two conditions that could explain any physiological differences found. These included attention to the stimuli, the engagement of the subject in a particular type of psychophysical task, and the general subject vigilance.

The first response measure analyzed was the alpha-band oscillation that a brief sensory stimulus is known to produce. This measure is the major focus of this study. Although the stimuli evoked strong alpha-band oscillations, no differences were found in the magnitude of the post-stimulus alpha-band power between the attended and unattended conditions for either of the two behavioral tasks.

The second response measure analyzed was the n100 component of the ERF, a negative going peak in the response waveform that occurs approximately 100 ms after a stimulus is delivered. This measure was studied to facilitate a comparison between the current results and the evoked response literature, in which the n100 has been analyzed extensively. All stimuli evoked a measurable n100 in all behavioral conditions, and an enhancement in the amplitude of the n100 response in the right hemisphere was found during the attended condition of the vigilance task. No differences were found in the left hemisphere during the vigilance task and during the

inter-modal selective attention task. No differences were found in the latency of the n100 in any behavioral condition.

Previous predictions about alpha-band oscillation

Several previous investigations have indirectly suggested that alpha-band oscillations would be evoked under conditions of behavioral arousal and that they could be changed as a result of attentional state. In particular, studies of intra-modal selective attention in the visual system, in which a subject attended to a stimulus in one hemifield while ignoring a stimulus in the contralateral hemifield, have shown that the basic evoked response potential (ERP) shows an alternating sequence of peaks and troughs with approximately a 100 ms period (Johannes et al. 1995). These components have been suggested to reflect the activation of distinct visual areas (Mangun et al. 1993). However, they could also be considered in frequency space, where they could be interpreted as an alpha-band oscillation. Selective attention increased the amplitude of several of these components (Johannes, et al. 1995), suggesting that evoked alpha-band power would have increased in the attended condition.

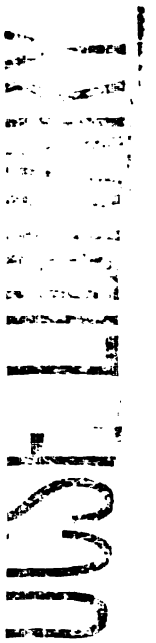

Studies conducted using brain slice recording techniques have demonstrated that alpha-band oscillations can be recorded in the thalamus and cortex, both in the local field potentials and intracellularly in certain cell types. These oscillations occur spontaneously and in response to intracellularly injected current. In the thalamus, oscillations in this frequency range are called spindles, and are the result of a interplay between the

excitatory cells of the thalamic relay nuclei and the inhibitory cells of the associated thalamic reticular nuclei (Bal et al. 1995; Bal et al. 1995). In the cortex, oscillations in this frequency range are evoked by sensory stimuli as in-place oscillations of the local field potential, and multi- and single unit activity. Responses to subsequent stimuli that occur during the troughs of the oscillation are suppressed (Schoner et al. 1992; Sameshima and Merzenich 1993). The oscillations are generated by a endogenous properties of a network of layer V pyramidal cells (Silva et al. 1991) called bursting cells that project to subcortical targets such as the superior colliculus (Hallman et al. 1988). In both of these examples, the application of neuromodulators that are thought to be involved in arousal, such as noradrenaline, serotonin, and acetylcholine (Wang and McCormick 1993; Lee and McCormick 1996), cause neurons to depolarize. This in turn causes the networks to cease generating spontaneous oscillations and alters the response properties of the cells involved such that intracellularly injected current generates a flatter, more sustained response instead of an oscillation. This slice data has been suggested to be the cellular correlate of the EEG changes that accompany the shift from the sleeping to the waking state in the case of thalamic spindles or the shift from a relaxed state to an attentive state in the case of cortical alpha rhythm (Steriade, et al. 1993). In opposition to the ERP intra-modal selective attention experiment discussed above, these studies have suggested that alpha-band oscillations would not be evoked under conditions in which an alert subject attended a demanding psychophysical task.

The data from the current study shows that alpha-band oscillations are evoked by stimuli under conditions of behavioral arousal and selective attention. These oscillations are unaffected by inter-modal selective attention and vigilance. This is consistent with the basic result of visual intra-modal selective attention experiments, in which an evoked oscillation is seen, but suggests that the task demands of the intra-modal and inter-modal selective attention experiments are different enough that attentional enhancement of the ERF is seen in the former but not the latter. Together, these behavioral studies suggest that slice studies showing that the application of neuromodulators causes a shift away from low frequency oscillations do not fully reflect the operation of these systems in the awake, behaving human.

Previous predictions about n100 amplitude

In 1973, using a dichotic listening task in which a subject attended to stimuli delivered to one ear and ignored stimuli delivered to the other ear Hillyard et. al. (Hillyard et al. 1973) demonstrated that attended stimuli evoked a larger n100 component than did unattended stimuli. Many studies have now extended this result to show that the enhancement of n100 is the result of a negative difference (Nd) potential beginning at the time of the n100 and extending for several hundred milliseconds thereafter, depending on the nature of the experimental design. This negativity has been hypothesized to reflect a shift of computational resources towards an attended stimulus. Recently, an Nd effect has been demonstrated in the auditory system using MEG (Woldorff et al. 1993). These data suggested that the Nd effect was a

direct effect on early cortical responses, and confirmed that it was a cortical source that could be recorded with either EEG or MEG techniques. Nd-like potentials have also been recorded in intra-modal selective attention studies within the visual and somatosensory modalities, suggesting that the Nd reflects a generalized mode of cortical processing.

In the current study, an Nd effect was found in the amplitude of the n100 response in the right hemisphere during the vigilance experiment. The lack of evidence for an effect of attention on the n100 in the left hemisphere could be due to the fact that the amplitude of the left hemisphere responses was weaker, making small differences more difficult to detect. The lack of an n100 effect in the inter-modal selective attention experiment was a surprise. This may reflect basic differences in the attentional demands of intra- and inter-modal selective attention tasks.

Previous work on intra-modal selective attention

Although many studies have looked at intra-modal selective attention, few have examined inter-modal selective attention. A recent ERP study by Woods et. al. (Woods et al. 1992) used a methodology that was similar to our own. Subjects were presented with both auditory and visual stimuli simultaneously, switching on a block-by-block basis between auditory frequency discrimination and a visual length discrimination. Auditory and visual ERP's showed an enhancement of both the n100 and p200 components when attention was directed to the appropriate sensory modality. These data

were interpreted as suggesting that modality-specific attentional modulations occur even in inter-modal selective attention tasks.

The most likely explanation of the discrepancy between this result and the current study is that EEG and MEG recordings are sensitive to different cortical current sources, as discussed by Kaufman et. al (Kaufman et al. 1981) and Mahncke (Mahncke 1998). It is possible that the current sources that gave rise to the attentionally sensitive component of the evoked response in the EEG study of Woods et. al. were not the same as the current sources recorded in the current MEG study. In particular, a careful study by Mangun et. al. (Mangun, et al. 1993) concluded that the attentionally sensitive n100 and p40 components of the visual ERP were due to current sources in extrastriate and not primary visual cortex. An attentionally insensitive early component of the response was found to have a source in primary visual cortex. These data suggested that visual responses in primary visual cortex were not sensitive to the attentional state of the subject. The attentionally sensitive visual ERP peaks recorded with EEG by Woods et. al. are likely to have extrastriate sources as well, in which case they are not comparable to the ERF waveforms recorded in the current study with MEG, which are likely to be the result of the repetitive reactivation of a local cortical region in primary sensory cortex (Mahncke 1998).

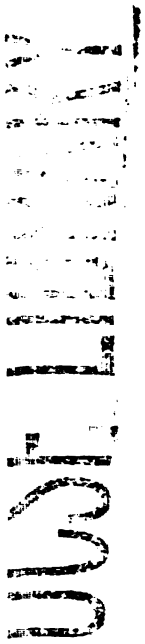

The lack of effect of selective attention in the inter-modal selective attention experiment on the n100 response component contrasts strongly with the effects of selective attention on that response component

demonstrated using MEG recording in intra-modal selective attention tasks (Woldorff, et al. 1993). The stimuli and recording techniques used in both experiments are similar, allowing these data sets to be meaningfully compared. The differences in the results between the two experiments suggest that attentional systems may act to selectively enhance attended stimuli and/or suppress unattended stimuli when they are presented in the same sensory modality, but that those attentional systems do not alter the processing of stimuli when they are presented in different sensory modalities. This situation can be interpreted as the cortex making a dynamic assessment and adjustment of its computational resources depending upon the nature of the task. In the intra-modal case, where stimuli could interfere with one another at relatively early stages of processing, attention differentiates the response to relevant and irrelevant stimuli at that early processing stage, allowing downstream stages of sensory processing within that sensory modality to allocate limited resources more effectively to the relevant stimuli. In the inter-modal case, the stimuli can not interfere with each other in the early, monomodal sensory areas, so there is no need the differentiate the responses in those regions with attention. In this case, the early stages of stimulus processing appears to be identical, suggesting that the stage at which unattended stimuli are discarded from sensory processing is later in the intra-modal case than in the inter-modal case.

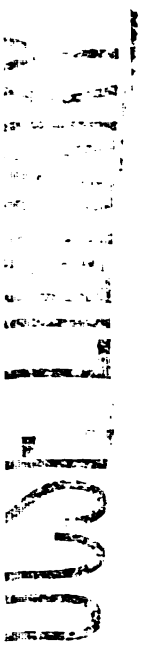

The relationship between attention and evoked oscillations

The main result of the current study is that strong alpha-band oscillations are evoked by sensory stimulation even when the subject is performing a demanding psychophysical task. Previous reports regarding the spontaneous alpha rhythm have usually stated that it is found under conditions of quiet, relaxed wakefulness, and that arousal desynchronizes the EEG, which is manifested by a shift from low frequency power to high frequency, gamma-band power (Steriade, et al. 1993; Steriade, et al. 1996). The fact that strong evoked alpha-band power is seen under psychophysically demanding behavioral conditions demonstrates that this traditional view of rhythmogenesis in the brain is incomplete. This presents an interesting conundrum, first noted by Bartley and Bishop in 1933: how a stable perceptual state is maintained in the face of an ongoing slow rhythm? (Bartley and Bishop 1933). If a stimulus evokes an alpha-band oscillation and that oscillation affects the response to subsequent stimuli, as has been shown in previous work, then perceptual events after an oscillation-evoking stimulus should themselves follow an alpha-band oscillation. For example, in a signal detection paradigm, one might predict that it would be easier to detect weak stimuli that occurred on the peak of the evoked alpha-rhythm following a strong stimulus and more difficult to detect weak stimuli in the troughs of that oscillation. Therefore, forward masking functions could look oscillatory, with peaks in detectability at 100, 200, and 300ms intervals. Future psychophysical experiments designed to test this and similar hypotheses will

reveal whether these oscillations are manifested in perceptual performance or if the cortex has specific mechanisms for maintaining temporal stability in an oscillatory environment.

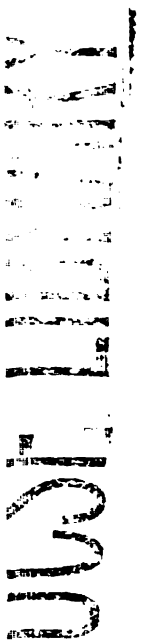

Figure 1: Schematic diagram of the inter-modal attention experiment. Auditory and somatosensory stimuli are both presented during a single trial. Subjects attend to and discriminate the intervals defined by the stimuli of one sensory modality while ignoring stimuli in the other sensory modality. A: Example trial in which the subject attends somatosensory and ignores auditory. B: Example trial in which the subject attends auditory and ignores somatosensory.

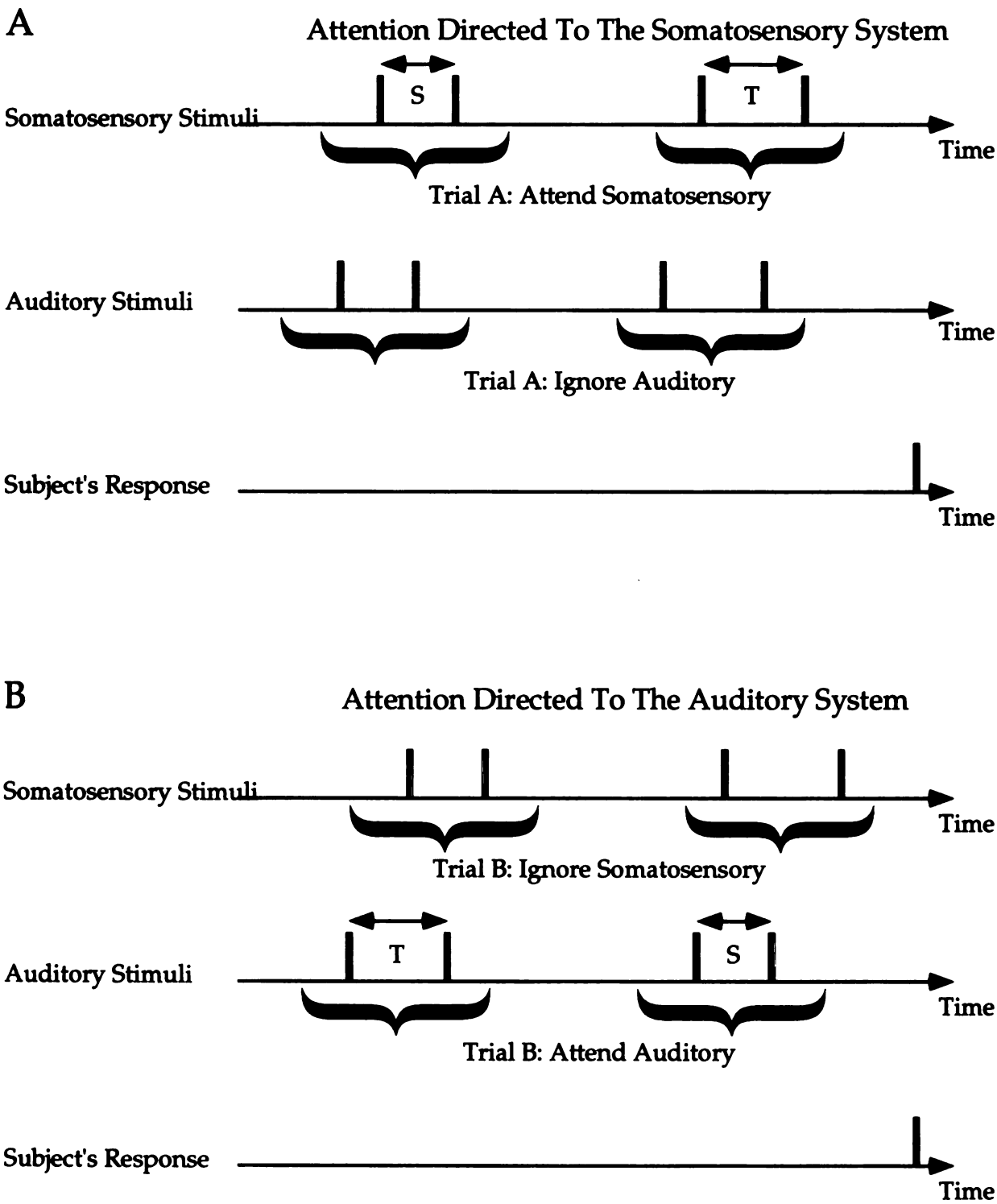
A
Attention Directed To The Somatosensory System
Somatosensory Stimuli
S
T
Time
Trial A: Attend Somatosensory
Auditory Stimuli
Time
Trial A: Ignore Auditory
Subject's Response
Time
B
Attention Directed To The Auditory System
Somatosensory Stimuli
Time
Trial B: Ignore Somatosensory
Auditory Stimuli
T
S
Time
Trial B: Attend Auditory
Subject's Response
Time

Figure 2: Schematic diagram of the vigilance experiment. Only auditory stimuli are used. A: Example trial in which the subject ignores all stimuli and makes no responses. B: Example trial in which the subject attends the stimuli and discriminates their amplitude.

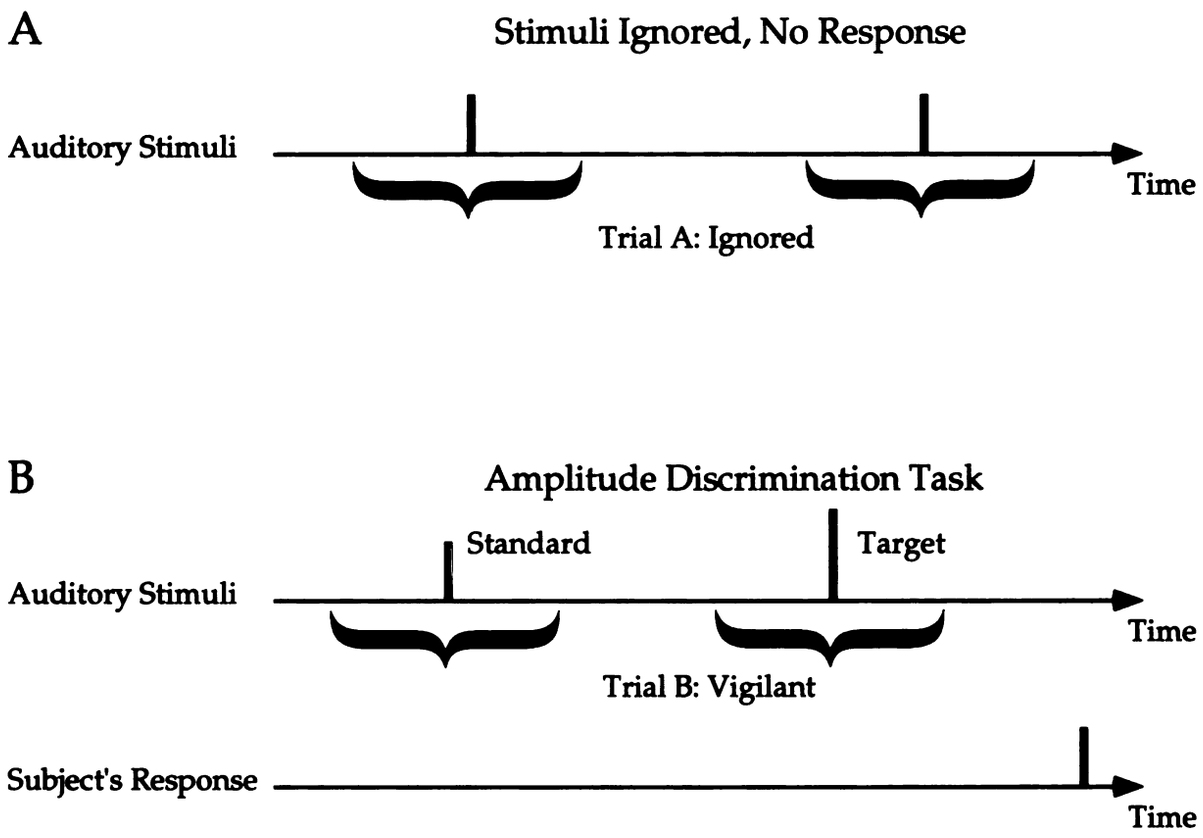
A
Stimuli Ignored, No Response
Auditory Stimuli
Time
Trial A: Ignored
B
Amplitude Discrimination Task
Standard
Target
Auditory Stimuli
Time
Trial B: Vigilant
Subject's Response
Time

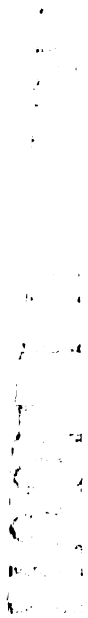

Figure 3: Example psychophysical performance for one trial block in one subject. The red line indicates the psychometric function for the attended somatosensory stimuli. The green line indicates the psychometric function for the unattended auditory stimuli.

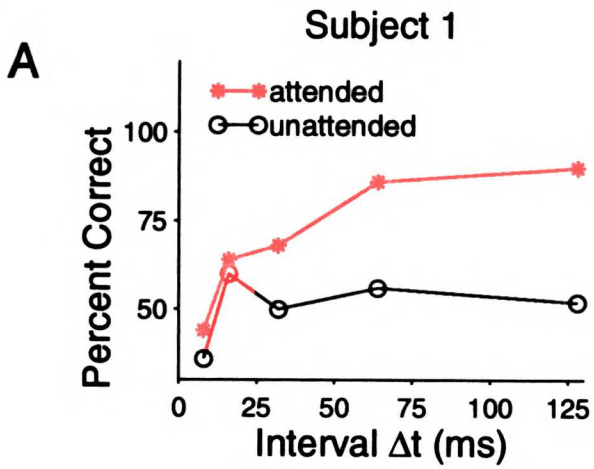
A
Subject 1
attended
unattended
Percent Correct
100
75
50
0
25
50
75
100
125
Interval Δt (ms)

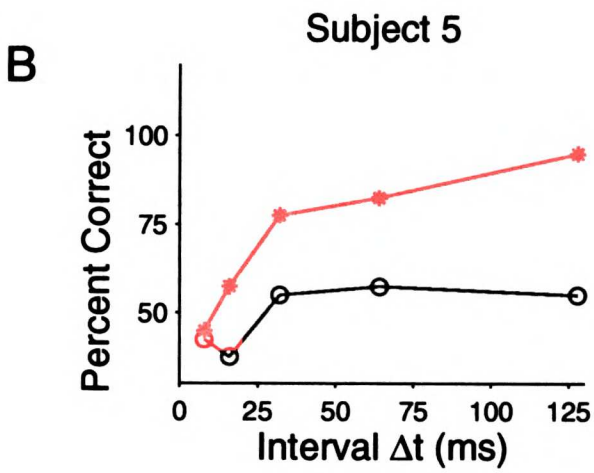
B
Subject 5
Percent Correct
100
75
50
0
25
50
75
100
125
Interval Δt (ms)

Figure 4: Example attended and unattended impulse responses from the inter-modal attention experiment. A: Waveform of somatosensory impulse response to the first stimulus of the pair for a single channel in one subject. Red, impulse response in attended condition. Green, impulse response in unattended condition. Blue, time of stimulus. B: Waveform of somatosensory impulse response to the second stimulus of the pair for a single channel in the same subject as A. C: Waveform of auditory impulse response to the first stimulus of the pair for a single channel in a different subject. D :Waveform of auditory impulse response to the second stimulus of the pair for a single channel in a the same subject as C.

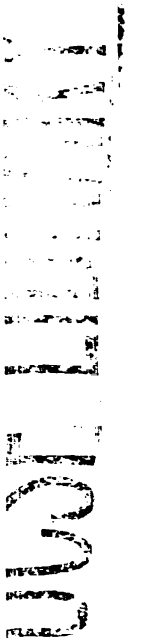

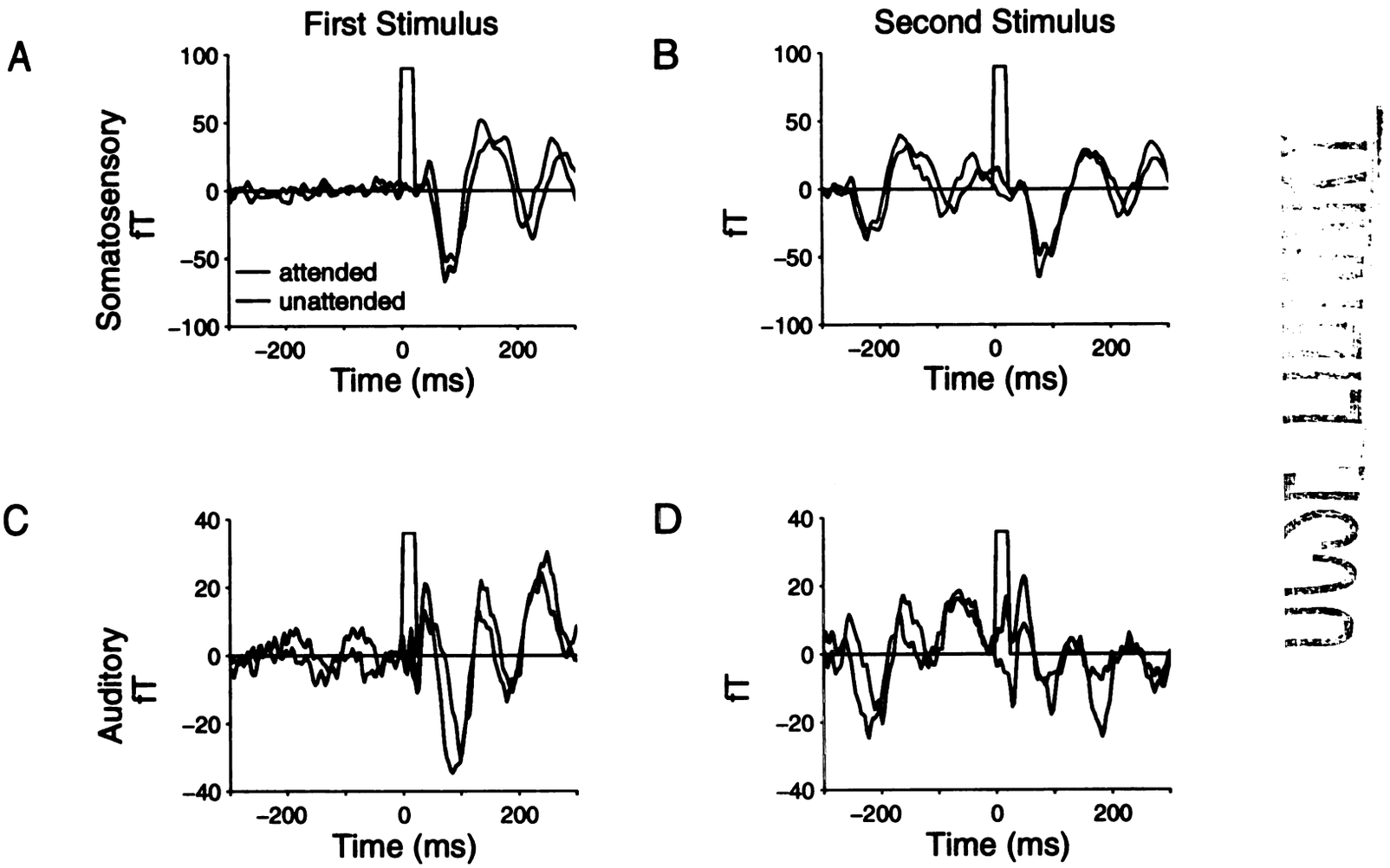
A
First Stimulus
Somatosensory
fT
100
50
0
−50
−100
attended
unattended
−200
0
200
Time (ms)
B
Second Stimulus
fT
100
50
0
−50
−100
−200
0
200
Time (ms)
C
Auditory
fT
40
20
0
−20
−40
−200
0
200
Time (ms)
D
fT
40
20
0
−20
−40
−200
0
200
Time (ms)

Figure 5: Summary of evoked alpha-band power in the inter-modal attention experiment. A: Data for the somatosensory system. The normalized ordinate represents the fraction of total post-stimulus power in the alpha-band for each stimulus condition. The data are grouped into responses to the first stimulus on the left and responses to second stimulus on the right. For each stimulus type, four bars are shown. The green bars represent the response to the stimulus in the unattended condition, with the pre-stimulus condition on the left (dark green) and the post-stimulus condition on the right (light green). The red bars represent the response to the stimulus in the attended condition, with the pre-stimulus condition on the left (dark red) and the post-stimulus condition on the right (light red). Error bars are standard errors. B: Data for the auditory system, same conventions as A. ANOVA shows that alpha-band power is significantly increased in the post-stimulus period in all conditions, but that there are no significant differences between the attended and unattended state in any condition (see text for details).

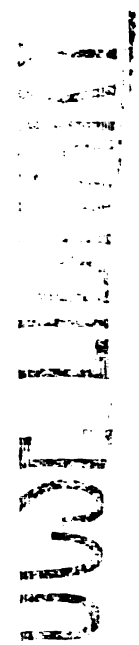

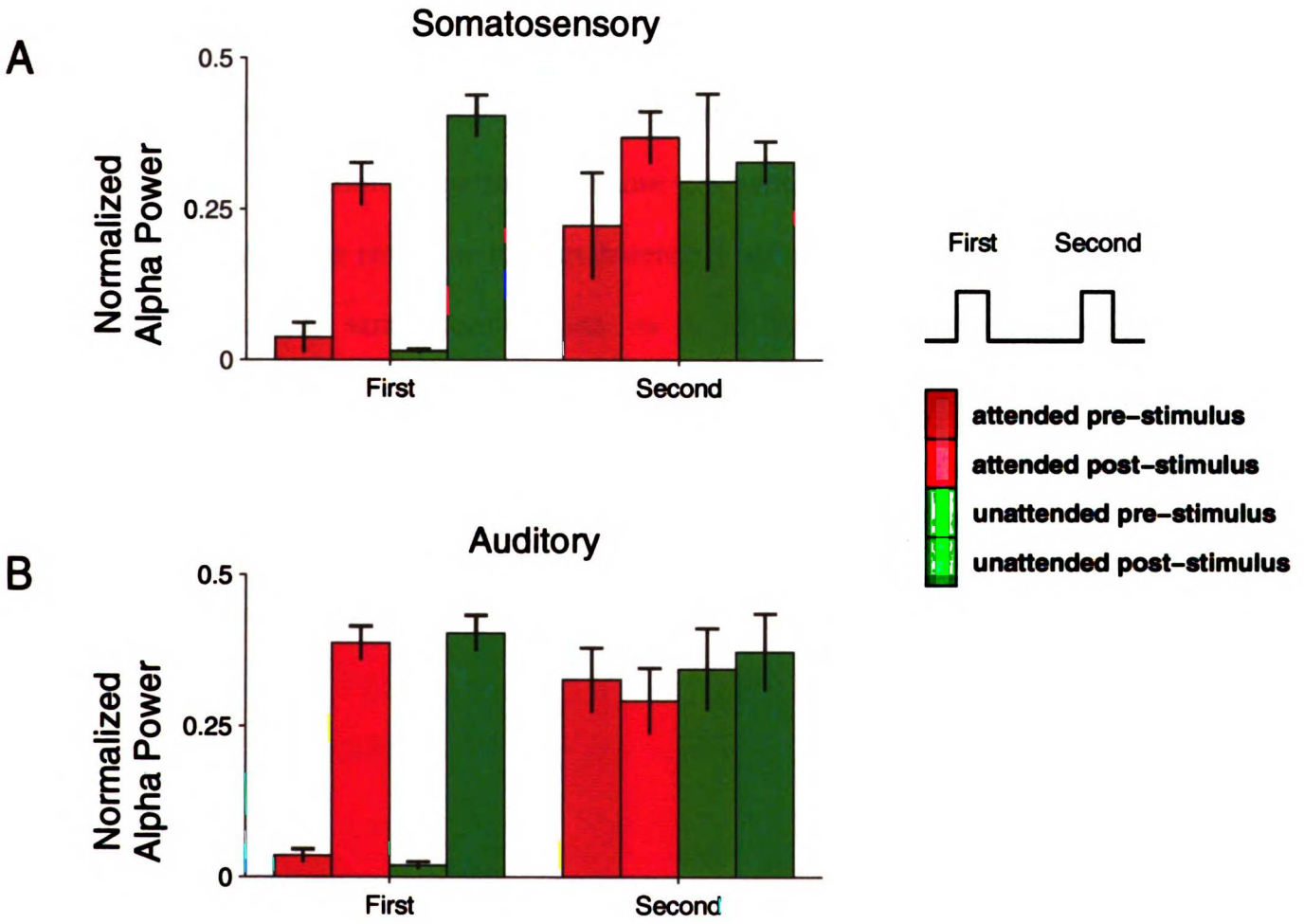

Figure 6: A: Summary of the amplitude of the response to somatosensory stimuli in the inter-modal attention experiment. The responses to the first and second stimulus of the interval pair are shown for each subject. Unattended responses are marked with a star and attended responses are marked with a circle. A line connects the unattended and attended response for each individual subject to make across subject trends more clear. ANOVA shows no significant amplitude differences across subjects (see text for details). B: Summary of the amplitude of the response to auditory stimuli in the inter-modal attention experiment, same conventions as A. C: Summary of the latency of the response to somatosensory stimuli in the inter-modal attention experiment, same conventions as A. D: Summary of the latency of the response to auditory stimuli in the inter-modal attention experiment, same conventions as A. ANOVA shows no significant latency difference across subjects (see text for details).

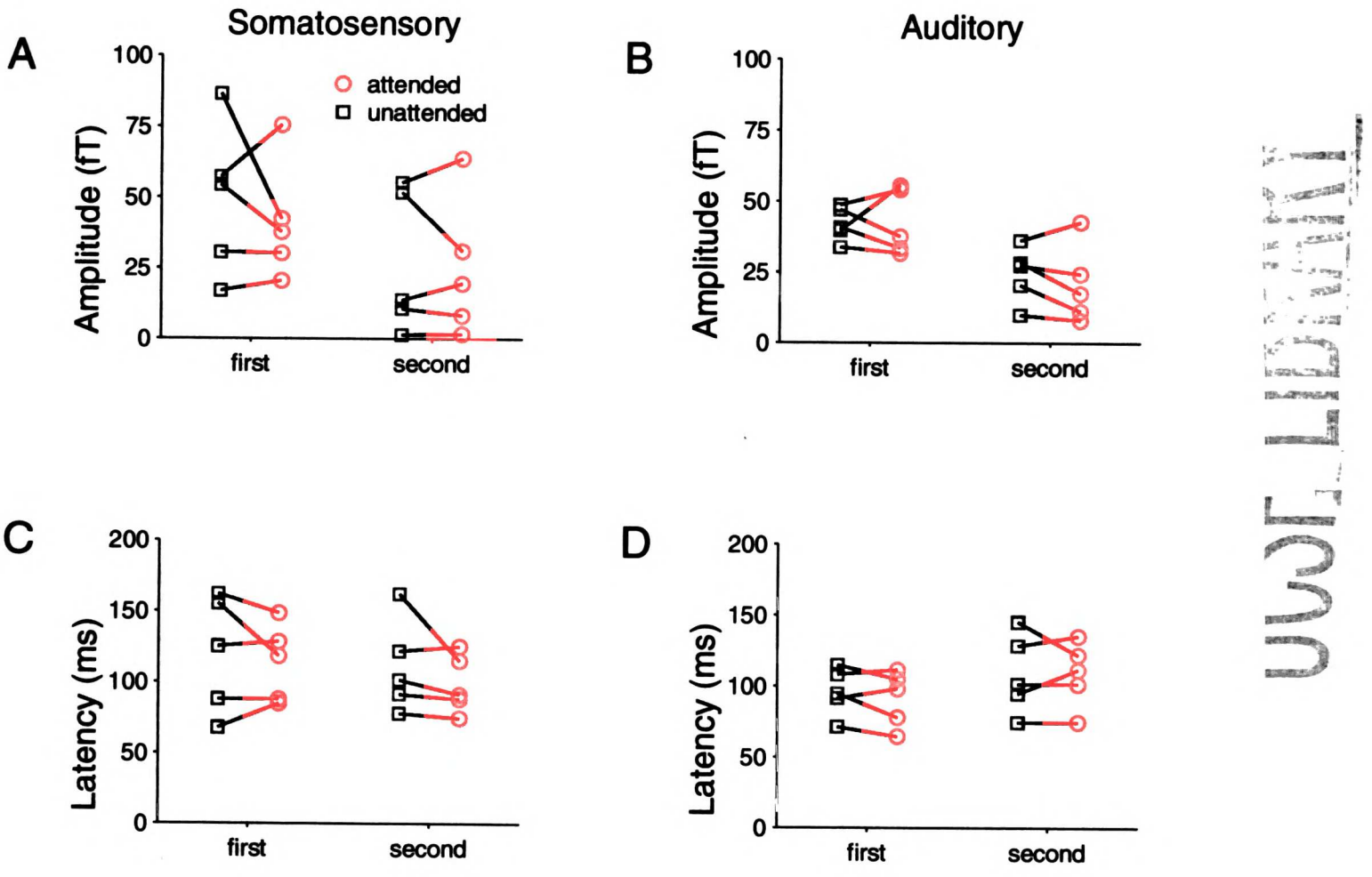

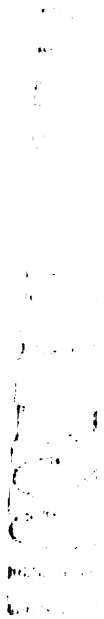

Figure 7: A : Example attended and unattended impulse responses from the vigilance experiment. A: Waveform of auditory impulse response in one subject. Same conventions as figure 4. B : Summary of evoked alpha-band power in the vigilance experiment. The data are grouped into responses to the left hemisphere on the left and responses to the right hemisphere on the right. For each hemisphere, four bars are shown. The green bars represent the response to the stimulus in the unattended condition, with the pre-stimulus condition on the left (dark green) and the post-stimulus condition on the right (light green). The red bars represent the response to the stimulus in the attended condition, with the pre-stimulus condition on the left (dark red) and the post-stimulus condition on the right (light red). Error bars are standard errors. ANOVA shows that alpha-band power is significantly increased in the post-stimulus period in all conditions, but that there are no significant differences between the attended and unattended state in any condition (see text for details). C :Summary of the amplitude of the response in the vigilance experiment. The responses in the left and right hemispheres are shown for each subject. Unattended responses are marked with a star and attended responses are marked with a circle. A line connects the unattended and attended response for each individual subject to make across subject trends more clear. ANOVA shows no significant differences across subjects; however, a paired t-test shows a significant effect of attention in the right hemisphere only (see text for details). D : Summary of the latency of the

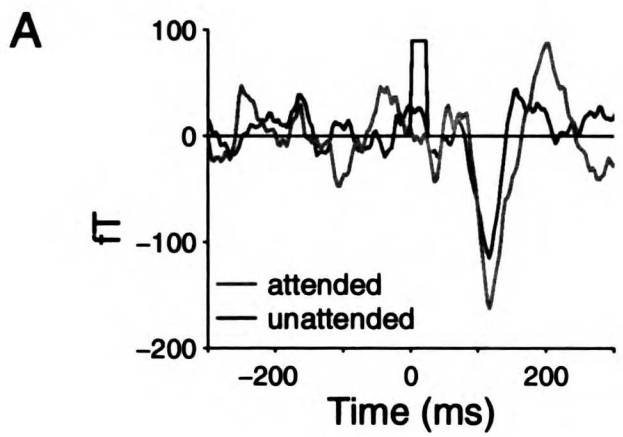
A
100
0
−100
−200
fT
attended
unattended
−200
0
200
Time (ms)

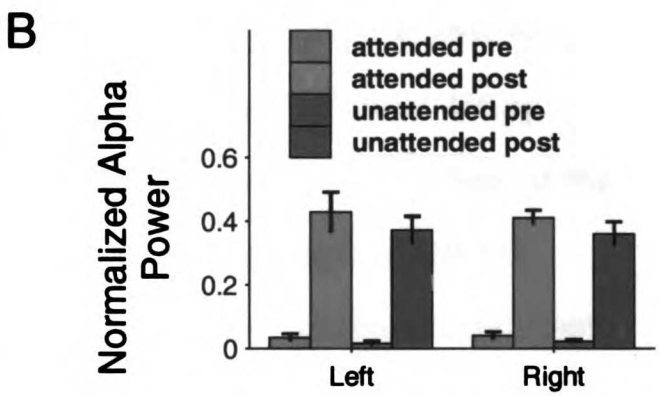
B
attended pre
attended post
unattended pre
unattended post
Normalized Alpha Power
0.6
0.4
0.2
0
Left
Right

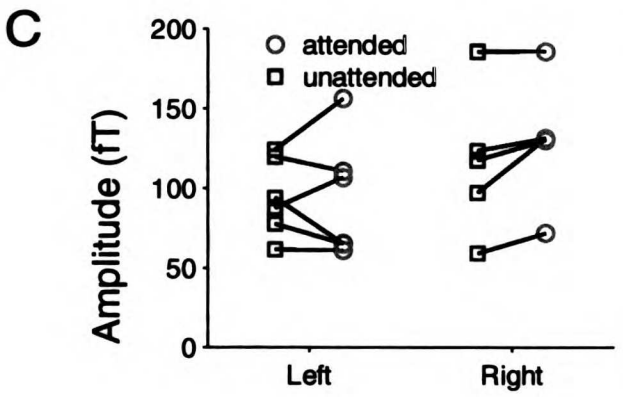
C
attended
unattended
Amplitude (fT)
200
150
100
50
0
Left
Right

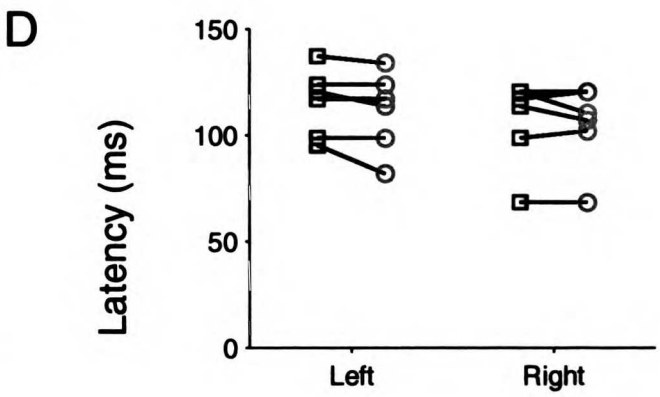
D
Latency (ms)
150
100
50
0
Left
Right

References:

Bal T, von Krosigk M, and McCormick DA (1995) Role of the ferret perigeniculate nucleus in the generation of synchronized oscillations in vitro. Journal of Physiology (London) 483:665-685.

Bal T, von Krosigk M, and McCormick DA (1995) Synaptic and membrane mechanisms underlying synchronized oscillations in the ferret lateral geniculate nucleus in vitro. Journal of Physiology (London) 483:641-663.

Barlow JS (1993) The Electroencephalogram. Cambridge:MIT Press. 456 pp.

Bartley SH and Bishop GH (1933) The cortical response to stimulation of the optic nerve in the rabbit. American Journal of Physiology 103:159-172.

Guido W, Lu SM, Vaughan JW, Godwin DW, and Sherman SM (1995) Receiver operating characteristic (ROC) analysis of neurons in the cat's lateral geniculate nucleus during tonic and burst response mode. Visual Neuroscience 12:723-741.

Hallman LE, Schofield BR, and Lin CS (1988) Dendritic morphology and axon collaterals of corticotectal, corticopontine, and callosal neurons in layer V of primary visual cortex of the hooded rat. Journal of Comparative Neurology 272:149-160.

Hillyard SA, Hink RF, Schwent VL, and Picton TW (1973) Electrical signs of selective attention in the human brain. Science 182:177-180.

Johannes S, Munte TF, Heinze HJ, and Mangun GR (1995) Luminance and spatial attention effects on early visual processing. Cognitive Brain Research 2:189-205.

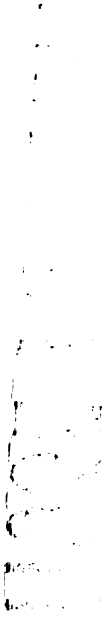

Kaufman L, Okada Y, Brenner D, and Williamson SJ (1981) On the relation between somatic evoked potentials and fields. International Journal of Neuroscience 15:223-239.

Lee KH and McCormick DA (1996) Abolition of spindle oscillations by serotonin and norepinephrine in the ferret lateral geniculate and perigeniculate nuclei in vitro. Neuron 17:309-321.

Mahncke HW (1998) Oscillations and temporal processing and sensory cortex. Thesis:University of California, San Francisco.

Mangun GR, Hillyard SA, and Luck SJ (1993) Electrocortical substrates of visual selective attention. Cambridge:MIT Press. 219-243 pp.

Murthy VN and Fetz EE (1996) Oscillatory activity in sensorimotor cortex of awake monkeys: synchronization of local field potentials and relation to behavior. Journal of Neurophysiology 76:3949-3967.

Nagarajan SS, Blake DT, Wright BA, Byl N, and Merzenich MM (1998) Practice-related improvements in somatosensory interval discrimination are temporally specific but generalize across skin location, hemisphere, and modality. Journal of Neuroscience 18:1559-1570.

Nunez PL (1995) Neocortical Dynamics and Human EEG Rhythms. New York:Oxford Press. 708 pp.

Regan D (1989) Human Brain Electrophysiology. New York:Elsevier Science. 672 pp.

Rougeul A, Bouyer JJ, Dedet L, and Debray O (1979) Fast somato-parietal rhythms during combined focal attention and immobility in baboon and

squirrel monkey. Electroencephalography and Clinical Neurophysiology 46:310-319.

Salmelin R and Hari R (1994) Characterization of spontaneous MEG rhythms in healthy adults. Electroencephalography and Clinical Neurophysiology 91:237-248.

Sameshima K and Merzenich MM (1993) Intrinsic oscillator contributions to response properties of SI cortical neurons. Society for Neuroscience Abstract.

Schoner G, Kopecz K, Spengler F, and Dinse HR (1992) Evoked oscillatory cortical responses are dynamically coupled to peripheral stimuli. Neuroreport 3:579-582.

Silva LR, Amitai Y, and Connors BW (1991) Intrinsic oscillations of neocortex generated by layer 5 pyramidal neurons. Science 251:432-435.

Steriade M, Contreras D, Amzica F, and Timofeev I (1996) Synchronization of fast (30-40 Hz) spontaneous oscillations in intrathalamic and thalamocortical networks. Journal of Neuroscience 16:2788-2808.

Steriade M and Llinas RR (1988) The functional states of the thalamus and the associated neuronal interplay. Physiology Reviews 68:649-742.

Steriade M and McCarlet RW (1990) Brainstem Control of Wakefullness and Sleep. New York:Plenum Press. 497 pp.

Steriade M, McCormick DA, and Sejnowski TJ (1993) Thalamocortical oscillations in the sleeping and aroused brain. Science 262:679-685.

Wang Z and McCormick DA (1993) Control of firing mode of corticotectal and corticopontine layer V burst-generating neurons by norepinephrine, acetylcholine, and 1S,3R- ACPD. Journal of Neuroscience 13:2199-2216.

Woldorff MG, Gallen CC, Hampson SA, Hillyard SA, Pantev C, Sobel D, and Bloom FE (1993) Modulation of early sensory processing in human auditory cortex during auditory selective attention. Proceedings of the National Academy of Science (USA) 90:8722-8726.

Woods DL, Alho K, and Algazi A (1992) Intermodal selective attention. I. Effects on event-related potentials to lateralized auditory and visual stimuli. Electroencephalography and Clinical Neurophysiology 82:341-355.

Wright BA, Buonomano DV, Mahncke HW, and Merzenich MM (1997) Learning and generalization of auditory temporal-interval discrimination in humans. Journal of Neuroscience 17:3956-3963.

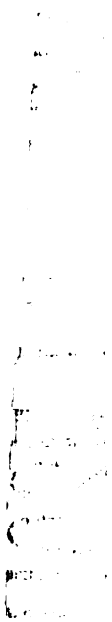

LAMINAR ANALYSIS OF SENSORY EVOKED ALPHA-BAND CORTICAL OSCILLATIONS

Chapter 4

Abstract:

Many studies have demonstrated that brief visual, somatosensory, or auditory stimuli can evoke low frequency oscillations in the alpha band (7-13 Hz) in sensory cortices in anesthetized animals and awake humans. These oscillations may play a role in processing temporal information in the range of hundreds of milliseconds. However, the anatomical source of these evoked oscillations is unclear, making it difficult to constrain hypotheses about their functional role. The primary purpose of this study was to define the laminar distribution of these oscillatory phenomena in the primary auditory cortex.

Evoked local field potentials and multi-unit spike activity were recorded at 100 μ intervals from the pia through the white matter in perpendicularly-oriented penetrations through the primary auditory cortex of pentobarbital anesthetized female rats with a carbon fiber electrode. Evoked electrical activity was filtered from 1-100 Hz to isolate field potentials and from 300-10000 Hz to isolate multi-unit spike activity. Responses to fifty presentations of a 250 μs positive going click were recorded at each depth.

The evoked response was divided into two parts: an onset response consisting of the total power in the first 50 ms post-stimulus, and an evoked alpha band response consisting of the power in the 7–13 Hz frequency range from 50-400 ms post-stimulus. The evoked alpha band power in the field potential and in the multi-unit spike response was relatively low and constant in the upper layers, reached a peak in layer 5, then decreased through layer 6 and the white matter. There was a dissociation between the strength of

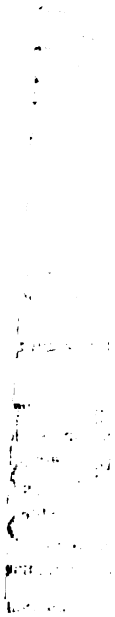

the onset response and the strength of the alpha-band oscillations in both the field potential signal and the multi-unit spikes, indicating that the ability of layer five to generate strong alpha-band oscillations was not a simple consequence of elevated responsivity in that layer. Current source density analysis was consistent with a role for layer 5 cells with extended apical dendrites in the generation of alpha-band oscillations. Single trial analysis indicated that although low-frequency (1-5 Hz) activity was prevalent in the pre-stimulus and post-stimulus periods, alpha-band activity was specifically enhanced and phase reset by sensory stimulation. These results are consistent with both the known bursting properties of layer 5 cells *in vitro*, and with previous studies of the spontaneous alpha rhythm. These data indicate that the evoked alpha band responses seen previously in anesthetized animals and awake humans originate predominately in layer 5.

Introduction:

In 1929, Berger discovered the alpha rhythm, a spontaneous oscillation with a frequency between 7-13 Hz found in the electroencephalogram of awake humans (Adrian and Matthews 1934). These oscillations were found to be generated by the visual cortex and were only present when the visual system was unstimulated, either when the subject closed their eyes or when they were in a dark room (Adrian and Yamagiwa 1935). As a result, it was concluded that the alpha rhythm was the extra-cranial manifestation of spontaneous neural activity in the visual system. Psychophysical correlates of this spontaneous rhythm were established by presenting visual stimuli at defined phases of the ongoing rhythm. These studies have shown effects of the phase of the alpha rhythm on visual temporal framing (Varela et al. 1981; Gho and Varela 1988), reaction time, and stimulus detectability. Similar spontaneous rhythms have now been found over the somatomotor cortex and auditory cortex (Tiihonen et al. 1991), suggesting that this intrinsic spontaneous rhythmicity is a general property of sensorimotor cortex.

Recently, sensory evoked oscillations with frequencies in the alpha-band have been found in both anesthetized animals (Schoner et al. 1992; Sameshima and Merzenich 1993) and in awake humans (Mahncke 1998). These studies have shown that brief sensory stimuli in the visual, auditory, and somatosensory modalities evoke an alpha-band oscillation in neural activity in the appropriate sensory cortex. This oscillation persists for several hundred milliseconds and affects the responsivity of the cortex to subsequent

stimuli, causing a depression of the onset response when a subsequent stimulus occurs in the trough of the evoked oscillation.

To gain a better understanding of the function of these sensory evoked oscillations, it would be useful to know the neural mechanisms by which they are generated. Spontaneous and evoked alpha-band oscillations that are dependent upon the integrity of cortical layer 5 have been recorded in vitro using cortical slices (Silva et al. 1991; Flint and Connors 1996). However, the relevance of these oscillations to those seen in vivo is unclear because they were only visible under conditions that favored enhanced activity of the NMDA receptor. A laminar study of the spontaneous alpha rhythm in the awake dog has been conducted that concluded that layer 5 cells were the cortical source of this rhythm (Lopes da Silva and Storm van Leeuwen 1977; Lopes da Silva and Storm van Leeuwen 1978); however, the relationship between the spontaneous rhythm and the sensory evoked relationship is unknown.

There were two main goals of these experiments. The first was to determine the laminar distribution of sensory-evoked alpha-band oscillations. The second was to determine whether a sensory stimulus initiates a new alpha-band oscillation or phase-resets an ongoing oscillation.

Methods:

Animal preparation

Experiments were conducted in eight female Sprague-Dawley albino rats (280-330 g). Surgical anesthesia was induced by an intraperitoneal injection of 0.35 ml sodium pentobarbital (CONC). A tracheotomy was performed to ease breathing, and the jugular vein was cannulated to allow administration of fluids. A state of areflexia was maintained through the remainder of the experiment with a continuous infusion of sodium pentobarbital in normal saline (1:17) administered intravenously. A heating pad was used to maintain body temperature at 38° Celsius. Reflexes were monitored to control the depth of anesthesia. The rat was placed in a custom designed head holder that stabilized the head while allowing access to the pinnae. Following a midline incision, a craniotomy was performed to expose the upper part of the left cortical hemisphere. The dura was removed and the exposed brain was covered in mineral oil.

Neurophysiological recording

Recordings were made with single carbon fiber (10 μ tip diameter, 1-3 MΩ) microelectrodes. Electrodes were inserted into the brain perpendicular to the surface and recordings were at 100 μ intervals from the pia until responses were no longer evident, at a depth of 1600-2000 μ. Electrical activity was split into two channels, the first for recording evoked field data and the second for recording multi-unit spike data. Evoked field data was amplified, band-pass filtered (1 Hz - 100 Hz), sampled at 300 Hz, and saved to disk. Multi-unit data

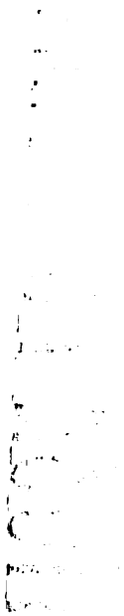

was amplified and band-pass filtered (300 Hz - 10 kHz). Spikes were detected by a threshold crossing and spike waveforms were then digitized at 30 kHz and saved to disk for off-line analysis. Data acquisition was controlled by a PC (Datawave Systems).

Primary auditory cortex was identified before performing the quantitative experiments described above by recording multi-unit activity from a depth of 500-600 μ, which corresponds to the layer 4 of rat auditory cortex. Recording from at least seven sites delineated primary auditory cortex as a region of cortex with sites that had short (8-16 ms) latencies to tonal stimuli, well defined tuning curves, and an appropriately oriented topographic organization of characteristic frequencies (CFs).

Stimulus generation and control

Recording was performed in a double walled sound attenuated chamber. All stimuli were generated under PC control by a D/A board (Spectrum Scientific). Sound was generated with 16 bit resolution at a 96 kHz sampling rate. Pure tone stimuli for receptive field mapping were 50 ms in duration, including a 5 ms ramp at each end. Click stimuli were 250 μs positive going square pulses. The sound level was calibrated (Bruel and Kjaer sound level meter) such that a 250 pps click train had a sustained amplitude of 70 dB SPL. Click trains exhibited broad-band frequency spectra. Stimuli were presented monaurally through a sound tube directed into the contralateral ear.

Experimental protocol

At each recording depth, fifty single clicks were presented with an inter-stimulus interval of 3000±500 ms. Data collection at each depth took approximately three minutes, and an entire penetration took approximately 1 hour. As a result of the short length of time spent recording from a single penetration and the use of an infusion anesthesia protocol, little change in the responsivity in a given penetration was seen. This was verified in a subset of the penetrations by recording multi-unit tuning curves in layer 4 during the sequence of laminar recordings and a second time at that depth after the deepest recording had been completed.

Data Analysis

Most analyses were performed with Matlab (The Mathworks). Evoked potential and spike data from single trials were aligned to stimulus onsets to create average event-related potentials (ERP's) and post-stimulus time histograms (PSTH's).

Current source density (CSD) analysis was performed on the ERP data. The CSD at any point along a perpendicular penetration through the cortex is equal to the second spatial derivative of the field potential (Mitzdorf 1985). This quantity was estimated from the field data by spatially filtering the ERP data from each penetration with a 8 bin (800 μ) Hamming window, then taking the 1 bin (100 μ) difference along the spatial difference twice. CSD analysis depends on the knowledge of the response patterns from adjacent depths in a recording penetration. The responses evident in the ERP's can be

compared because they represent average activity at the depth across many trials. Since recordings were made sequentially through the cortex, CSD estimates for single trials could not be made because the activity recorded at one depth for one trial is not related in a meaningful way to activity recorded at the next depth for one trial. Thus all single trial analyses are confined to field potential recordings.

Power spectra of ERP's, CSD's, and PSTH's were estimated using a multi-taper method with time-bandwidth factor between 2 and 4. Bandwidths were calculated as the width of the power spectrum 3 dB down from the amplitude of the peak. Alpha-band power was calculated from the power spectra by averaging the power in the 7-13 Hz range. The entire pre-stimulus period was used to estimate the alpha-band power in the pre-stimulus condition. The period from 50-500 ms post-stimulus period was used to estimate the alpha-band power in the post-stimulus condition to exclude the initial high-frequency onset response transient. The strength of this onset response was quantified by taking the mean of the root mean square of the response waveform in the 0-50 ms post-stimulus period, which is equivalent to measuring the total power in this period. A comparable estimate of background power was made by taking the mean value of the root-mean-square of the entire pre-stimulus period.

For some analyses, it was necessary to calculate the interval between various peaks in the pre-stimulus and post-stimulus periods of the single trial ERPs. The raw data from a given single trial was smoothed using a band-

pass filter between 3-20 Hz. The time of each peak of the smoothed waveform was calculated. The mean pre-stimulus period was calculated by averaging the intervals between all pre-stimulus peaks. The time of the peak immediately before the stimulus was noted, as was the time of the rebound response following the stimulus. The smoothing procedure allowed these peaks to be detected easily and accurately using an automated algorithm based on differentiating the waveform because low amplitude noisy peaks were eliminated. However, the short latency onset response was also eliminated. Since the latency of this peak was very reliable across trials and recording sites and depths, the exact time of its occurrence was determined by finding the largest peak in the raw waveform in a 5-25 ms post-stimulus window. The times of these peaks were used to calculate two relevant intervals: the "intrinsic period," which was the interval between the immediate pre-stimulus peak and the post-stimulus rebound peak, and the "evoked period," which was the interval between the onset peak and the post-stimulus rebound peak. The relations between the mean pre-stimulus period, the intrinsic period, and the evoked period express the degree to which the stimulus interacts and resets the ongoing oscillatory activity.

Results:

Evoked oscillations in averaged responses

The intra-cortically evoked field response to a single click stimulus recorded from primary auditory cortex is shown in figure 1a. The stimulus is shown in the blue trace, and data recorded from a representative penetration at depths of 300 μ and 800 μ are shown in the red and green traces respectively. Each data trace is the average of 50 single trials. At each depth, a strong, short-latency onset response is seen that reverses polarity between the two recording depths. The 300 μ recording shows a subsequent rebound response followed by baseline activity. The 800 μ recording shows a long-lasting oscillatory response with a frequency in the alpha band.

The intra-cortically evoked field recordings from all depths of a single penetration are shown in figure 1b. Depths are represented on the ordinate and the color represents the strength and polarity of the evoked field, with blue representing negative potentials and red representing positive potentials. Strong oscillations can be seen in the lower cortical layers, particularly in layer 5. Somewhat weaker oscillations are seen in the upper cortical layers.

The depth profile of the pre-stimulus and post-stimulus alpha-band powers of the field potential signal averaged across 43 penetrations are shown in figure 2a. The red graph shows the depth profile for the post-stimulus condition. At each depth of each penetration, the power spectrum of the field response was calculated across a 50-500 ms post-stimulus window. This

window was chosen to exclude the initial onset transient which, due to its brief timecourse, contributes only high frequency power.. The alpha-band power was calculated by averaging this power spectrum across the 7-13 Hz range, yielding a depth profile for each penetration. Each profile was normalized to its peak value and all post-stimulus profiles were averaged together.

The green graph shows the depth profile for the pre-stimulus condition. At each depth of each penetration, the power spectrum of the field response was calculated across the entire 1 second pre-stimulus time period. The pre-stimulus alpha-band power was calculated by averaging this power spectrum across the 7-13 Hz range, yielding a depth profile for each penetration. Each profile was normalized to the peak value of the post-stimulus profile for that penetration, and all pre-stimulus profiles were averaged together.

Post-stimulus alpha-band power is elevated relative to pre-stimulus alpha-band power at all depths, but shows a peak at a depth of 800 μ in layer 5. Analysis of variance (ANOVA) with depth as a repeated measure shows that the depth distribution of post-stimulus alpha-band power is not uniform ($p < 0.0001$, d.o.f. = 15, $F = 21.808$). A similar ANOVA shows that the depth distribution of mean pre-stimulus power is also not uniform ($p < 0.002$, d.o.f. = 15, $F = 2.846$). However, the variations in the pre-stimulus profile are quite small compared to the post-stimulus profile.

The elevation of post-stimulus alpha-band power in layer 5 could occur for two reasons. The first is that layer 5 neurons could generate stronger

alpha-band oscillations than other layers. The second is that layer 5 neurons could generate stronger field potentials, due to the cell packing or cell size in that layer. To determine which of these possibilities was the case, the short-latency onset response power was calculated at each depth. If the peak in post-stimulus alpha-band power seen in layer 5 was due to an increased overall responsiveness in that layer, then the depth profiles of the alpha-band and onset power response should have the same shape. Finding a difference between these depth profiles would indicate that the peak in alpha-band power found in layer 5 was not simply due to stronger overall responsivity in that layer.

To obtain the onset response power profile, at each depth of each penetration the power spectrum of the field response was calculated across a 0-50 ms post-stimulus window, chosen to include the initial onset transient. The post-stimulus onset response power was calculated by summing this power spectrum, yielding a depth profile for each penetration. Each profile was normalized to its peak value and all post-stimulus profiles were averaged to produce the red graph shown in figure 2b. As a control, the depth profile of the mean pre-stimulus power is shown in green. At each depth of each penetration, the mean value of the power spectrum of the field response across the entire pre-stimulus time period was calculated, yielding a depth profile for each penetration. Each profile was normalized to the peak value of the post-stimulus onset response profile for that penetration and all pre-

stimulus profiles were averaged to produce the green graph shown in figure 2b.

Onset responses are large in the upper layers, decrease to a minimum in layer 4, and reach another peak in layer 5 before decreasing in layer 6. ANOVA with depth as a repeated measure shows that the depth distribution of post-stimulus onset response power is not uniform ($p < 0.0001$, d.o.f. = 15, $F = 21.808$). A similar ANOVA shows that the depth distribution of mean pre-stimulus power is not uniform ($p < 0.002$, d.o.f. = 15, $F = 2.846$); however, it is relatively flat compared to the onset response profile. The depth profiles of the post-stimulus alpha-band power and the onset power are significantly different as shown by a Kolmogorov-Smirnov test ($p < 0.001$, d.o.f. = 15, $Dmax = 0.494$).

These data indicate that although alpha-band power is evoked by sensory stimuli in all layers, layer 5 generates the strongest alpha-band oscillations. This layer-specific enhancement is not due to generally stronger responses in this layer, because the upper layers are capable of generating a very strong onset response even though they do not generate strong alpha-band power. Thus there is a dissociation between the ability of a cortical layer to generate an onset response and an alpha-band oscillation and that layer 5 neurons are uniquely specialized to convert a large onset response into a large alpha-band oscillation.

A limitation of the study of intra-cortically evoked field potentials is that an electric field is detectable at a distance from the current source that actually

generates it (Mitzdorf 1985). Using the evoked field potentials and making a specific set of assumptions regarding current flow in the cortical tissue, it is possible to calculate the locations of the current sources that give rise to those field potentials. Current source density (CSD) data from the example site shown in figure 1 is shown in figure 3. The current response to a single click stimulus is shown in figure 3a. The stimulus is shown in the blue trace, and calculated currents at depths of 300 μ and 800 μ are shown in the red and green traces respectively. The ordinate is in arbitrary current units due to the nature of the current source density calculation. At both depths a strong onset response is seen followed by rhythmic oscillations in the alpha-band range. Both the onset response and the oscillatory response are opposite polarities at the two depths.

The current sources and sinks from a single penetration are shown in figure 3b. Depths are represented on the ordinate and the color represents the strength and direction of the current, with blue representing current sinks and red representing current sources. Strong oscillations can be seen in both the upper and lower cortical layers, particularly in layer 5.

The depth profile of the pre-stimulus and post-stimulus alpha-band powers of the current source signal averaged across 43 penetrations are shown in figure 4a. These profiles were generated in an identical fashion to the field potential profiles, except using the current source waveforms as data. The post-stimulus alpha-band power in the current signal (red) shows peaks at a depths of 200 μ, in layer 2/3 and at 800 μ in layer 5. ANOVA with depth as a

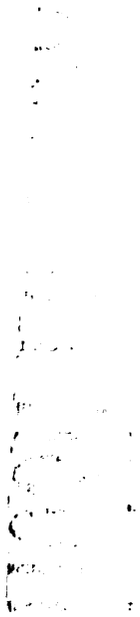

repeated measure shows that the depth distribution of post-stimulus alpha-band power is not uniform ($p < 0.0001$, d.o.f. = 13, $F = 13.475$). The pre-stimulus alpha-band power in the current signal (green) shows a small peak at a depth of 200 μ in layer 2/3. ANOVA with depth as a repeated measure shows that the depth distribution of pre-stimulus alpha-band power is not uniform ($p < 0.0001$, d.o.f. = 13, $F = 21.702$).

These data suggest that sensory stimulation induces alpha-band oscillations in current sources and sinks that are strongest in layers 2/3 and 5. Since total current flow into a neuron must sum to zero (Mitzdorf 1985), the opposed currents in layer 2/3 and layer 5 are likely to reflect current flow into and out of neurons with processes in both layers. A neuronal population with these characteristics is the pyramidal cells of layer 5, which have cell bodies in layer 5 and dendrites extending into the upper layers.

The depth profile of the onset response and mean pre-stimulus powers of the current source signal averaged across 43 penetrations are shown in figure 4b. These profiles were generated in an identical fashion to the field potential profiles, except using the current source waveforms as data. The post-stimulus onset response power in the current signal (red) shows peaks at a depths of 200 μ, in layer 2/3 and at 800 μ in layer 5. ANOVA with depth as a repeated measure shows that the depth distribution of post-stimulus alpha-band power is not uniform ($p < 0.0001$, d.o.f. = 13 $F = 40.643$).

The profiles for the alpha-band power and the onset response are not significantly different as shown by a Kolmogorov-Smirnov test ($p > 0.05$,

d.o.f. = 13, Dmax = 0.355), suggesting that the strength of the evoked oscillation is related to the strength of the initial response.

The mean pre-stimulus power in the current signal (green) shows a small peak at a depth of 200 μ in layer 2/3. ANOVA with depth as a repeated measure shows that the depth distribution of the mean pre-stimulus power is not uniform ($p < 0.0001$, d.o.f. = 13, $F = 31.114$). The upper layer peak in both alpha-band power and mean pre-stimulus power suggests high levels of spontaneous current flow in these layers.

Multi-unit spike data from a representative site is shown in figure 5. The multi-unit response to a single click stimulus recorded at a depth of 500 μ, in layer 4, is shown in figure 5a. A strong onset is seen followed by a return to baseline activity. The multi-unit response to a single click stimulus recorded at a depth of 800 μ, in layer 5, is shown in figure 5b. A strong onset is seen followed by a rhythmic oscillation in the alpha-band range.

The PSTH's from a single penetration are shown in figure 5c. Depths are represented on the ordinate and the color represents the strength of the response, with blue no response and red representing a large response. Oscillations are evident in layer 5. In general across all sites, and shown particularly at this site, there was very little spiking activity in the upper cortical layers. The depth at which the first spikes were found varied across penetrations from 200 μ to 500 μ.

The average depth profiles of the pre-stimulus and post-stimulus alpha-band powers of the multi-unit signal are shown in figure 6b. The exact

number of sites averaged at each depth varies because the depth at which multi-unit activity was first detected varied from penetration to penetration and depths with no activity were not included in the average. These profiles were generated in an identical fashion to the field potential profiles, except using the multi-unit data. The post-stimulus alpha-band power (red) shows a peak at a depth of 800 μ in layer 5. ANOVA with depth as a repeated measure shows that the depth distribution of the post-stimulus alpha-band power is not uniform ($p < 0.0001$, d.o.f. = 13, $F = 16.06$). The depth distribution of the pre-stimulus alpha band power (green) appears quite flat, although a similar ANOVA shows a significant effect of depth ($p < 0.0001$, d.o.f. = 13, $F = 4.691$).

The average depth profiles of the onset response and mean pre-stimulus powers of the multi-unit signal are shown in figure 6b. These profiles were generated in an identical fashion to the field potential profiles, except using the multi-unit data. The post-stimulus onset response power (red) very broad distribution with no clear peak, indicating . ANOVA with depth as a repeated measure shows that the depth distribution of the onset response power is not uniform ($p < 0.0001$, d.o.f. = 13, $F = 20.28$). The pre-stimulus power (green), equivalent to the background firing rate, is essentially flat, although ANOVA shows a significant factor of depth ($p < 0.0001$, d.o.f. = 13, $F = 9.494$). These data demonstrate that sensory stimulation causes rhythmic firing of neurons that is strongest in layer 5.

The depth profiles of the post-stimulus alpha-band power and the onset power are significantly different as shown by a Kolmogorov-Smirnov test

($p < 0.001$, d.o.f. = 14, Dmax = 0.559). This dissociation between the onset response and the oscillatory response indicates that layer 5 are uniquely capable of generating strong alpha-band oscillations.

The peak frequencies and 3 dB bandwidths of the average power spectra associated with each measured response type at each layer are summarized in table 1. Generally, across all layers, peak frequencies are within the alpha range, although exceptions exist. Specifically in layer 5, peak frequencies of all measures are within the alpha range.

Table 1:

Layer	Field Potential	CSD	Multi-Unit
1	8.8±4.7	8.8±4.8	no spikes
2/3	6.6±3.6	8.8±5.2	no spikes
4	8.8±3.8	8.8±4.1	6.5±3.4
5	8.8±4.7	8.8±4.9	10.8±2.7
6	8.8±5.1	4.4±4.1	10.8±4.5

Evoked oscillations in single trial responses

The post-stimulus oscillations seen in the evoked field data could arise from two different mechanisms. One possibility is that the cortex is quiescent until a sensory stimulus occurs, at which point it generates an alpha-band oscillation. If this were the case, each single trial would look like the average response. A second possibility is that the cortex is continually engaged in oscillatory activity that is reset by sensory stimulation. If this were the case,

the pre-stimulus activity and the post-stimulus activity in each single trial would be very similar. The effect of sensory stimulation would be to shift the phase of the ongoing oscillation. When these single trials are averaged, the pre-stimulus oscillations would average to zero because they are not phase-aligned, whereas the post-stimulus oscillations, having been reset to the same phase by the stimulus, would appear in the average.

To illustrate this point, the average response at a 800 μ depth recording site, shown in figure 7a, was compared to a single trial response from that same recording site and depth, shown in figure 7b. The average response shows very low pre-stimulus activity followed by a sharp onset response and a long-lasting alpha-band oscillation. The single trial shows very high pre-stimulus activity that is comparable to the high level of post-stimulus activity. The sharp onset response is still visible immediately following the stimulus.

The power spectra of these representative traces is shown in figure 8. The pre-stimulus (green) and post-stimulus (red) power spectra of the average response is shown in figure 8a. The pre-stimulus power spectrum is flat and low amplitude and the post-stimulus power spectrum is much larger with a peak in the alpha-band range. The alpha-band power of this average response is quantified in figure 8b, in which it is seen that there is very little alpha-band power in the pre-stimulus condition relative to the post-stimulus condition. The pre-stimulus (green) and post-stimulus (red) power spectra of a single trial response is shown in figure 8c. The pre-stimulus power

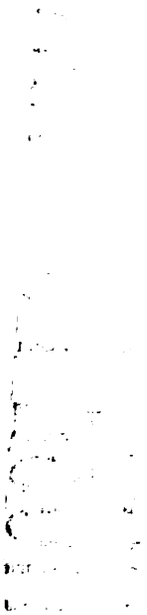

spectrum is now seen to have a broad peak in the alpha band range. The post-stimulus power spectrum has a peak in the alpha-band range and a secondary low frequency peak. The alpha-band power of this single trial response is quantified in figure 8d, in which it is seen that there is more alpha-band power in the pre-stimulus condition relative to the post-stimulus condition than in the case of the average data.

The relationship between the single trial pre-stimulus, single trial post-stimulus, and trial-averaged post-stimulus power spectra in single trials is quantified in figure 9. Pre-stimulus (green) and post-stimulus (red) power spectra are shown sorted by cortical layer and averaged across approximately 1500 single trials. The scale on the left ordinate refers to these spectra. In all layers, sensory stimulation causes a small increase in the frequency peak of the power spectrum, but the overall impression is of similarity between the pre-stimulus and post-stimulus power spectra. Peak frequencies and 3 dB bandwidths were calculated from the data and are shown in table 2. The peak frequencies for both time periods are substantially lower than the alpha-band range. Although the peaks for the post-stimulus period appear to be slightly higher than those for the pre-stimulus period, this could be a sampling error due to the low density of spectral points in these very low regions of the power spectrum.

Post-stimulus (blue) power spectra are shown sorted by cortical layer and averaged across the trial-averaged field potential responses from 43 penetrations. The scale on the right ordinate refers to these spectra. Unlike

the spectra from the single trial waveforms, the peaks in the trial-averaged power spectra lie inside the alpha range in all layers except layer 2/3 (table 2). The difference power spectra between the single trial post-stimulus and single-trial pre-stimulus power spectra were also calculated (data not shown). The peaks of the difference spectra include the alpha range in layers 2/3 and 4 and are centered in the alpha range in layer 1,5, and 6 (bandwidths could not be calculated for layers 1 and 6 because the peak was less than 3 dB above 0).

Table 2: Power Spectra Peaks

Layer	Single Trial Pre-Stimulus	Single Trial Post-Stimulus	Trial-Averaged Post-Stimulus	Single Trial Difference
1	3.15±3.26	4.41±3.67	8.82±4.75	8.5
2/3	3.15±3.01	4.41±3.64	6.61±3.61	5.00±8.82
4	3.15±3.31	4.41±3.51	8.82±3.87	5.00±8.30
5	3.15±3.32	4.41±4.23	8.82±4.76	9.00±4.21
6	3.15±2.52	4.41±3.00	8.82±5.13	9

The relationship between the pre-stimulus and post-stimulus alpha-band power in single trials is quantified in figure 10. The distribution of the log ratio of the post-stimulus alpha-band power to the pre-stimulus alpha-band power, sorted by cortical layer, is shown in histogram form. A ratio of 0 on this log scale represents the condition in which the pre-stimulus and post-stimulus conditions have equal alpha-band power. Negative numbers represent cases in which the pre-stimulus alpha-band power exceeds the post-

stimulus alpha-band power; and positive numbers represent cases in which the post-stimulus alpha-band power exceeds the pre-stimulus alpha-band power. The alpha-band power ratio is significantly greater than zero in all layers ($p < 0.0005$ for all layers except layer 1, $p < 0.02$ for layer 1). ANOVA shows a significant effect of layer on alpha-band power ($p < 0.0001$, d.o.f. = 4. $F = 21.86$). This effect is still significant following the removal of layer 5 data ($p < 0.0001$, d.o.f = 3, $F = 10.01$), but removing both the layer 5 and 6 data shows that the differences between layer 1, 2/3, and 4 are not significant ($p > 0.25$, d.o.f. = 2, $F = 1.32$). These data demonstrate that layer 5 generates the largest increase in alpha-band power as a result of stimulation, confirming the impression seen in figure 9. The alpha-band power increase following stimulation is quantified in table 3.

Table 3:

Layer	Alpha Band Power Increase
1	7%
2/3	13%
4	15%
5	50%
6	34%

Data in the previous three figures suggests that ongoing oscillations are prevalent in the pre-stimulus condition. Since post-stimulus oscillations are evident in the averaged data, the stimulus must phase-align the post-

stimulus oscillations. This issue was examined quantitatively in layer 5 recordings by comparing three intervals: the mean period in the pre-stimulus activity, the interval between the immediate pre-stimulus peak and the first post-stimulus oscillatory response peak, and the interval between the short-latency onset response and the first post-stimulus oscillatory response peak. These intervals are shown for a representative single trial in figure 11a. The raw data is shown in the dark green trace and a low-pass filtered version of the raw data is shown in the light green trace. The filtered data was used to calculate the mean pre-stimulus period and the times of the immediate pre-stimulus peak (left-most red start) and the first post-stimulus oscillatory response peak (right-most red start). The central star marks the time of the short-latency onset response, calculated from the raw data.

At one extreme, the sensory stimulation could have no effect on the ongoing oscillation. This hypothesis predicts that the interval between the pre-stimulus peak and the post-stimulus oscillatory response peak, called the "intrinsic period," would be the same as the mean pre-stimulus period. At the other extreme, the sensory stimulus could completely reset the ongoing oscillation. This hypothesis predicts that the interval between the onset response to the stimulus and the post-stimulus oscillatory response peak, called the "evoked period," would be the same as the mean pre-stimulus period.

These hypotheses are examined in figure 11b, in which the relationship between the mean pre-stimulus period and both the evoked period and the

intrinsic period is shown. The mean pre-stimulus period for each single trial is plotted against the evoked period (red) and the intrinsic period (green) for that trials. The mean pre-stimulus period is 91±12 ms (s.d.), the evoked period is 87±36 ms (s.d.) and the intrinsic period is 173±51 ms. Paired t-tests show that there is no significant difference between the mean pre-stimulus period and the evoked period ($p > 0.25$) and that there is a significant difference between the mean pre-stimulus period and the intrinsic period ($p < 0.0001$). These data support the hypothesis that a sensory stimulus completely resets the ongoing oscillation.

Another approach to address the same issue is found in the relationship between the phase of the ongoing oscillation at which the stimulus occurs and the evoked period in each trial. The hypothesis that sensory stimulation has no effect on the ongoing oscillation predicts that these quantities will be inversely related: if the sensory stimulus occurs immediately following a peak in the pre-stimulus activity, there will be a long evoked period and if the sensory stimulus occurs substantially after a peak in the pre-stimulus period, there will be a short evoked period. Alternatively, the hypothesis that sensory stimulation completely resets the ongoing oscillation predicts that there will be no relationship between these quantities: regardless of the phase of the ongoing oscillation at which the sensory stimulation occurs, an identical evoked period will follow it. This data is shown in figure 11c. A least squares regression line relating these two values has a slope of 0.19±0.03 (s.e.), with a correlation value r^2 of 0.16. Although the slope is significantly different from

zero ($p < 0.0001$, d.o.f. = 1745, $t = 6.89$) as is the correlation ($p < 0.0001$, d.o.f. = 1745, $t = 18.42$), it is of the opposite sign as that predicted by the hypothesis of no interaction between the ongoing oscillation and the sensory stimulus, demonstrating that the sensory stimulus resets the ongoing oscillation.

However, the positive slope and correlation value suggest that a weak interaction occurs between the time at which the stimulus occurs during the ongoing oscillation and the period of the evoked oscillation. When sensory stimuli occur greater than 150 ms after a pre-stimulus peak, very few short evoked periods are seen. Conversely, when sensory stimuli occur immediately after a pre-stimulus peak, very few long evoked periods are seen. Both of these effects could be related to cortical excitability. From figure 11b, its clear some variability exists in the mean pre-stimulus period, which ranges from 70 - 130 ms. When very long pre-stimulus periods are prevalent, the cortex is oscillating very slowly. This condition of depressed cortical oscillatory activity could in turn cause the evoked oscillation to have a long period. When short pre-stimulus periods are prevalent, the cortex is oscillating at a higher frequency, potentially causing the evoked oscillation to be faster.

Discussion:

Two important results are demonstrated in this work. First, neurons in cortical layer five generate strong alpha-band oscillations in response to sensory stimulation. Alpha-band power in the trial-averaged post-stimulus field responses and in the multi-unit spike responses is strongest in layer 5. The current source density profile is consistent with the oscillatory activation of pyramidal cells in layers five in which the current flow through the cell bodies in layer five is balanced by opposite current flow in the apical dendrites in the upper layers.

Analysis of single trials shows that in layer 5 the difference between the post-stimulus and pre-stimulus power spectra, representing the change in power induced by the stimulus, peaks in the alpha band. Quantification of the pre-stimulus and post-stimulus alpha-band power reveals that sensory stimulation causes a greater increase in alpha band power in layer 5 than in any other layer.

The second major result from this study is that sensory stimulation specifically resets the phase of ongoing background alpha-band oscillations. Spectral analysis of pre-stimulus and post-stimulus periods of single trials demonstrates that the total power in each time period is very similar and that the spectral peaks in both cases are in the delta range (1-5 Hz). The duration of the first period of the post-stimulus oscillation is identical to the period of the pre-stimulus oscillation and is not affected by the phase of the ongoing

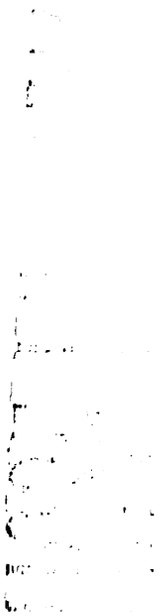

oscillation at which that stimulus occurs, indicating that a full reset has occurred.

Previous studies on the existence of the alpha band rhythm

Substantial data exists from earlier studies in anesthetized animals to confirm that a local region of cortex is capable of oscillatory activity in the alpha band following sensory stimulation. A repetitive response of the cortex to sensory stimulation was first observed by Bartley and Bishop (Bartley and Bishop 1933) who found that stimulation of the optic nerve was followed by several cycles of a 5 Hz oscillation in the surface potential of the visual cortex. The finding of repetitive responses to sensory stimulation was repeated in the somatosensory (Adrian 1941) and auditory (Bremer 1943; Bremer 1949) cortices. Modern studies have replicated these results using intracortically recorded local field potentials (LFP) and single and multi-unit activity in anesthetized animals. In particular, it has been shown that a brief somatosensory stimulus evokes a long-lasting alpha-band oscillation in the somatosensory cortex of both rats (Schoner, et al. 1992; Sameshima and Merzenich 1993) and monkeys (Sameshima and Merzenich 1993). This oscillation persisted for up to one second and altered the response to a subsequent stimulus in a phase-dependent manner (Kopecz et al. 1993; Sameshima and Merzenich 1993). Multi-site recording revealed the evoked oscillation to be synchronous across the activated cortex (Sameshima and Merzenich 1993). Studies in awake humans using MEG recording over somatosensory cortex have demonstrated stimulus-evoked oscillations that

last for 300 ms that alter the response to a subsequent stimulus in a phase-dependent manner (Mahncke 1998), confirming that these oscillations are functionally relevant in the awake human.

These evoked oscillations were considered to be the counterpart of the spontaneous alpha rhythm, discovered by Berger in humans in 1929. This rhythm was subsequently studied by Adrian (Adrian and Matthews 1934; Adrian and Yamagiwa 1935), who found that its source was in the occipital lobe and that it was only present when the visual cortex was unstimulated. It was considered to be the endogenous rhythm of the unstimulated brain, and its disappearance during vision was attributed to either desynchronization or inhibition. The same rhythm has subsequently been found over visual cortex with MEG recording, (Cohen 1968; Cohen 1972), over somatomotor cortex with EEG recording (Gastaut et al. 1954) and MEG recording (Tiihonen et al. 1989), and over auditory cortex with MEG recording (Tiihonen, et al. 1991). Each of these oscillations is suppressed by sensory stimulation of the appropriate modality. This suppression, frequently called "alpha blocking," (Williamson et al. 1997) is in apparent conflict with the data presented in this paper, in which sensory stimulation evokes an alpha-band oscillation. This difference is likely to arise from the different stimuli used in alpha-blocking studies and the current study. In alpha-blocking experiments, the stimuli used are usually several hundred milliseconds in duration, whereas in the current experiments, the stimuli were under 5 ms in duration. These differences suggest a general model of alpha-band cortical dynamics in

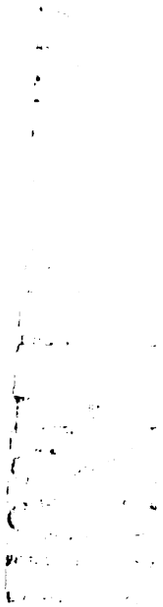

which spontaneous oscillations are suppressed by extended stimuli, as shown in previous work, and reset by brief stimuli, as shown in this work. It is likely that the offset of a extended stimulus resets or initiates a phase-locked alpha-band oscillation, as has been suggested by several lines of experiments (Williamson, et al. 1997; Mahncke 1998).

Previous studies on the laminar distribution of spontaneous alpha band rhythms

Lopes da Silva and Storm van Leeuwen have conducted a series of studies examining spontaneous alpha-band oscillations in the awake dog. They concluded that the current sources underlying the alpha rhythm were likely to be in layer 5 (Lopes da Silva and Storm van Leeuwen 1977; Lopes da Silva and Storm van Leeuwen 1978), and the cortico-cortico coherences were stronger than thalamo-cortical coherences (Lopes da Silva et al. 1973). This evidence was used to argue that the cortex was the generator of the alpha rhythm and that intracortical circuitry as well as thalamocortical circuitry contributed to this rhythm (Lopes da Silva et al. 1980). The data from the current study support and extend these previous results by showing that layer 5 neurons are the source of sensory evoked alpha-band oscillations. These results also suggest that the spontaneous and sensory evoked alpha-band oscillations have identical cortical generators and reflect activity of the same population of neurons.

Isolated cortical slices kept in a low magnesium bath exhibit spontaneous field potential oscillations in the alpha-band range (Silva, et al. 1991). These

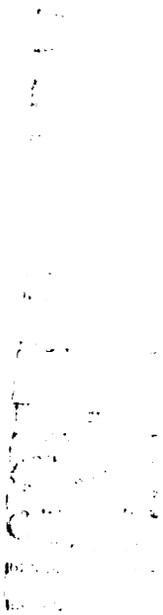

oscillations were recorded through all layers of the slice, but disappeared when the slice was sectioned to remove layer 5, demonstrating that they were caused by neurons in layer 5. These oscillations were dependent on NMDA receptor activity, as was suggested by their enhancement with low magnesium baths and by their abolition with the application of the NMDA receptor antagonist AP5 (Silva, et al. 1991; Flint and Connors 1996). The strength of these oscillations as a function of cortical layer was not quantified in that study. These field potential oscillations are likely to be caused by a population of pyramidal cells found in layer 5 called "intrinsic bursters" as a result of their ability to generate bursty spiking activity in the alpha-band frequency range. This cell population has been found to differ from other pyramidal cells in layer 5 in being superficially located (Larkman and Mason 1990), having a thick apical dendrite that projects into layer 1 (Larkman and Mason 1990), and by their projections to subcortical targets including the superior colliculus and pons (Schofield et al. 1987; Hallman et al. 1988). These results are similar to those in the current study in that alpha-band oscillations are seen in all cortical layers but are dominant in layer 5. Although the absolute requirement for the presence of layer 5 in generating alpha-band oscillations could not be assayed with the current techniques, the fact that layer 5 generated the strongest alpha-band power in all measures suggests that it is intimately involved in generating these oscillations.

Dinse et. al. have recently reviewed their work on sensory-evoked low frequency oscillations (Dinse et al. 1997). In a laminar study of unit activity in

somatosensory cortex evoked by single taps to the receptive field on the skin, they reported oscillatory peaks in the PSTH's of units in all laminae, although these oscillations may be strongest in the middle layers, where every unit generated more than one oscillatory peak. In the current study, oscillations in multi-unit responses were also found in all layers, but were clearly strongest in layer 5. This result can not be compared directly with the Dinse et. al. study because the strength of the oscillations was not quantified in that work.

Relationship to modulation transfer functions

Many previous studies have examined the ability of the auditory cortex to respond to cycles of a repetitive stimulus. This ability is described as a modulation transfer function (MTF), which expresses either the amplitude or the phase locking of the neural response as a function of the stimulus rate. Peripheral afferents have been found to respond to every cycle of a repetitive stimulus up to rates of several hundred hertz. Neurons more centrally located in the inferior colliculus (Langner and Schreiner 1988) and thalamus (Creutzfeldt et al. 1980) typically follow less well, with most not responding to rates over 100 Hz. In turn, neurons in the auditory cortex typically do not respond well to stimuli at rates higher than 20-30 Hz and function as low or band pass filters. Many neurons in the auditory cortex exhibit a best modulation rate in the alpha-band range (Schreiner and Urbas 1986). The evoked alpha-band oscillations characterized might exhibit a resonance with sensory stimuli, which could cause neurons exhibiting these oscillations to prefer stimuli delivered at rates of near 10 Hz. The laminar

specificity of these oscillations suggests that it would be interesting to conduct a laminar study of MTFs to determine if neurons with a peak MTF in the alpha-band range were preferentially located in layer 5.

Ionic basis of these oscillations

A persistent tetrodotoxin-sensitive sodium current has been reported to be involved with the generation of these oscillations (Franceschetti et al. 1995; Guatteo et al. 1996), but the complete cellular basis of these oscillations remains unclear. Since these neurons burst when depolarized with intracellular current injection and these oscillations persist after mechanical dissociation (Guatteo et al. 1994), it is likely that the oscillations are generated by endogenous cellular properties and do not require network effects to operate. Bursting activity in the thalamus occurs when thalamocortical relay cells are in a hyperpolarized state. This deinactivates calcium channels, which cause a slow depolarization. This in turn eventually opens sodium channels, causing a burst of spikes. The depolarization inactivates the calcium channel, causing a return to a hyperpolarized state (Bal et al. 1995). Although the burst frequency in the thalamic system is controlled by the dynamics of neuronal interplay between the excitatory cells of the relay nucleus and the inhibitory cells of the associated reticular nucleus (von Krosigk et al. 1993; Bal et al. 1995), similar ionic mechanisms may underlie the endogenous oscillations found in cortical layer 5 cells.

Interpretation of laminar specificity, active dendrites

Data from the current study in combination with previous studies suggests that a population of bursting neurons in layer 5 of the cerebral cortex generates alpha-band oscillations spontaneously and in response to sensory stimulation. Two possibilities exist to explain the fact that these oscillations are detectable, although weaker, throughout the other layers of the cortex. The first is that the source of the recorded oscillations is the neurons in these other layers whose activity has been entrained by the ability of the layer 5 network to synchronize cortical oscillations. The second is that the source of the recorded oscillations is the processes of the oscillatory layer 5 neurons, in which case neurons in the other layers may not oscillate at all. These possibilities can not be distinguished with the current data set. Apical dendrites from oscillatory layer five cells could contribute at all layers to both the field potential signal, because current passes through them, and the multi-unit signal, because they exhibit action potentials. This question would be best addressed with in vivo intracellular recording where the oscillatory responses of a single cell could be examined and then the precise anatomical position of the cell determined by filling the cell.

It is now well established that the dendrites of layer 5 cells exhibit a number of active conductances that can support the propagation of action potentials. Since these conductances include calcium and sodium, the possibility exists that the dendrites of layer 5 cells could, in themselves, support the generation of alpha-band oscillations. The data from the current

study demonstrates that current rhythmically flows into and out of cells in layer 2/3, consistent with current flow through active dendrites of layer 5 cells. Interestingly, the pre-stimulus current flow alpha-band activity is quite high in the upper layers even after extensive trial averaging. This suggests that the dendrites of layer 5 cells might exhibit spontaneous alpha-band oscillations while the cell bodies themselves are relatively quiescent.

Relevance to MEG

The current data have implications for the generation of extra-cranial magnetic fields detectable with magnetoencephalography (MEG). Based on physical arguments, the source of alpha-band oscillations recorded with MEG in awake humans has been postulated to be the apical dendrites of layer 5 cells. In the current work, it is shown that this cell class exhibits stimulus evoked oscillations that are very similar to those seen in the awake human. Given that the alpha-band oscillations are strongest in layer 5 and that in human somatosensory cortex these cells are optimally oriented for the generation of extra-cranial magnetic fields, it seems very likely that this cell population produces the magnetic signal recorded in humans. This result suggests that future work performed in animal models to gain a better physiological understanding of the magnetic signals recorded in humans should target layer 5, cells rather than indiscriminately record from all cortical depths.

Evoked oscillations in single trial responses

Averaging neural responses over trials is done to increase the signal to noise ratio of the data, where noise is defined as activity that is not temporally locked to the stimulus presentation. The fact that the single trials show important differences from the trial-averaged responses in their background activity and power spectra indicates that these components are not temporally locked to sensory stimulation. The temporally structured "noise" in the current system deserves future study as it may affect responses to stimuli on a trial by trial basis, perhaps contributing to physiological and perceptual variability.

Data from single trials indicate that although ongoing alpha band oscillations appear to be present in the pre-stimulus period, as shown by the single trial power spectra and by the mean period of the pre-stimulus oscillatory activity, very low frequency power (1 - 5 Hz) dominates the field potential activity. In the post-stimulus period, very low frequency power continues to dominate the spectra despite an enhancement of alpha-band power. This very low frequency power is not as prevalent in the trial-averaged field responses, as is seen by the peaks of those power spectra in the alpha range. This suggests that both the amplitude and phase of ongoing low frequency oscillations are unaffected by sensory stimulation, but that the alpha-band oscillations are enhanced and phase-aligned by sensory stimulation. The source of the very low frequency oscillations is not clear; however one possibility is that they are delta waves. These are typically

described as a regular oscillation in the 1-5 Hz range that occurs during sleep. Recently, Flint and Connors (Flint and Connors 1996) have shown that oscillations at this frequency can be found in cortical slices and are caused by a population of cells in layer 2/3. If these oscillations are present in the current experimental conditions, their amplitude and phase do not appear to be affected by sensory stimulation.

Global model

The data from the current study demonstrate that sensory stimulation evokes an alpha-band oscillation in neural activity that is strongest in cortical layer 5. Oscillatory activity could affect both the inputs to these neurons and the outputs from them. Due to their extended apical dendrites, these neurons are ideally suited for integrating the activity of an entire cortical column. The relative efficacy of these inputs is likely to be affected by the phase of the oscillation at which they occur, suggesting that these neurons are be integrating activity over ~100 ms periods or sampling activity at ~100 ms intervals. These oscillations also must affect the encoding of cortical outputs. Oscillatory layer 5 neurons are the output units of the cortex, projecting to subcortical targets such as the spinal cord, superior colliculus, pons, and striatum. Their rhythm may serve a purpose in driving their subcortical targets by delivering information at a specific rate or by ensuring reliable synaptic transmission through repetitive firing. By affecting the basic transformation of inputs to outputs through the cortex, alpha-band

oscillations are likely to have a significant affect on sensory and motor processing of events at this time scale.

Figure 1: Example intra-cortical evoked field potential recording data from a single penetration through A1. A: Each trace is the average of 50 responses to a click delivered at time 0. Purple trace recorded at a depth of 300 μ. Green trace recorded at a depth of 800 μ. Note polarity reversal in the short latency onset response and strong alpha-band oscillations in 800 μ trace. B: Reconstruction of the field activity recorded through the depth of the cortex in a single penetration. Blue represents field negativities, red represents field positivities. Approximate cortical layers boundaries are shown in horizontal black lines.

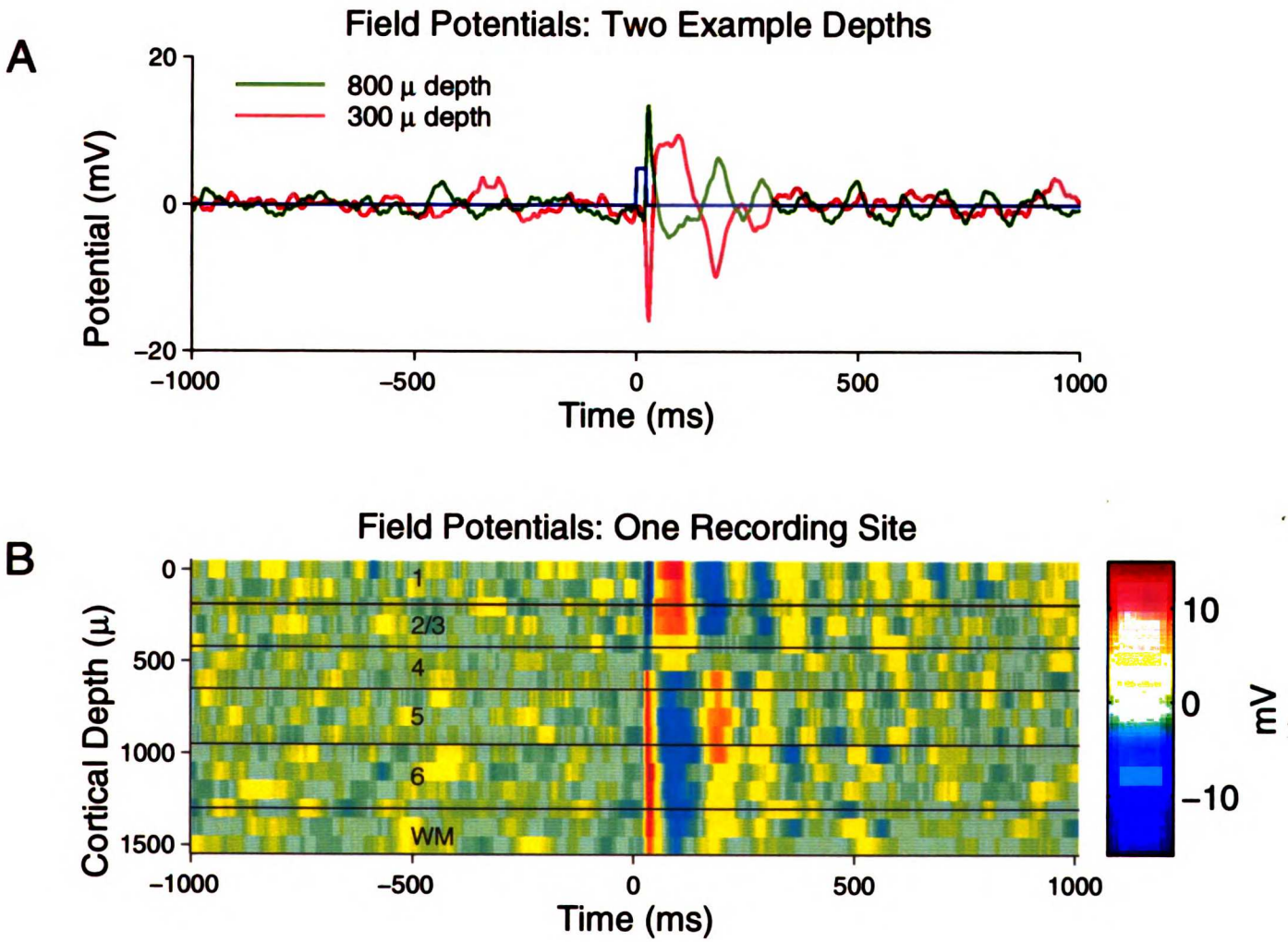
A
Field Potentials: Two Example Depths
800 μ depth
300 μ depth
Potential (mV)
20
0
-20
-1000
-500
0
500
1000
Time (ms)
B
Field Potentials: One Recording Site
Cortical Depth (μ)
0
500
1000
1500
1
2/3
4
5
6
WM
-1000
-500
0
500
1000
Time (ms)
10
0
-10
mV

Figure 2: Summary of intra-cortical evoked field potential recording data from 43 recording sites. A: Red graph is the average profile of the post-stimulus alpha-band power. A depth profile was constructed for each penetration by calculating the alpha band power (50-500 ms post-stimulus) at each depth. Profiles were normalized to their peak values and then averaged. Analysis of variance (ANOVA) with depth as a repeated measure shows the depth distribution of post-stimulus alpha-band power is not uniform ($p < 0.0001$, d.o.f. = 15, $F = 15.247$). Blue graph is the average profile of the pre-stimulus alpha-band power. A depth profile was constructed for each penetration by calculating the alpha band power over the entire pre-stimulus period at each depth. Profiles were normalized to the peak post-stimulus alpha-band power and then averaged. Analysis of variance (ANOVA) with depth as a repeated measure shows the depth distribution of pre-stimulus alpha-band power is not uniform ($p < 0.0025$, d.o.f. = 15, $F = 2.385$). B: Red graph is the average profile of the post-stimulus onset response power. A depth profile was constructed for each penetration by calculating the total power (0-50 ms post-stimulus) at each depth. Profiles were normalized to their peak values and then averaged. Analysis of variance (ANOVA) with depth as a repeated measure shows the depth distribution of post-stimulus onset response power is not uniform ($p < 0.0001$, d.o.f. = 15, $F = 21.808$). Blue graph is the average profile of the pre-stimulus power. A depth profile was constructed for each penetration by calculating the mean total power over the entire pre-stimulus period at each depth. Profiles were normalized to the

peak post-stimulus onset response power and then averaged. Analysis of variance (ANOVA) with depth as a repeated measure shows the depth distribution of mean pre-stimulus power is not uniform ($p < 0.002$, d.o.f. = 15, $F = 2.846$). Error bars are standard errors.

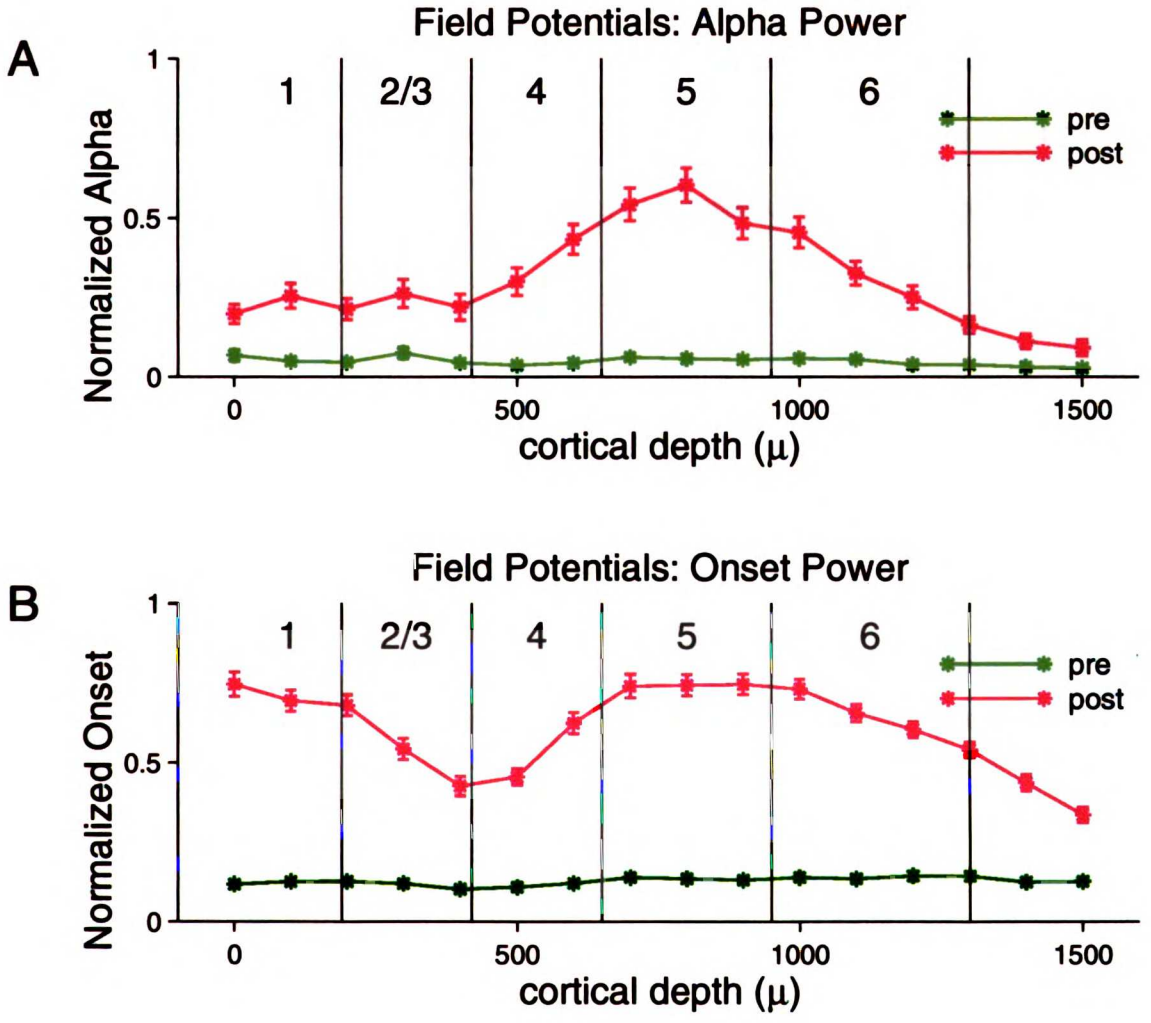
A
Field Potentials: Alpha Power
Normalized Alpha
1
0.5
0
1
2/3
4
5
6
pre
post
0
500
1000
1500
cortical depth (μ)
B
Field Potentials: Onset Power
Normalized Onset
1
0.5
0
1
2/3
4
5
6
pre
post
0
500
1000
1500
cortical depth (μ)

Figure 3: Example current source density recording data from a single penetration. A: Each trace is the current source density at a particular depth calculated from the evoked field potential average of 50 responses to a click delivered at time 0. Outward current is up and inward current flow is down. Ordinate is in arbitrary current units. Purple trace for a depth of 300 μ. Green trace for a depth of 800 μ. Note strong alpha-band oscillations are 180 out of phase in the two traces. B: Reconstruction of the CSD calculated through the depth of the cortex in a single penetration. Blue represents current sinks, red represents current sources. Approximate cortical layers boundaries are shown in horizontal black lines.

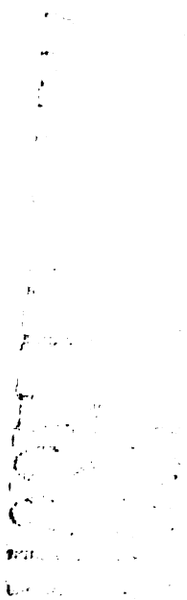

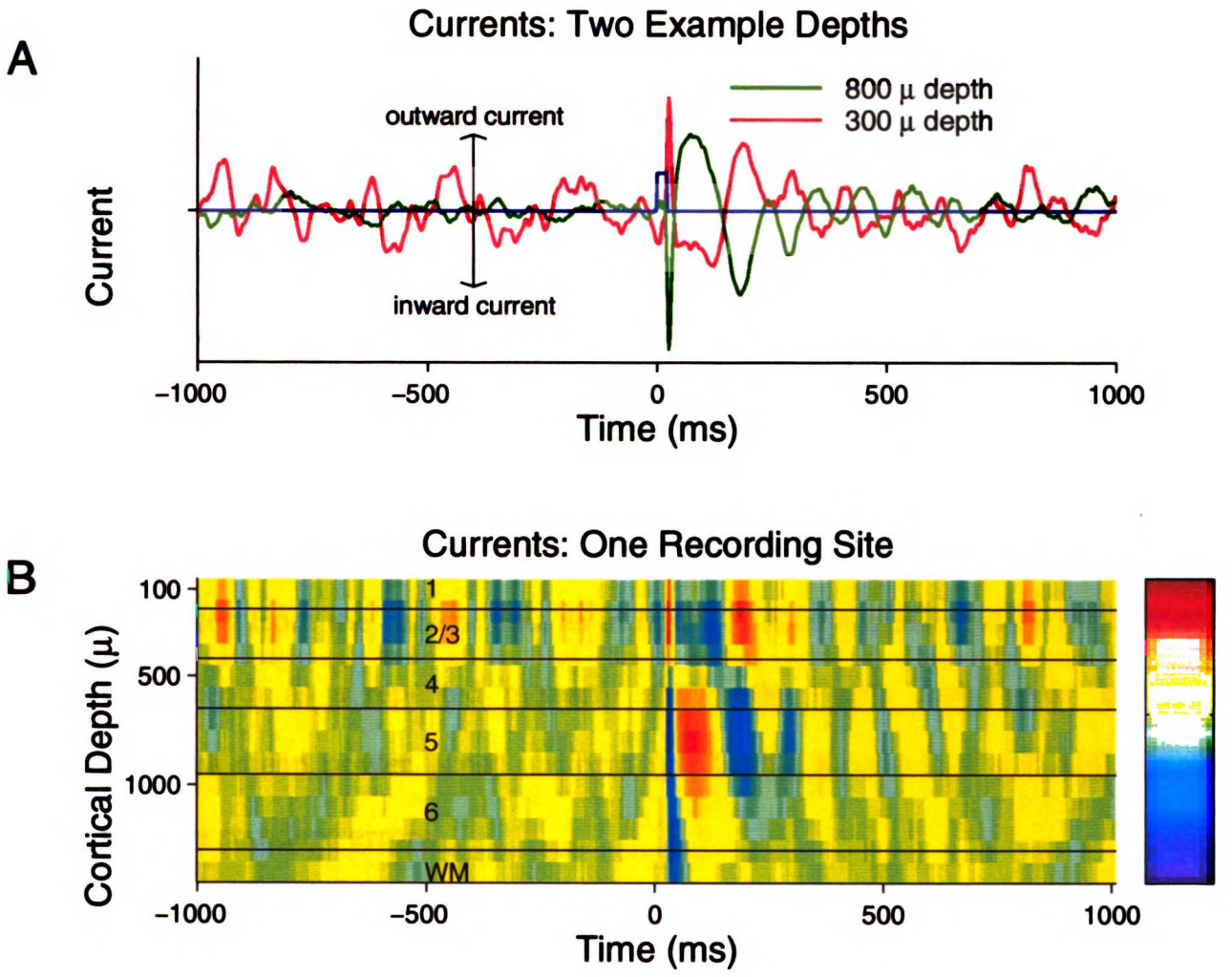
A
Currents: Two Example Depths
800 μ depth
300 μ depth
outward current
inward current
Current
−1000
−500
0
500
1000
Time (ms)
B
Currents: One Recording Site
Cortical Depth (μ)
100
500
1000
1
2/3
4
5
6
WM
−1000
−500
0
500
1000
Time (ms)

Figure 4: Summary of current source data from 43 recording sites. A: Red graph is the average profile of the post-stimulus alpha-band power, calculated from the current data as in figure 2. Analysis of variance (ANOVA) with depth as a repeated measure shows the depth distribution of post-stimulus alpha-band power is not uniform ($p < 0.0001$, d.o.f. = 13, $F = 13.475$). Blue graph is the average profile of the pre-stimulus alpha-band power, calculated from the current data as in figure 2. Analysis of variance (ANOVA) with depth as a repeated measure shows the depth distribution of pre-stimulus alpha-band power is not uniform ($p < 0.0001$, d.o.f. = 13, $F = 21.702$). B: Red graph is the average profile of the post-stimulus onset response power, calculated from the current data as in figure 2. Analysis of variance (ANOVA) with depth as a repeated measure shows the depth distribution of post-stimulus onset response power is not uniform ($p < 0.0001$, d.o.f. = 13 $F = 40.643$). Blue graph is the average profile of the pre-stimulus power, calculated from the current data as in figure 2. Analysis of variance (ANOVA) with depth as a repeated measure shows the depth distribution of pre-stimulus mean power is not uniform ($p < 0.0001$, d.o.f. = 13, $F = 31.114$). Error bars are standard errors.

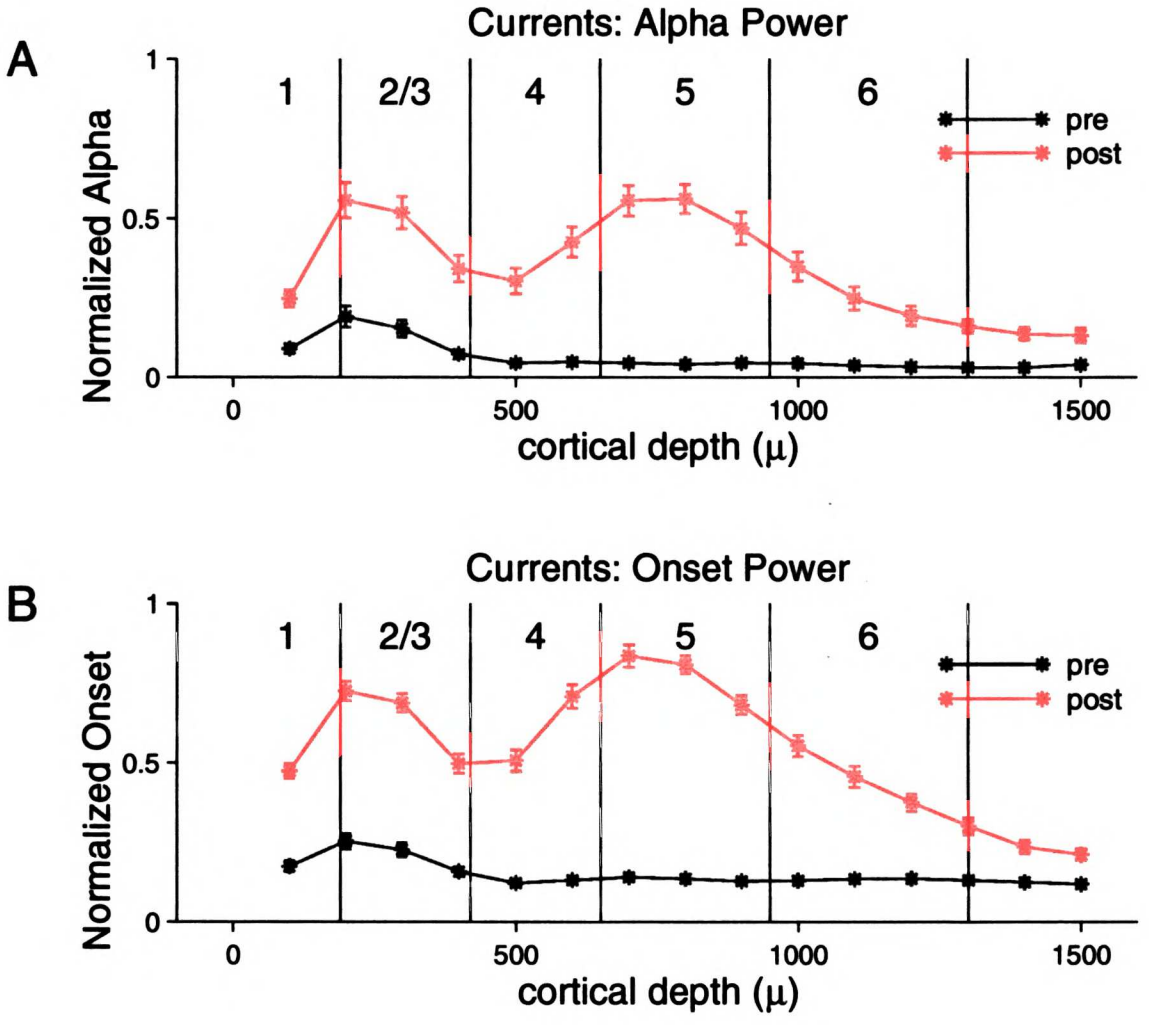
A
Currents: Alpha Power
Normalized Alpha
1
0.5
0
1
2/3
4
5
6
pre
post
0
500
1000
1500
cortical depth (μ)
B
Currents: Onset Power
Normalized Onset
1
0.5
0
1
2/3
4
5
6
pre
post
0
500
1000
1500
cortical depth (μ)

Figure 5: Example multi-unit spike data from a single penetration. A: Post-stimulus time histogram (PSTH) averaged over 20 responses to a click delivered at time 0. Note strong onset response but no post-stimulus oscillations. B: Post-stimulus time histogram (PSTH) averaged over 50 responses to a click delivered at time 0. Note strong alpha-band oscillations. C: PSTHS's through the depth of the cortex in a single penetration. Blue represents low activity, red represents high activity. Cortical layers boundaries are shown in horizontal black lines.

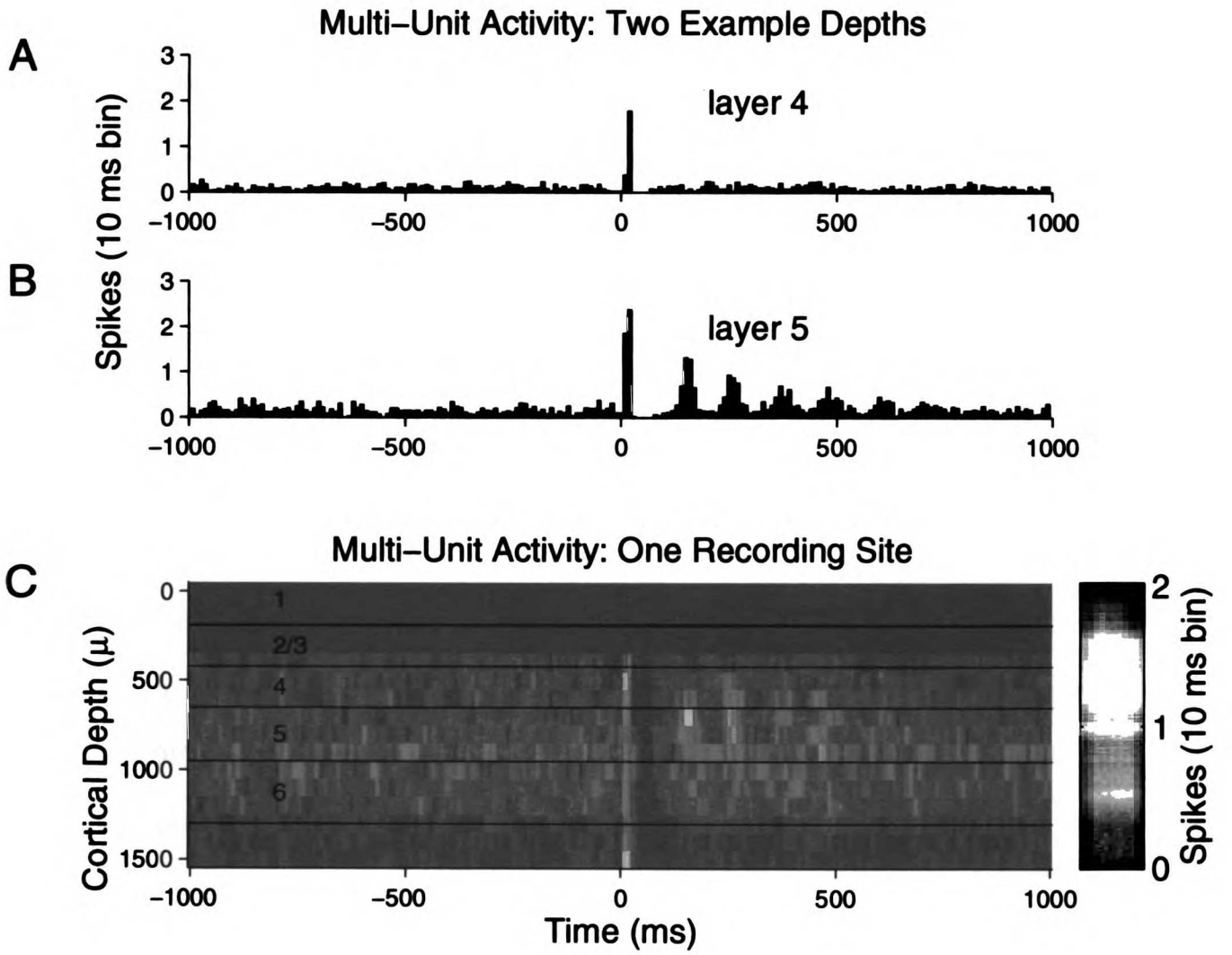
Multi–Unit Activity: Two Example Depths
A
B
layer 4
layer 5
Spikes (10 ms bin)
3
2
1
0
–1000
–500
0
500
1000
C
Multi–Unit Activity: One Recording Site
Cortical Depth (μ)
0
500
1000
1500
1
2/3
4
5
6
Time (ms)
Spikes (10 ms bin)
2
1
0

Figure 6: Summary of PSTH data from 43 recording sites. The exact number of sites at each depth depends on the number of sites where adequate multi-unit activity was recorded (see methods). A: Red graph is the average profile of the post-stimulus alpha-band power in the PSTH, calculated from the spike data as in figure 2. ANOVA with depth as a repeated measure shows that the depth distribution of post-stimulus alpha-band power is not uniform ($p < 0.0001$, d.o.f. = 13, $F = 16.06$). Blue graph is the average profile of the pre-stimulus alpha band power in the PSTH, calculated from the spike data as in figure 2. ANOVA with depth as a repeated measure shows that the depth distribution of post-stimulus alpha-band power is not uniform ($p < 0.0001$, d.o.f. = 13, $F = 4.691$). B: Red graph is the average profile of the post-stimulus onset response power in the PSTH, calculated from the spike data as in figure 2. ANOVA with depth as a repeated measure shows that the depth distribution of post-stimulus onset response power is not uniform ($p < 0.0001$, d.o.f. = 13, $F = 20.28$). Blue graph is the average profile of the pre-stimulus mean power in the PSTH, calculated from the spike data as in figure 2. ANOVA with depth as a repeated measure shows that the depth distribution of post-stimulus alpha-band power is not uniform ($p < 0.0001$, d.o.f. = 13, $F = 9.494$). Error bars are standard errors.

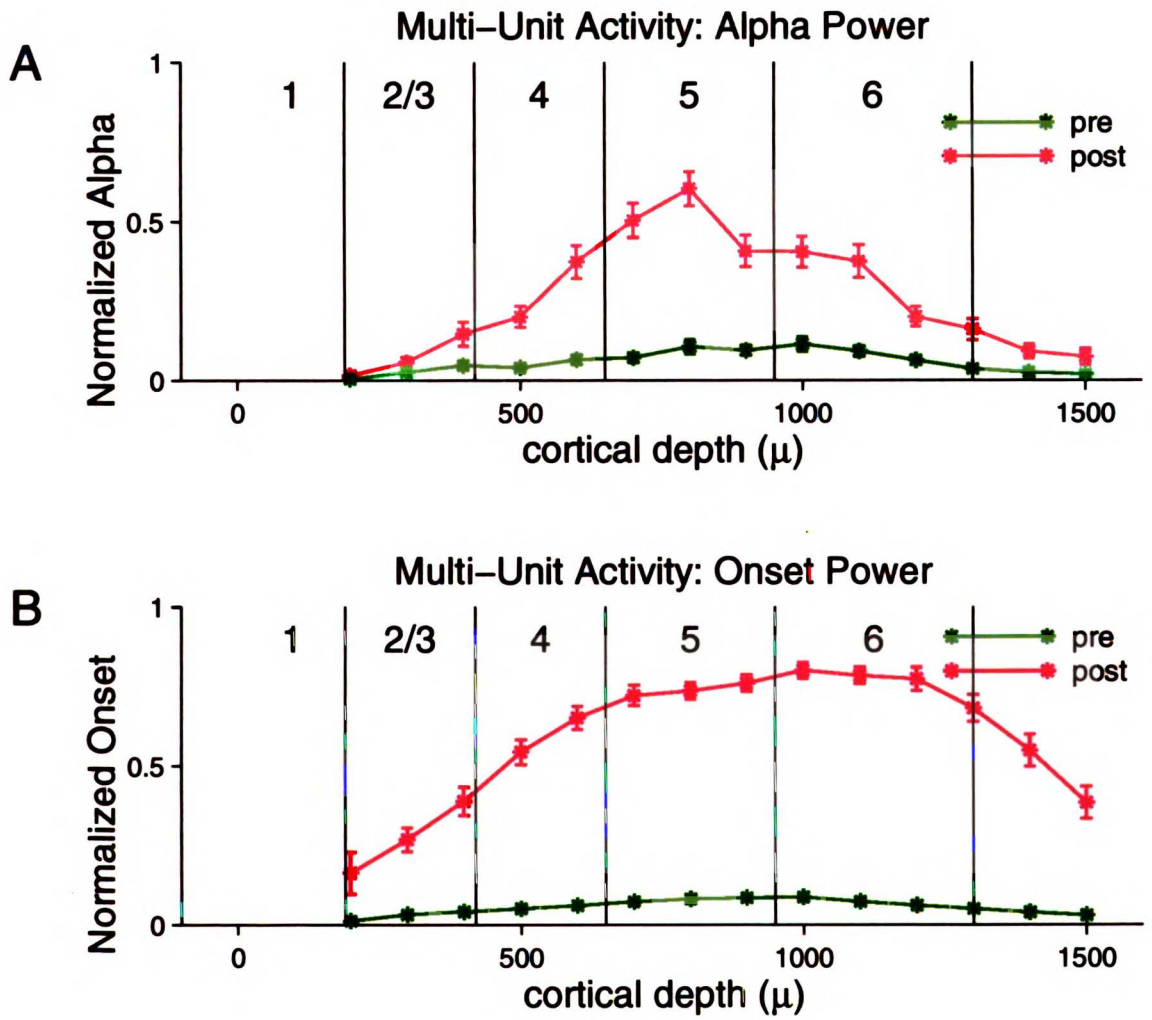
A
Multi–Unit Activity: Alpha Power
Normalized Alpha
1
0.5
0
1
2/3
4
5
6
pre
post
0
500
1000
1500
cortical depth (μ)
B
Multi–Unit Activity: Onset Power
Normalized Onset
1
0.5
0
1
2/3
4
5
6
pre
post
0
500
1000
1500
cortical depth (μ)

Figure 7: A: Average intra-cortically evoked field potential response recorded at 800 μ depth in response to 50 presentations of a click at time 0. Note lack of background activity, sharp onset response, and long lasting alpha-band oscillation. B: Single intra-cortically evoked field potential response recorded at 800 μ depth in response to a single presentation of a click at time 0 (same site as A). Note large, rhythmic background activity at approximately the same amplitude and frequency as evoked activity. The onset response is remains readily identifiable.

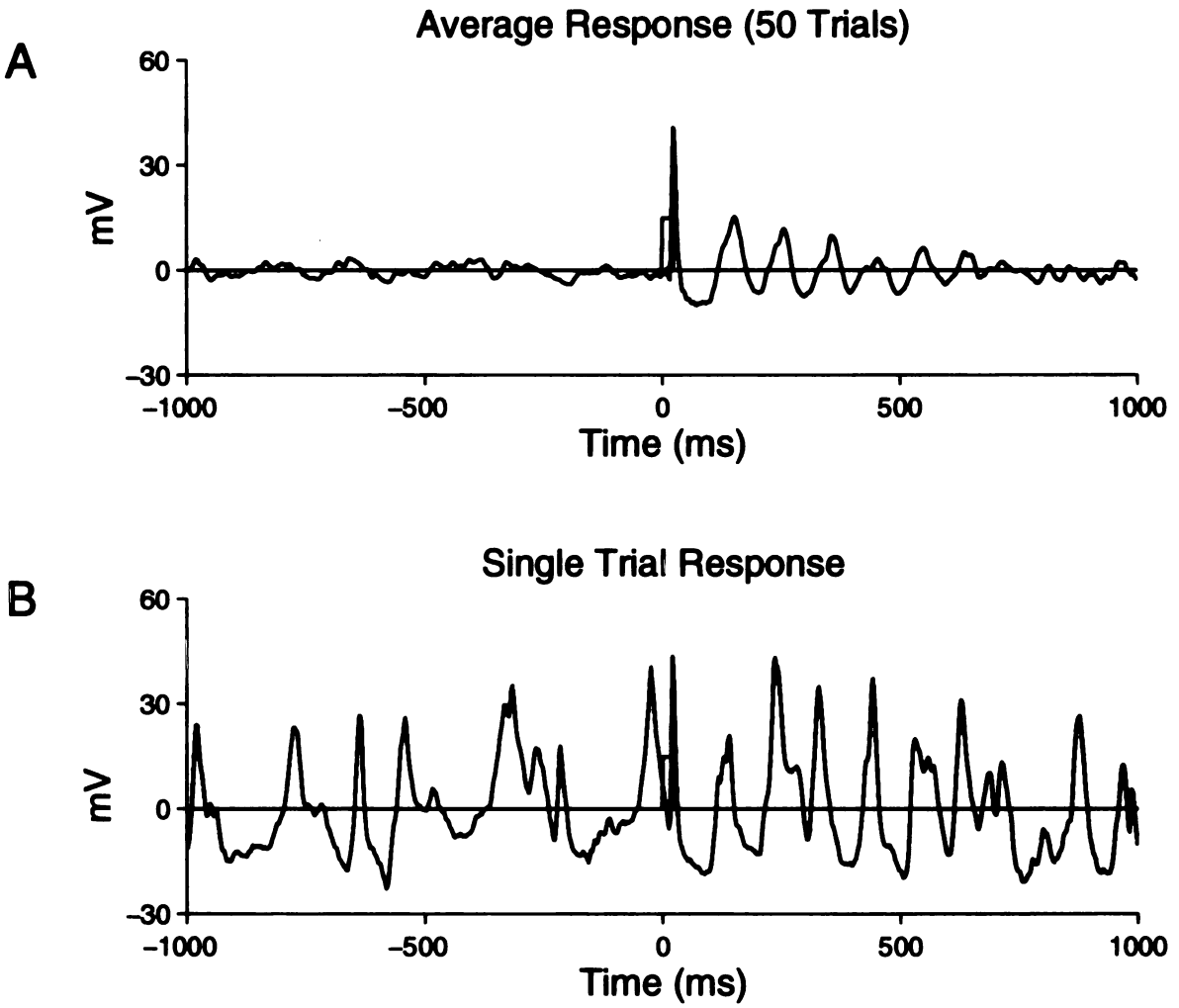
A
Average Response (50 Trials)
60
30
0
-30
mV
-1000
-500
0
500
1000
Time (ms)
B
Single Trial Response
60
30
0
-30
mV
-1000
-500
0
500
1000
Time (ms)

Figure 8: A: Power spectrum of average response to a click from figure 7a. Green trace is the pre-stimulus power spectrum, red trace is the post-stimulus power spectrum. Note very low total pre-stimulus power and strong alpha-band post-stimulus power. B: Pre-stimulus (green) and post-stimulus (red) alpha-band power calculated from A. C: Power spectrum of single trial response to a click from figure 7b. Green trace is the pre-stimulus power spectrum, red trace is the post-stimulus power spectrum. Note high total powers in pre-stimulus and post-stimulus conditions. D: Pre-stimulus (green) and post-stimulus (red) alpha-band power calculated from C.

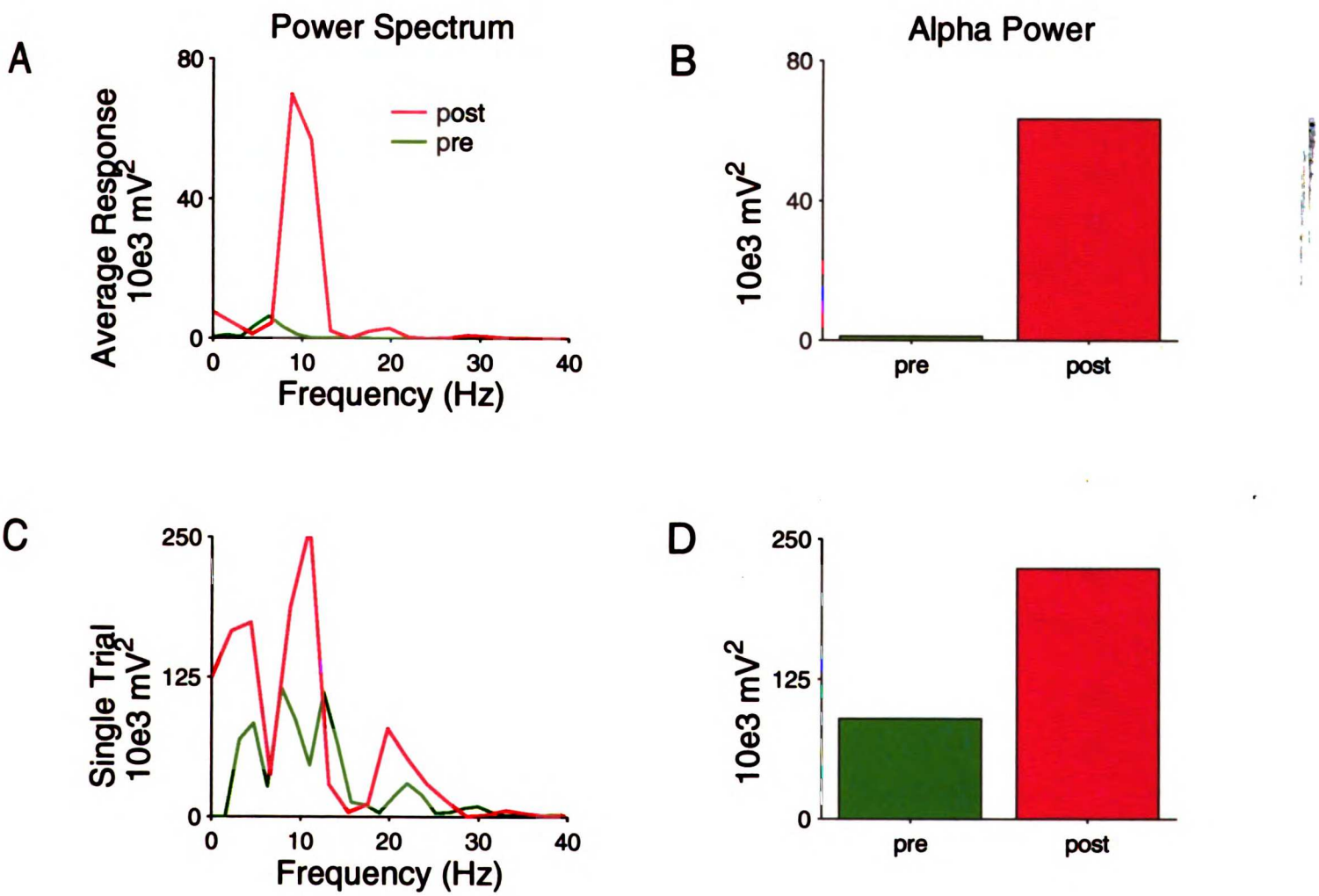
A
Power Spectrum
Average Response
10e3 mV2
80
40
0
post
pre
0
10
20
30
40
Frequency (Hz)
B
Alpha Power
10e3 mV2
80
40
0
pre
post
C
Single Trial
10e3 mV2
250
125
0
0
10
20
30
40
Frequency (Hz)
D
10e3 mV2
250
125
0
pre
post

Figure 9: Average pre-stimulus (green) and post-stimulus (red) power spectra of single trial responses across trials sorted by recording depth. Error bars are standard errors. Note comparable total powers in both time periods and an increase in the post-stimulus power in the alpha-band range. Avererage post-stimulus power spectra of the trial-averaged response (blue).

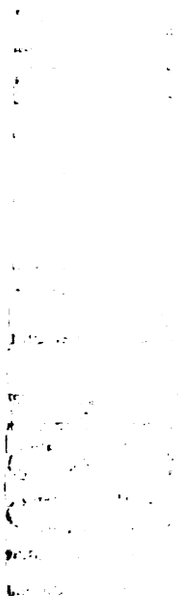

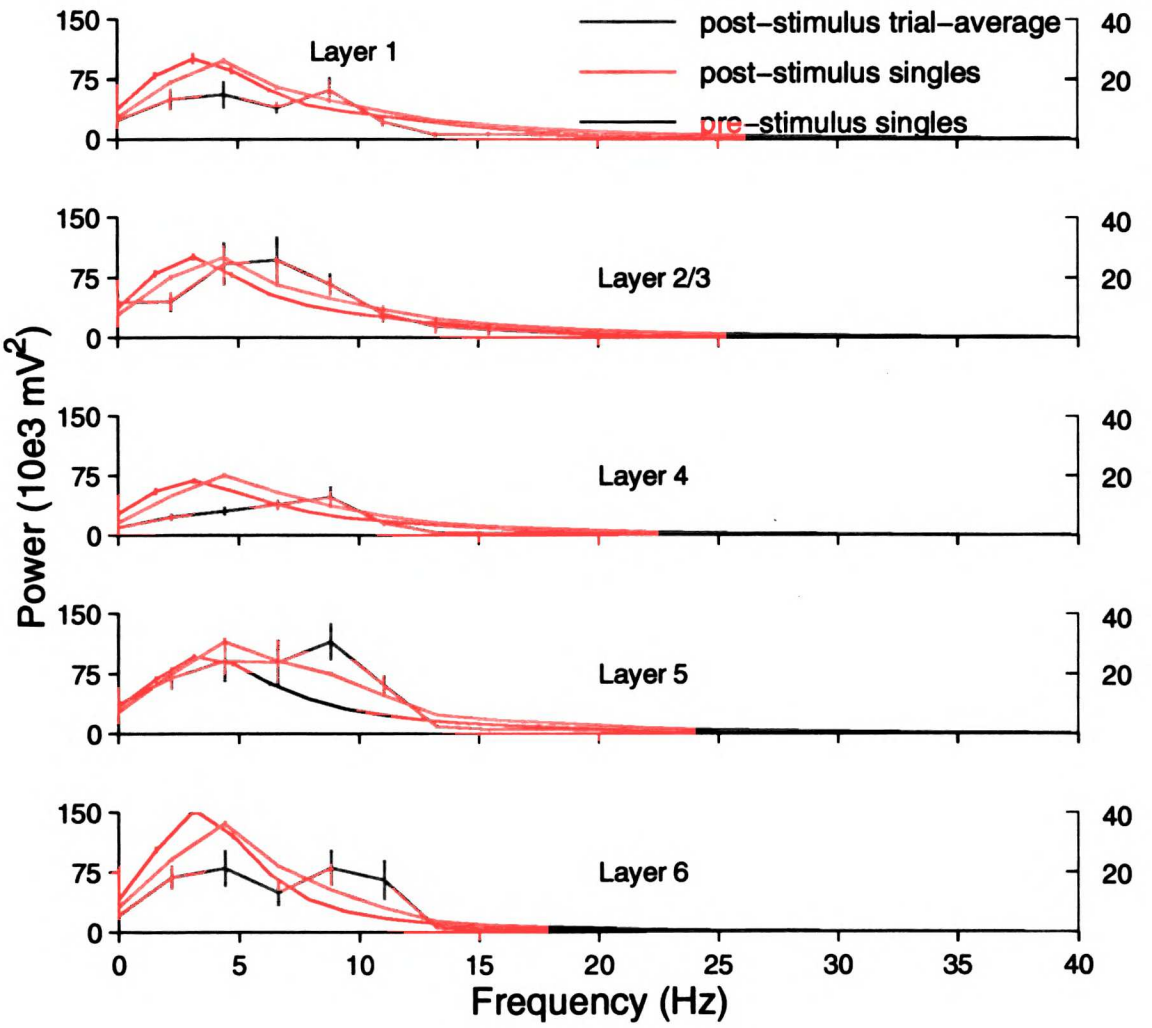
post–stimulus trial–average
post–stimulus singles
pre–stimulus singles
Layer 1
Layer 2/3
Layer 4
Layer 5
Layer 6
150
75
0
40
20
Power (10e3 mV²)
0
5
10
15
20
25
30
35
40
Frequency (Hz)

Figure 10: Distributions of log of ratios of pre-stimulus alpha-band power to post-stimulus alpha-band power of single trials across trials sorted by recording depth. Number of trials per layers same as figure 9. Vertical line represents mean of each layer distribution. Alpha-band power ratio is significantly greater than zero in all layers ($p < 0.0005$ for all layers except layer 1, $p < 0.02$ for layer 1). ANOVA shows a significant effect of layer on alpha-band power ($p < 0.0001$, d.o.f. = 4. $F = 21.86$).

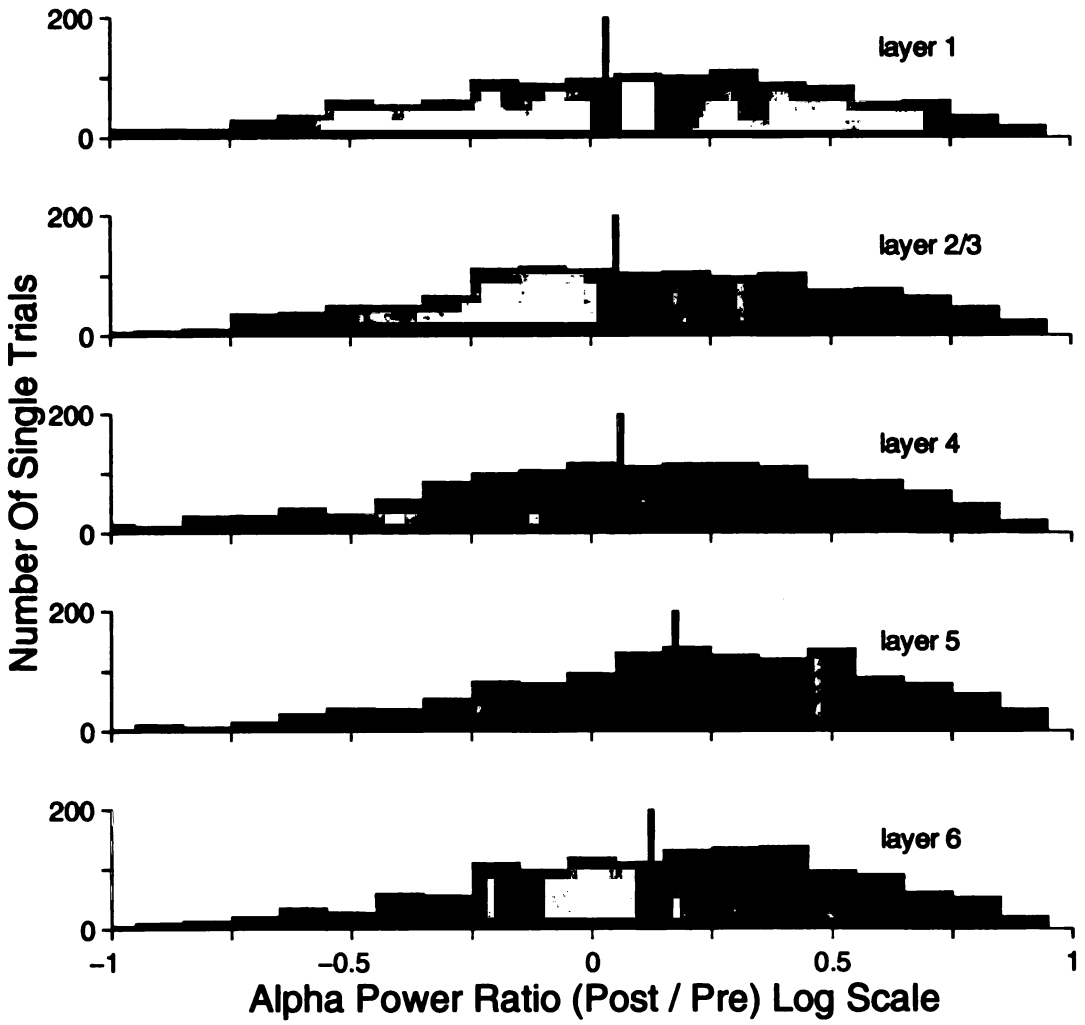
200
0
layer 1
200
0
layer 2/3
200
0
layer 4
200
0
layer 5
200
0
layer 6
Number Of Single Trials
−1
−0.5
0
0.5
1
Alpha Power Ratio (Post / Pre) Log Scale

Figure 11: A: Single trial field potential recording from layer 5. Dark green trace is the raw data, filtered from 1-100 Hz. Light green trace is smoothed data, filtered from 3-20 Hz. Blue trace represents stimulus. Red stars mark relevant peaks. Left-most star marks the time of the immediate pre-stimulus peak, calculated from the smoothed data. Center star marks the time of the onset response, calculated from the raw data. Right-most star marks the time of the first rebound response, calculated from the smoothed data. B: Plot of mean pre-stimulus period versus the intrinsic period (green) and the evoked period (red). Intrinsic period is calculated as the interval between the immediate pre-stimulus peak and the rebound response. Evoked period is calculated as the interval between the onset response and the rebound response. Paired t-tests show no significant difference between the pre-stimulus periods (mean 91±12 ms) and the evoked periods (mean 87±36 ms) ($p > 0.25$) and a significant difference between the pre-stimulus periods and the intrinsic periods (mean 173±51 ms) ($p < 0.0001$). C: Plot of the interval between the immediate pre-stimulus peak and the onset response versus the evoked period as defined in B. Regression analysis shows a significant trial by trial correlation between these measures

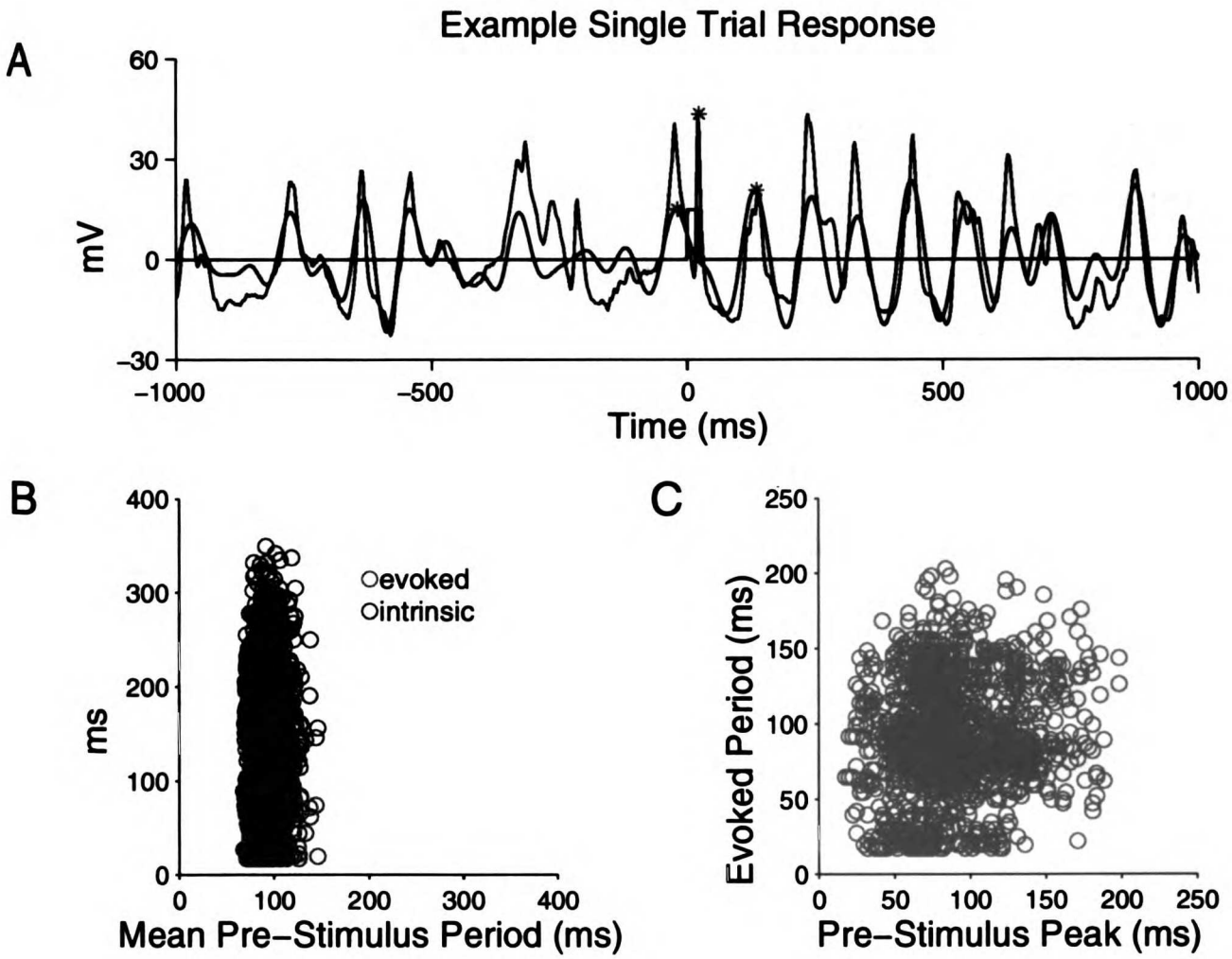
A
Example Single Trial Response
60
30
0
-30
mV
-1000
-500
0
500
1000
Time (ms)
B
400
300
200
100
0
ms
evoked
intrinsic
0
100
200
300
400
Mean Pre-Stimulus Period (ms)
C
250
200
150
100
50
0
Evoked Period (ms)
0
50
100
150
200
250
Pre-Stimulus Peak (ms)

References:

Adrian ED (1941) Afferent discharges to the cerebral cortex from peripheral sense organs. Journal of Physiology 100:159-191.

Adrian ED and Matthews BHC (1934) The Berger rhythm: potential changes from the occipital lobes in man. Brain 57:355-385.

Adrian EH and Yamagiwa K (1935) The origin of the Berger rhythm. Brain 58:323-351.

Bal T, von Krosigk M, and McCormick DA (1995) Role of the ferret perigeniculate nucleus in the generation of synchronized oscillations in vitro. Journal of Physiology (London) 483:665-685.

Bal T, von Krosigk M, and McCormick DA (1995) Synaptic and membrane mechanisms underlying synchronized oscillations in the ferret lateral geniculate nucleus in vitro. Journal of Physiology (London) 483:641-663.

Bartley SH and Bishop GH (1933) The cortical response to stimulation of the optic nerve in the rabbit. American Journal of Physiology 103:159-172.

Bremer F (1943) Etude oscillographique des responses sensorielles de l'aire acoustique corticale chez le chat. Archives International Physiology 53:53-103.

Bremer F (1949) Consideration sur l'origine et la nature des "ondes" cerebrales. Electroencephalography and Clinical Neurophysiology 1:177-193.

Cohen D (1968) Magnetoencephalography: Evidence of magnetic fields produced by alpha-rhythm currents. Science 161:784-786.

Cohen D (1972) Magnetoencephalography: Detection of the brain's electrical activity with a superconducting magnetometer. Science 175:664-666.

Creutzfeldt O, Hellweg FC, and Schreiner C (1980) Thalamocortical transformation of responses to complex auditory stimuli. Experimental Brain Research 39:87-104.

Dinse HR, Kruger K, Akhavan AC, Spengler F, Schoner G, and Schreiner CE (1997) Low-frequency oscillations of visual, auditory and somatosensory cortical neurons evoked by sensory stimulation. International Journal of Psychophysiology 26:205-227.

Flint AC and Connors BW (1996) Two types of network oscillations in neocortex mediated by distinct glutamate receptor subtypes and neuronal populations. Journal of Neurophysiology 75:951-957.

Franceschetti S, Guatteo E, Panzica F, Sancini G, Wanke E, and Avanzini G (1995) Ionic mechanisms underlying burst firing in pyramidal neurons: intracellular study in rat sensorimotor cortex. Brain Research 696:127-139.

Gastaut H, Dongier M, and Courtois G (1954) On the significance of 'wicket rhythms' ('rythmes en arceau') in psychosomatic medicine. Electroencephalography and Clinical Neurophysiology 6:687-695.

Gho M and Varela FJ (1988) A quantitative assessment of the dependency of the visual temporal frame upon the cortical rhythm. Journal of Physiology (Paris) 83:95-101.

Guatteo E, Bacci A, Franceschetti S, Avanzini G, and Wanke E (1994) Neurons dissociated from neocortex fire with 'burst' and 'regular' trains of spikes. Neuroscience Letters 175:117-120.

Guatteo E, Franceschetti S, Bacci A, Avanzini G, and Wanke E (1996) A TTX-sensitive conductance underlying burst firing in isolated pyramidal neurons from rat neocortex. Brain Research 741:1-12.

Hallman LE, Schofield BR, and Lin CS (1988) Dendritic morphology and axon collaterals of corticotectal, corticopontine, and callosal neurons in layer V of primary visual cortex of the hooded rat. Journal of Comparative Neurology 272:149-160.

Kopecz K, Schoner G, Spengler F, and Dinse HR (1993) Dynamic properties of cortical evoked (10 Hz) oscillations: theory and experiment. Biological Cybernetics 69:463-473.

Langner G and Schreiner CE (1988) Periodicity coding in the inferior colliculus of the cat. I. Neuronal mechanisms. Journal of Neurophysiology 60:1799-1822.

Larkman A and Mason A (1990) Correlations between morphology and electrophysiology of pyramidal neurons in slices of rat visual cortex. I. Establishment of cell classes. Journal of Neuroscience 10:1407-1414.

Lopes da Silva FH and Storm van Leeuwen W (1977) The cortical source of the alpha rhythm. Neuroscience Letters 6:237-241.

Lopes da Silva FH and Storm van Leeuwen W (1978) The cortical alpha rhythm in dog: the depth and surface profile of phase. New York:Raven Press. 319-333 pp.

Lopes da Silva FH, van Lierop THMT, Chreijer CF, and Storm van Leeuwen W (1973) Organization of thalamic and cortical alpha rhythms: spectra and coherences. Electroencephalography and Clinical Neurophysiology 35:627-639.

Lopes da Silva FH, Vos JE, Mooibroek J, and Van Rotterdam A (1980) Relative contributions of intracortical and thalamo-cortical processes in the generation of alpha rhythms, revealed by partial coherence analysis. Electroencephalography and Clinical Neurophysiology 50:449-456.

Mahncke HW (1998) Oscillations and temporal processing and sensory cortex. Thesis:University of California, San Francisco.

Mitzdorf U (1985) Current source-density method and application in cat cerebral cortex: investigation of evoked potentials and EEG phenomena. Physiological Reviews 65:37-100.

Sameshima K and Merzenich MM (1993) Intrinsic oscillator contributions to response properties of SI cortical neurons. Society for Neuroscience Abstract.

Schofield BR, Hallman LE, and Lin CS (1987) Morphology of corticotectal cells in the primary visual cortex of hooded rats. Journal of Comparative Neurology 261:85-97.

Schoner G, Kopecz K, Spengler F, and Dinse HR (1992) Evoked oscillatory cortical responses are dynamically coupled to peripheral stimuli. Neuroreport 3:579-582.

Schreiner CE and Urbas JV (1986) Representation of amplitude modulation in the auditory cortex of the cat. I. The anterior auditory field (AAF). Hearing Research 21:227-241.

Silva LR, Amitai Y, and Connors BW (1991) Intrinsic oscillations of neocortex generated by layer 5 pyramidal neurons. Science 251:432-435.

Tiihonen J, Hari R, Kajola M, Karhu J, Ahlfors S, and Tissari S (1991) Magnetoencephalographic 10-Hz rhythm from the human auditory cortex. Neuroscience Letters 129:303-305.

Tiihonen J, Kajola M, and Hari R (1989) Magnetic mu rhythm in man. Neuroscience 32:793-800.

Varela FJ, Toro A, John ER, and Schwartz EL (1981) Perceptual framing and cortical alpha rhythm. Neuropsychologia 19:675-686.

von Krosigk M, Bal T, and McCormick DA (1993) Cellular mechanisms of a synchronized oscillation in the thalamus. Science 261:361-364.

Williamson SJ, Kaufman L, Lu ZL, Wang JZ, and Karron D (1997) Study of human occipital alpha rhythm: the alphon hypothesis and alpha suppression. International Journal of Psychophysiology 26:63-76.

STIMULUS RATE GOVERNS INTEGRATION TIME IN THE AUDITORY CORTEX

Chapter 5

Abstract:

Auditory cortical neurons usually respond to the onset of a stimulus with a burst of activity that subsides to substantially lower levels during the remaining duration of the stimulus. The dynamics of this form of adaptation bear important implications for the processing of spatiotemporally complex stimuli by the cortex. In particular, recovery from this form of adaptation will govern responses to stimuli that occur sequentially in time. Many aspects of recovery of excitability have not been closely examined to date. The goals of this experiment were (1) to measure the time course of recovery from adaptation in auditory cortical field A1 for a broadband stimulus, and (2) to determine if the recovery of excitability is dependent on the temporal structure of the conditioning stimulus.

Multiple-unit activity was recorded from the auditory cortex of Nembutal anesthetized rats. A conditioning stimulus/probe stimulus paradigm was used to define the time course of the recovery of excitability following stimulation. Conditioning stimuli were click trains presented at rates between 50 and 500 pulses per second (pps). Probe stimuli were identical click trains or single clicks separated by variable intervals from the conditioning stimulus offset. The amplitude and latency of the onset response to probe stimuli were used to measure recovery from adaptation.

It was found that (1) responses to probe stimuli exhibited a recovery of excitability characterized by increasing response amplitudes and decreasing response latencies as a function of the inter-stimulus interval (ISI). A 100 ms

long 125 pps conditioning click train required, on average, a 49 ms inter-stimulus interval (ISI) for the amplitude of the response to the probe click train to rise to 50% of the activity generated by a control train presented in isolation. A 38 ms ISI was required for the latency of the response to the second click train to decrease to twice the value of a control train. (2) The time course of recovery of excitability did not vary significantly as a function of conditioning click train duration. (3) The time course of recovery of excitability did vary systematically as a function of the pulse rate of the conditioning click train. Post–stimulus excitability recovered more quickly following click trains with higher rates than those with lower rates. The function relating conditioning click train rate to recovery time was quite linear from 50 pps to 333 pps, saturating at higher rates than 333 pps. (4) The rate of the conditioning click train did not affect the frequency of alpha-band post-stimulus oscillations.

These results parallel psychophysical findings and suggest specific physiological mechanisms by which sequentially occurring stimuli are segregated and integrated in the auditory cortex.

Introduction:

Neural activity in the cerebral cortex exhibits considerable variation in the time domain. At the gross level of evoked potentials, background activity fluctuates in the 10 Hz frequency range, and oscillations in the alpha (Poeppel et al. 1996) and gamma bands (Singer 1993) can be evoked by sensory stimulation. Behavioral arousal can shift the cortex from a state marked by synchronized high-amplitude slow-wave oscillations to a state marked by desynchronized low-amplitude rapid oscillations (Steriade et al. 1993). At the level of single unit activity, similar oscillatory responses to sensory stimuli are seen. Individual neurons can also exhibit bursts of high frequency activity followed by long pauses (Lisman 1997). Intracellular recording reveals a host of temporally varying properties. Neurons have intrinsic properties leading them to respond differentially to injected current, exhibiting either fast spiking, regular spiking, bursting (Connors and Gutnick 1990), or chattering behavior (Gray and McCormick 1996). Influences from other neurons include slow IPSP's and neuromodulators such as acetylcholine and norepinephrine (McCormick et al. 1993), all of which can alter the temporal structure of ongoing and evoked activity.

These intrinsic temporal dynamics of the cortex interact with the temporal structures of incoming sensory stimuli. The cortical response to stimuli is a combination between the driving forces inherently represented by the incoming inputs and the intrinsic cortical dynamics. This interaction must often distort the representation of the temporal structures of the inputs,

either degrading or enhancing the response to specific temporal patterns, as well as convert temporal information to a spatial code. One well studied example of the interactions has been explored in the interplay between intrinsic alpha frequency dynamics of the auditory cortex and temporally modulated stimuli (Kenmochi and Eggermont 1997). The temporal properties of auditory neurons have been earlier assayed by presenting a gradated series of click trains with different click repetition rates. It is usually found that cortical neurons do not respond well to rates higher than 20 Hz and frequently have a bandpass filter shape centered near 10 Hz (Schreiner and Urbas 1988; Eggermont 1994). Cortical neurons oscillate at frequencies near 10 Hz after sensory stimulation (Schoner et al. 1992; Kopecz et al. 1993). It has been suggested that this intrinsic feature is what limits cortical responsiveness to high click rates (Eggermont 1992). By this interpretation, the excitatory-inhibitory dynamics of the cortex simply prevent it from being able to respond to clicks that occur too close together in time. The temporal properties of any complex stimulus are reshaped by this interplay with the intrinsic dynamics of the cortex. To understand how complex auditory signals like speech are actually represented by cortical networks, it is critical that the principles of this recoding be understood.

Another neural process that plays a role in sculpting the temporal response of the nervous system to a sensory stimulus is adaptation. Neurons at most levels of the nervous system respond to a sustained stimulus by decrementing their response from the initial level of activity to a lower steady

state value. This adaptation can allow them to use effectively a relatively narrow dynamic range of response to cover a wide dynamic range of stimuli. In the retina, for example, photoreceptors must respond to levels of illumination that can vary over six log units of intensity. The dynamic range of photoreceptor output, however, can only vary over two log units. By adapting to the ambient light level, photoreceptors can efficiently encode changes around the mean light level that are behaviorally important to the animal. Similarly, visual cortical cells adapt to the ambient contrast in order to effectively use the dynamic range of their response to indicate changes in contrast around the mean (Ohzawa et al. 1982; Ohzawa et al. 1985).

Neural adaptation can have a large effect on perception. The waterfall illusion (Nakayama 1985), for example, is induced by presenting a pattern moving in a single direction to a subject for several seconds. When the subject subsequently views a stationary pattern, she reports that it appears to be moving slowly in the direction opposite to the first direction. Exposure to the moving pattern induces a direction specific adaptation of directionally selective neurons (Petersen et al. 1985). It has been suggested that the subsequent response to the stationary pattern may be unbalanced across the population of directionally selective neurons. making the stationary pattern appear to drift in the direction opposite to the adapting direction (Petersen, et al. 1985).

The temporal properties of adaptation provide an additional response feature to the cortex. If adaptation and recovery from adaptation occur on the

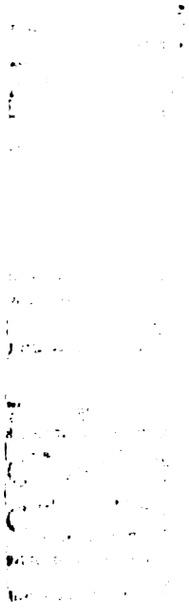

same time scale as the temporal variations in stimuli, these neuronal properties will shape the response to temporally varying stimuli. In particular, the timecourse and specificity of adaptation may govern such processes as the integration and segregation of sequentially occurring stimuli. It is surprising, therefore, that relatively little attention has been paid to the important role that adaptation may play in processing temporally varying information. We have studied these issues in the primary auditory cortex using click train stimuli with the goals of (1) measuring the time course of the recovery from adaptation following a click train and (2) determining the effect of the temporal structure of the click train on response recovery.

Methods:

Animal preparation

Experiments were conducted in 18 female Sprague-Dawley albino rats (280-330 g). Surgical anesthesia was induced by an intraperitoneal injection of 0.35 ml sodium pentobarbital (CONC). A tracheotomy was performed to ease breathing, and the jugular vein was cannulated to allow administration of fluids. A state of areflexia was maintained through the remainder of the experiment with a continuous infusion of sodium pentobarbital in normal saline (1:17) administered intravenously. A heating pad was used to maintain body temperature at 38° Celsius. Reflexes were monitored to control the depth of anesthesia. The rat was placed in a custom designed head holder that stabilized the head while allowing access to the pinnae. Following a midline incision, a craniotomy was performed to expose the upper part of the left cortical hemisphere. The dura was removed and the exposed brain was covered in mineral oil.

Neurophysiological recording

Multi-unit recordings were made with either parylene coated tungsten microelectrode pairs (tip separation 250-400 μ, resistance 1-3 MΩ, F. Haer) or single carbon fiber (10 μ tip diameter, 1-3 MΩ) microelectrodes. Electrodes were inserted into the brain perpendicular to the surface and advanced to a depth of 500-600 μ, which corresponds to the layer 4 of rat auditory cortex (Roger and Arnault 1989). Neuronal activity was amplified, band-pass filtered (300 Hz-10 kHz) and displayed on an oscilloscope. Data acquisition was

controlled by a PC (Datawave Systems). Spikes were detected by a threshold crossing and spike waveforms were then digitized at 30 kHz and saved to disk for off-line analysis. Primary auditory cortex was identified as a region of cortex with sites that had short (8-16 ms) latencies to tonal stimuli, well defined tuning curves, and an appropriately oriented topographic organization of characteristic frequencies (CF's) (Sally and Kelly 1988).

Stimulus generation and control

Recording was performed in a double walled sound attenuated chamber. All stimuli were generated under PC control by a D/A board (Spectrum Scientific). Sound was generated with 16 bit resolution at a 96 kHz sampling rate. Pure tone stimuli for receptive field mapping were 50 ms in duration, including a 5 ms ramp at each end. Click stimuli were 250 μs positive going square pulses. The sound level was calibrated (Bruel and Kjaer sound level meter) such that a 250 pps click train had a sustained amplitude of 70 dB. Click trains exhibited broad-band frequency spectra. Stimuli were presented monaurally through a sound tube directed into the contralateral ear.

Experimental protocol

A detailed tuning curve was generated by presenting tones ranging in frequency from 1 kHz to 32 kHz in 1/12th octave steps and ranging in amplitude from 0 dB to 75 dB in 15 dB (SPL) steps. CF's were determined from the tips of typically V-shaped tuning curves. Tuning curves were constructed before and after a full experimental stimulus set (see below) was presented to ensure recording stability.

Recovery functions were obtained by presenting a conditioning stimulus and a probe stimulus separated by a parametrically varying series of silent inter-stimulus intervals (ISI's). For most experiments, the recovery function was investigated following two different conditioning stimuli. The first conditioning stimulus was always a standard 125 pps click train of 100 ms duration, the control stimulus. The second conditioning stimulus was a click train applied at a different rate. Conditioning stimuli of different rates had durations as close to 100 ms as possible; however, depending upon the exact period of the stimulus, the duration of the stimulus could be slightly less than 100 ms. Probe stimuli were usually identical to conditioning stimuli; however, in certain experiments as noted, single clicks were used as probe stimuli. Twenty repetitions of each ISI duration were presented to generate post-stimulus time histograms (PSTH's). Stimuli separated by all ISI's as well as both stimulus sets for different click rates were presented in a randomly interleaved fashion with inter-trial intervals of 2000-3000 ms.

Data analysis

All data analysis was performed with Matlab (Mathworks). Responses to clicks and click trains consisted of a burst of spikes with a latency between 8 and 16 ms that was finished within 30 ms of stimulus onset. No response locking was seen to the click train rates used in this study. Stimulus evoked activity was extracted from average PSTH's with an automated algorithm that looked for the maximum response in a 3 ms bin in a 30 ms duration post-stimulus time window. The amplitude of the response was measured by the

total number of spikes in the 3 ms bin. The latency of the response was measured from stimulus onset to the peak of the response. Response amplitudes and response latencies were plotted as a function of ISI.

Two parameters, the amplitude and latency recovery times, were estimated to characterize each recovery function. The amplitude recovery time was defined as the minimum length of the ISI required for the amplitude of the response to the probe stimulus to recover 50% of the amplitude of the response evoked by the probe stimulus presented in isolation. The latency recovery time was defined as the minimum length of the ISI required for the latency of the response to the probe stimulus to fall to twice the latency of the response evoked by the probe stimulus presented in isolation. Both amplitude and latency recovery functions were smoothed with a triangular filter five bins wide before the recovery time was calculated to facilitate measurement of recovery times. If the recovery time appeared to fall between two ISI's, the recovery time was estimated by interpolation. All analyses were performed automatically using MATLAB programs with the operator blind to the experimental condition.

In the first set of experiments, recovery times for a control conditioning stimulus (125 pps click train, 100 ms duration) and for one other conditioning stimulus were measured at each recording site. A normalized recovery time was calculated as the difference between the recovery time of the control conditioning stimulus and the experimental conditioning stimulus. This normalization allowed us to compensate for differences in baseline recovery

between recording sites caused by recording from different subregions in primary auditory cortex, by differences in anesthetic state, or by inter-animal differences.

Results:

Auditory cortical units do not respond to stimuli presented in very rapid succession

The response of a multi-unit cluster to a single click is shown in figure 1a. A strong evoked multi-unit response was seen, followed by a return to baseline activity. Figure 1b shows the response of the same cluster to a 200 ms click train with a 125 pps repetition rate (8 ms inter-click interval). An onset response similar to that recorded for a single click was seen. However, none of the subsequent clicks evoked an identifiable response. This is referred to as an adapted state because a stimulus that evoked a strong response when presented alone evoked no response when presented as an element of an ongoing click train. Figure 1c demonstrates that this adaptation was not simply the result of residual inhibition following the onset response to the first click. A second click delivered at 108 ms following the first click evokes a strong response. However, a click delivered at exactly the same time following the first click of a train did not evoke a response when the intervening interval was filled with the click train as shown in 1b. The 108 ms interval in 1c corresponds precisely to the time of occurrence of the thirteenth click of the click train in 1b, which did not evoke a response. Thus, the lack of response in the click train to a click that occurs 108 ms after the onset of the train was not due to simple inhibition following the onset response. Rather, the adaptation was maintained and extended by the

presence of the intervening clicks of the train. It was this adaptation that this study was designed to characterize.

Time course of recovery from adaptation

The time course of recovery from this form of adaptation was measured using a standard conditioning stimulus — probe stimulus method. The conditioning stimulus consisted of a 100 ms long, 125 pps click train. The probe stimulus was an identical click train. The time between the offset of the conditioning stimulus and the onset of the probe stimulus (termed the inter-stimulus interval or ISI) was a principle variable in this study. The response to a stimulus at a particular ISI is shown in figure 2. The objective of this paradigm was to quantify the amplitude of the response to the probe stimulus to measure recovery from cortical adaptation.

In figure 3a, the response to the probe stimulus after a parametric series of ISI's was plotted. The abscissa is the ISI and the ordinate is the average number of spikes per trial in the response to the probe over a 3 ms window. The response to the probe stimulus presented in isolation is shown by the horizontal line. The recovery function exhibits a monotonic increase with increasing gap duration until the gap duration reaches 65 ms, at which point the probe stimulus evokes a response equivalent to the response when presented in isolation.

The amplitude recovery time was defined as the minimum gap duration at which the probe stimulus evoked 50% of the response of the probe

stimulus presented in isolation. This time is shown by the vertical line in figure 3a and in this example was 45 ms.

The latency of the response to the probe stimulus was also quantified to measure recovery from cortical adaptation. In figure 3b, the latency of the response to the probe stimulus is plotted. The abscissa is the ISI and the ordinate is the latency of the response to the probe stimulus. The latency to the probe stimulus presented in isolation is indicated by the horizontal line. The recovery function exhibited a monotonic decrease with increasing gap duration. Note that even at the maximum gap tested, the latency of the response to the probe stimulus remained slightly elevated relative to the latency of the response to the control stimulus.

The latency recovery time was defined as the minimum gap duration at which the latency of the response to the probe stimulus had decreased to two times that of the response of the probe stimulus presented in isolation. It is marked by the vertical line in figure 3b and in this example was 32 ms.

The distribution of amplitude recovery times measured across 96 recording sites in 13 experiments is shown in figure 4a. The mean recovery time was 48 ms±13 ms (s.d.). A wide variation was seen across sites. The distribution of latency recovery times measured across 117 recording sites in 13 animals is shown in figure 4b. The mean recovery time was 39 ms±12 ms (s.d.). Again, a wide variation was seen across sites.

The rate of the conditioning stimulus affects the recovery time

It was hypothesized that the temporal structure of the conditioning stimulus would affect the rate of recovery from adaptation following the conditioning stimulus. This hypothesis was tested by comparing the recovery times measured with 125 pps stimuli to recovery times measured with stimuli of different pulse rates. The response to a 125 pps stimulus at a particular ISI is shown in figure 5a, and the response to a 250 pps stimulus at the same ISI recorded from the same site is shown in figure 5b.

The recovery functions of the two conditioning stimuli are shown in figure 6a. The responses to the probe stimuli presented in isolation were identical. Amplitude recovery functions, however, were different. The 125 pps conditioning stimulus, shown in stars, attained 50% recovery of amplitude at a 45 ms ISI. The amplitude recovery time for the 250 pps conditioning stimulus, shown in squares, was 22 ms. At every ISI, the probe stimulus following the 250 pps stimulus evoked a stronger response than the probe stimulus following the 125 pps stimulus. A normalized amplitude recovery time was defined as the amplitude recovery time of the 125 pps stimulus minus the amplitude recovery time of the 250 pps, which in this case was 23 ms.

The effect of the rate of the conditioning stimulus on the latency of the response to subsequent probe stimuli was also measured using this paradigm. The latency recovery functions following the two conditioning stimuli are shown in figure 6b. The latency of the responses to the probe stimuli

presented in isolation were very similar. The recovery functions were again quite different. The latency recovery time for the 125 pps conditioning stimulus was 32 ms, whereas the latency recovery time for the 250 pps conditioning stimulus was 16 ms. At most ISI's, the latency of the response to the probe stimulus following the 250 pps stimulus was less than the latency of the response to the probe stimulus following the 125 pps stimulus. The normalized latency recovery time was defined as the recovery time of the 125 pps stimulus minus the recovery time of the 250 pps, which in this case was 16 ms.

The dependence of the amplitude recovery time on the rate of the conditioning stimulus is summarized in figure 7a. The 125 pps conditioning stimulus was presented at every site and the normalized recovery time of a second conditioning stimulus rate, either 50 pps, 200 pps, 250 pps, 333 pps, or 500 pps, was calculated relative to the 125 pps standard. This normalization allowed for the detection of differences in recovery times that might otherwise be obscured by the high variance of recovery time measurements across sites as seen in figure 4. A zero recovery time indicates that the stimulus had a recovery time identical to that of the 125 pps stimulus. Positive numbers indicate slower recovery times than that of the 125 pps stimulus; negative numbers indicate faster times. A clear relationship between the rate of the conditioning stimulus and the recovery time is seen. The more rapid the click repetition rate of the conditioning stimulus, the more quickly the site recovered excitability. In particular, there was a very

linear region from 50 pps to 333 pps. In this region, the recovery time shortened by 0.13 ms per pps change in the conditioning click train repetition rate. This slope is significantly different from zero (two-tailed t test, $p < 0.0001$, d.o.f = 82, t = -13.06). The normalized recovery times for 333 pps and 500 pps appeared to be identical, suggesting that adaptive processes had saturated at these rates.

The dependence of the latency recovery time on the rate of the conditioning stimulus is summarized in figure 7b. A zero normalized recovery time indicates that the stimulus had a recovery time identical to that of the 125 pps stimulus. Positive numbers indicate slower recovery times than that of the 125 pps stimulus; negative numbers indicate faster times. A clear relationship between the rate of the conditioning stimulus and the recovery time was seen. The more rapid the conditioning stimulus, the more quickly the site recovered excitability. A least-squares regression fit to these data excluding the 500 pps point shows that the latency recovery time shortens by 0.09 ms per 1 pps increase in the conditioning click train repetition rate. This slope is significantly different from zero (two-tailed t test, $p < 0.0001$, d.o.f = 98, t = -7.27).

The use of different probe stimuli did not affect the measurement of recovery time.

In studies discussed so far, the probe stimulus was identical to the conditioning stimulus. The differences seen in recovery times could therefore conceivably have been due to the differences in the probe stimuli rather than

the differences in the conditioning stimuli. Two lines of argument demonstrate that this is not this case. First, the onset response to a single click and to all click trains in the frequency ranges used in this study were identical. The average response to a single click at an example site is shown in figure 8a. The average response to a 125 pps click train at the same site is shown in figure 8b. The amplitude and shape of the response to each stimulus are clearly close to identical. Clicks subsequent to the first in a click train do not appear to contribute to the measured neural response at the level of the auditory cortex. Second, control experiments were performed using a 250 pps click train conditioning stimuli with either an identical click train or a single click as a probe stimulus. Recovery times were quantified from the amplitude of the responses to these probe stimuli. The results are shown in figure 8c. No statistically significant difference existed between the recovery times in experiments in which click trains were used as probe stimuli and experiments in which single clicks were used as probe stimuli (Mann-Whitney test, $p > 0.3$, d.o.f. = 9, $z = 0.568$). Taken together, these results support the hypothesis that the onset responses to click trains with different rates are identical and thus that the rate of the probe stimulus does not affect the measurement of the recovery time.

The rate of the conditioning stimulus, not the number of clicks, governs the recovery time.

The variable under study with this set of conditioning stimuli was click repetition rate. However, as a result of varying rate while keeping duration

constant, the total number of clicks delivered in a conditioning stimulus was also varied. To confirm that the differences in recovery times seen following various conditioning stimuli was due to differences in rate and not differences in total number of clicks delivered, control experiments were designed to distinguish between these two stimulus parameters. Conditioning stimuli were presented at 125 pps with a duration of either 100 ms or 200 ms. Single clicks were used as probe stimuli. Amplitude recovery times for these two conditioning stimuli are shown in figure 9. The two distributions are statistically identical (Wilcoxon test, $p > 0.25$, d.o.f. = 9, $z = 0.739$), suggesting that the recovery time following a 100 ms stimulus is the same as that following a 200 ms stimulus of the same rate, despite the fact that one contains twice as many clicks as the other. To confirm this lack of difference, the predicted difference in recovery times if the governing stimulus feature was number of clicks and not rate was calculated from figure 6a. The 200 ms, 125 pps stimulus in this experiment has the same number of clicks as the 100 ms, 250 pps stimulus in figure 6a, suggesting that it should exhibit a recovery time that is 16 ms more rapid than the control 100 ms, 125 pps stimulus. Thus the distribution for the 200 ms stimuli in figure 8 should be centered at 16ms. The actual distribution is significantly different from one centered at 16 ms (Mann-Whitney, $p < 0.025$, d.o.f. = 9, $z = 2.9859$). These data support the hypothesis that the difference in recovery times following stimuli of different rates is due to rate differences and not to the coincident difference in the number of clicks in the conditioning stimulus.

The rate of the conditioning stimulus does not alter the period of post-stimulus oscillations.

Earlier work from our laboratory and from others has demonstrated that the cortex undergoes rhythmic changes in excitability at a frequency of 10 Hz following a brief sensory stimulus. This oscillation is manifested by an initial refractory period that recovers to 50% of control excitability in about seventy milliseconds, followed by alternating periods of suppression and enhancement of the response to a probe stimulus. However, it is not known if stimulus properties can modify these oscillatory dynamics. The data presented in this paper demonstrates that excitability following a 100 ms duration, 250 pps click train recovers to 50% of control excitability in about forty milliseconds, indicating that recovery of excitability is more rapid following a click train than following a single click. A stimulus set was designed to determine if the frequency of post-stimulus oscillations was altered in a similar manner by measuring the amplitude of the response to a single click probe stimulus with an ISI range spanning several hundred milliseconds following conditioning stimuli that were either single clicks or 100 ms duration, 250 pps click trains. The click conditioning stimulus is outlined in figure 10a with an example PSTH. The amplitude recovery function derived from this stimulus configuration is shown in figure 10b. As expected, the amplitude of the responses to probe stimuli following a single click conditioning stimulus showed rhythmic changes with a frequency of approximately 10 Hz, as shown by the peaks in excitability at ISI's of 105 ms

and 195 ms. The click train conditioning stimulus is outlined in figure 11a with an example PSTH recorded from the same site as figure 10a. The amplitude recovery function derived from this stimulus configuration is shown in figure 11b. The amplitude of the responses to probe stimuli following the click train conditioning stimulus exhibit a much quicker initial return of excitability, as predicted from previous data in this paper. Excitability then cycled, with peaks at ISI's of 60 ms, 150 ms, and 255 ms following the offset of the click train. The oscillation period following each conditioning stimulus type was calculated by averaging these inter-peak times. This yielded an average period of 90 ms for the oscillation following the single click and an average period of 97.5 ms for the oscillation following the click train.

The average oscillatory period following a click or a click train is shown in the histogram in figure 12. The periods measured from the application of these two very different stimuli are not statistically different (Wilcoxon test, $p > 0.2$, d.o.f. = 28, $z = 1.09$), suggesting that although the rate of a conditioning stimulus can alter the rate at which the cortex recovers excitability following that stimulus, it does not alter the fundamental oscillatory processes of the cortex.

Discussion:

The goals of the present study were to examine the properties of the recovery of excitability in the auditory cortex following a stimulus that induces strong adaptation. A simple conditioning stimulus-probe stimulus methodology was employed to define recovery functions following click trains of various rates. These studies revealed that excitability, as quantified by the amplitude and latency of the response to a probe stimulus, recovered over the time period of tens of milliseconds. That recovery time was not a fixed property for a given cortical site, but instead, varied as a function of the characteristics of the conditioning stimulus. Specifically, excitability recovered more quickly following conditioning stimuli with higher input click rates.

Potential caveats

Multi-unit recording techniques were employed in this study. Previous studies of cortical feature selectivity have reported some differences in the spectral properties of single and multi-units. Schreiner and Sutter found that in the dorsal region of A1, the tuning curve bandwidths of multi-units were representative of the bandwidths of single units, whereas in the ventral region, multi-unit bandwidths were wider than those of single units (Schreiner and Sutter 1992). This was interpreted to mean that nearby single units in the ventral region of A1 exhibited a greater scatter in their CF's, making multi-unit bandwidths appear larger. South and Weinberger (South and Weinberger 1995) found similar interpretational difficulties in a study comparing various measures of the spectral receptive

fields of single and multi-units. These difficulties arise because multi-unit firing is the sum of the firing of the underlying single units, and can appear to be wider or more sensitive than the average single unit.

These studies do not suffer from these difficulties. The first major result, the fundamental measurements of recovery times derived from multi-unit responses, represent estimates of the minimal recovery time for single units. Some single units are likely to recover more slowly than these estimates, but none are likely to recover more quickly. The second major result, the difference in recovery times in multi-units depending upon the rate of the conditioning click train guarantees that some single units will exhibit this property. These measurements are based upon seeing a multi unit response to the probe under one condition, versus not seeing such a response in another condition. Some single units must exhibit this property for it to be seen with multi unit recording.

Relationship to modulation transfer functions

The acoustic energy of almost all natural auditory stimuli exhibits fluctuations in time. These variations, including effects stemming from frequency and amplitude modulations, carry important information about the nature of stimuli. Many previous studies have examined the responses of auditory neurons to parametrically varied stimuli such as click trains, AM tones, and repetitive FM sweeps. The ability of neurons to respond to each cycle of a repetitive stimulus is described as a modulation transfer function (MTF), which expresses either the amplitude or the phase locking of the

neural response as a function of the stimulus rate. Peripheral afferents are usually found to respond to every cycle of a repetitive stimulus up to rates of several hundred hertz. Neurons more centrally located in the inferior colliculus (Langner and Schreiner 1988) and thalamus (Creutzfeldt et al. 1980) typically follow less well than peripheral afferents with most neurons not responding to rates over 100 Hz. In turn, neurons in the auditory cortex typically function as low pass filters and do not respond well to stimuli at rates higher than 20-30 Hz.

Consistent with these previous reports regarding data from other species, it was found that auditory cortical units did not follow click trains with rates of 50 pps and above. The cellular and circuit processes that prevent cortical neurons from following high stimulus rates are not yet well understood. It is clear that most auditory cortical neurons have spontaneous rhythmic activity in the 10 Hz range, which interacts with repetitive inputs in a complex manner (Kenmochi and Eggermont 1997). This can cause an enhanced response to inputs in that frequency range as well as a frequency doubling behaviors, in which every other cycle of a 20 Hz stimulus drives a strong response in the cortex. The onset of a stimulus appears to start a 10 Hz oscillation whose first phase is inhibitory, allowing activity and responsiveness to begin to recover about one half cycle, or 50 ms, later (Schoner, et al. 1992). This 10 Hz activity is likely to be responsible for the complete suppression of spontaneous activity as well as unresponsiveness to

external stimuli that persists for approximately 50 ms following the onset of a stimulus.

Following this inhibition, a form of adaptation must occur to explain the lack of response to clicks in the train at a time where the second click of a two click series does evoke a strong response. This lack of responsiveness is notable because spontaneous activity has returned to baseline levels, suggesting that the cortex is not deeply inhibited at this time. This form of adaptation appears to be maintained by the ongoing stimulus, since it does not decay even during stimuli that last several hundred milliseconds. One hundred millisecond duration stimuli were used to study the recovery of excitability following this adaptation at a time point when the post-onset inhibitory response was no longer present. It was found that recovery of excitability following this adaptation occurred on the time scale of tens of milliseconds; during this recovery time, the amplitude of the response to the probe stimuli increased to control levels and the latency of the response to the probe decreased to control levels.

Cellular basis

These features are compatible with several mechanisms of adaptation, including postsynaptic inhibition and presynaptic depression. These two models of adaptation have been studied in the visual system through both experimental and theoretical approaches. Bonds and Heeger (Heeger 1992) have pointed out that visual cortical neurons must maintain orientation selectivity in the face of wide variations in input rate due to variations in

image contrast. One might imagine that as the contrast of a given stimulus was increased, the orientation tuning to that stimulus would widen, as the higher contrast stimulus would drive the neuron more effectively at poor orientations. However, orientation tuning bandwidth remains constant over a very wide range of contrasts, implying that responses are normalized for contrast. Heeger (Heeger 1992; Carandini and Heeger 1994) has suggested that this could occur by a process called divisive normalization, in which a neuron receives inhibition as a function of the total cortical activity. Thus, as contrast increases, average cortical activity increases, causing feedback inhibition, which in turn lowers cortical firing rates, preventing responses to inappropriately oriented stimuli.

The adaptation seen in the experiments discussed in this paper could be a case of feedback inhibition. For this to be true, a population of inhibitory cortical neurons must be active during the sustained stimulus, preventing other neurons from responding. This inhibition must be closely balanced to prevent the target cell from responding to the stimulus, while allowing it to fire at baseline levels. Although the dynamics of divisive normalization have not been well studied to date, one would predict that recovery from this form of inhibition would be governed by the off rate of GABA from its various receptors, and the membrane time constant of the cell.

A second model for the regulation of cortical activity that has recently been well studied in tissue slices is a form of synaptic depression. Finlayson and Cynader (Finlayson and Cynader 1995) recorded cortical cells

intracellularly while stimulating the same cortical column extracellularly. They found that post-synaptic activity underwent a depression during repetitive stimulation with a time constant in the range of 1-30s. Activity recovered with a somewhat slower time course. Abbott and colleagues (Abbott et al. 1997) performed similar experiments, recording field potentials in supragranular layers while stimulating layer IV at rates between 1 Hz and 100 Hz. They found a depression of evoked field strength that increased with increasing stimulation rate. Tsodyks and Markram (Tsodyks and Markram 1997) studied pairs of synaptically connected layer V pyramidal cells and also found a synaptic depression with a recovery rate in the range of hundreds of milliseconds. Carandini and Ferster (Carandini and Ferster 1997) recently studied contrast adaptation using in vivo intracellular recording and concluded that adaptation was caused by a tonic hyperpolarization that they attributed to a decrease in excitatory input. Each of these studies attributed the synaptic depression to a decreased presynaptic release probability and postsynaptic receptor desensitization. Like divisive normalization, presynaptic depression could provide a way for the cortex to downregulate saturating inputs.

The recovery of excitability following the delivery of repetitive input to the cortex in vivo occurs an order of magnitude more quickly than the studies in slice discussed above. However, it is possible that similar mechanisms may underlay both processes. The above studies all considered cortico-cortical connections only; however, in this study it is likely that the

properties of thalamocortical synapses are more relevant because units from layer IV were predominately studied. It is likely that the short latency responses recorded in this study are predominately due to input from thalamic cells that are well driven by the click train stimuli. Thalamocortical synapses are known to have very different properties from cortico-cortical synapses (Stratford et al. 1996), and these differences could include a more rapid recovery from synaptic depression.

Models: adaptation of inhibition

The most important finding in this study is the relationship between the rate of the conditioning stimulus and the recovery time. From the above work on adaptation in slices and the long inhibition seen following a single click in vivo studies, one might have predicted that a high rate click trains would drive a stronger adaptation that would recover more slowly than low rate click trains. The opposite was seen. This result may be explained in several ways. One possibility is that the inhibition is itself inhibited during the stimulus. The response generated by the last click in the train, including both excitatory and inhibitory components, will be a function of its proximity in time to the next to last click. At high click rates, the next to last click will inhibit the last click more effectively, lessening both the excitation and inhibition evoked by the last click. This lessened excitation would be seen as a quicker post-click-train recovery of excitability. A second possibility involves presynaptic depression. If presynaptic depression affects connections from excitatory neurons onto inhibitory neurons, then at high click rates that

connection will be strongly depressed. This may have the effect of lowering inhibition at high click rates, which could contribute to a quicker recovery of excitability. In general, any scheme that results in reduced inhibition at high click rates could account for these results.

Psychophysical parallels

There have been two psychophysical characterizations of perceptual effects relating to the onset of a stimulus following a short gap that bear on this study. In the first, Zwicker (Zwicker 1965) showed that the ability of a noise masker to inhibit the detection of a short probe tone was strongest when the probe was presented at the onset of the mask and decreased as the probe was presented later in the mask. This was interpreted to mean that the response to the noise masker adapted during its presentation, and that the amount of masking was proportional to the ongoing response to the masker. Zwicker then introduced short pauses into noise maskers and presented the probe at the onset of the noise following the pause. He found that at very short gaps, the threshold for the detection of the probe was identical to that when it was presented during the masker. As the gap duration increased, detection of the probe became progressively more difficult until the full masking effects as seen at the onset of the masker were again seen. A nearly complete recovery was seen at a 50 ms gap. This suggests that the adaptation to the noise masker recovered following the offset of the masker with a time course that was essentially finished at 50 ms, similar to the recovery of excitability seen in the current study.

The current results also bear an interesting similarity to psychophysical results found by Hafter and colleagues in a study of temporal integration. They presented stimuli binaurally with inter-aural time (Hafter and Dye 1983) or intensity differences (Hafter et al. 1983) designed to make the stimulus appear to be located to the left or the right of the listener. The ability of subjects to locate these stimuli on the azimuth was measured as a joint function of the number of clicks in a train and the rate of the train. It was found that at a given click train rate, subjects performed better with longer stimuli, suggesting that each additional click in the train added information to the subject's perception of location. However, at rates of 100 Hz and above, a form of adaptation was found in which each click in the train did not add as much information as predicted by standard models of stimulus integration. The auditory system places particular importance on the onset of a stimulus train when making judgments of spatial location. This adaptation could be reset by introducing a pause in the click train, effectively breaking it into two trains (Buell and Hafter 1991). Interestingly, the length of the pause required to reset the adaptation was proportional to the inter-click period of the train, such that slower click trains with larger inter-click periods required a longer pause to reset adaptation. Thus, adaptation persisted longer after a stimulus with a slow rate than after a stimulus with a high rate. This implies that the auditory system actively uses the rate of an ongoing stimulus to determine whether a subsequent stimulus is to be treated as part of that ongoing stimulus, or as the onset of a novel stimulus. If a series of stimuli are arriving

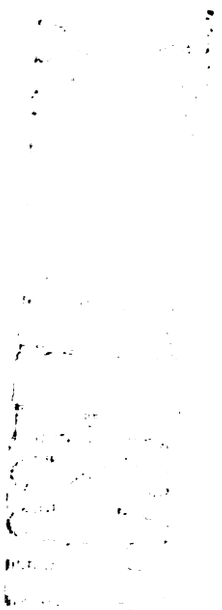

at a low rate, the auditory system waits for a while before it considers a subsequent stimulus to represent the onset of a new stimulus. Conversely, if stimuli are arriving at a high rate, the passage of only a short interval will indicate that the ongoing stimulus is finished and that the arrival of a new input indicates the onset of a novel stimulus. These psychophysical findings bear a strong similarity to the physiological results of the current study. Although the stimuli used in the current physiological study are significantly longer in duration than the psychophysical stimuli used by Hafter and colleagues, analogous physiological events at a short time scale may underlay the reset of adaptation witnessed in those experiments.

Implications: expectation and temporal integration

This study has shown that recovery of excitability following a click train stimulus in the auditory cortex takes on the order of tens of milliseconds and that this recovery time is a function of the rate of the stimulus, with higher rate stimuli causing a more rapid recovery and lower rate stimuli causing a slower recovery. This physiological property may provide a way for the cortex to adjust its integration time on a dynamic stimulus-dependent manner, which could have important consequences for perception. The cortex responds to isolated inputs with large amplitude, short latency responses. However, if the same input is presented as part of an ongoing stimulus, the cortex may not respond to it at all, as suggested by the lack of response to individual clicks during a train. Thus a response may indicate the onset of a novel stimulus whereas a lack of response may indicate that the input is

considered to be part of a larger stream. The current results suggest the period of time during which a subsequent input is considered to be part of the ongoing stimulus is longer following a low rate stimulus than a high rate stimulus.

This work constitutes the beginnings of an effort to elucidate the fundamental physiological and psychophysical processes by which sequentially occurring inputs are integrated and segregated into distinct perceptual objects. While this work has addressed the fact that the integration time is dynamically determined on the basis of the input rate, presumably temporal integration will be affected by many other stimulus features as well, such as frequency and location in space. The importance of temporal integration for sensory processing is particularly evident when it is disrupted, as is the case in disorders such as specific language impairment and dyslexia.

Figure 1: The response of auditory cortical units to click stimuli presented in rapid succession. Stimuli are represented by vertical slashes. A: Average response over twenty trials of a cluster recording to a single click at t = 100 ms. B: Response to a 125 pulses per second (pps) click train with a duration of 100 ms starting at t = 100 ms. C: Response to two single clicks separated by 108 ms.

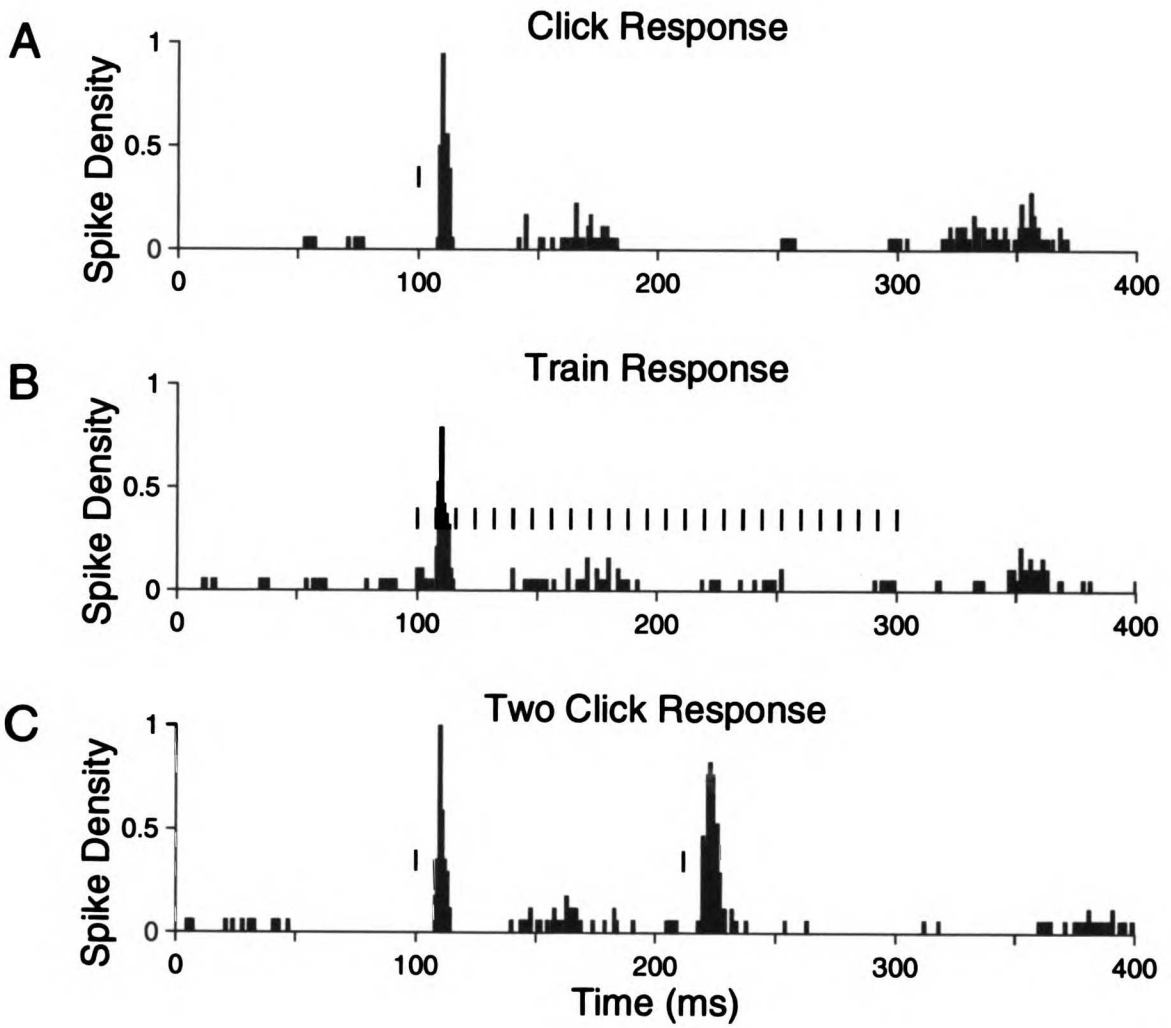
A
Click Response
Spike Density
1
0.5
0
0
100
200
300
400
B
Train Response
Spike Density
1
0.5
0
0
100
200
300
400
C
Two Click Response
Spike Density
1
0.5
0
0
100
200
300
400
Time (ms)

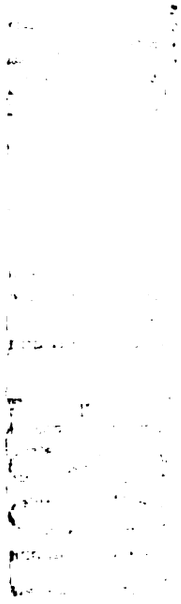

Figure 2: Conditioning stimulus – probe stimulus methodology. A diagram of the stimulus configuration used in these experiments and an example PSTH for 125 pps conditioning stimulus and 41 ms ISI. Data are from the same site as figure 1.

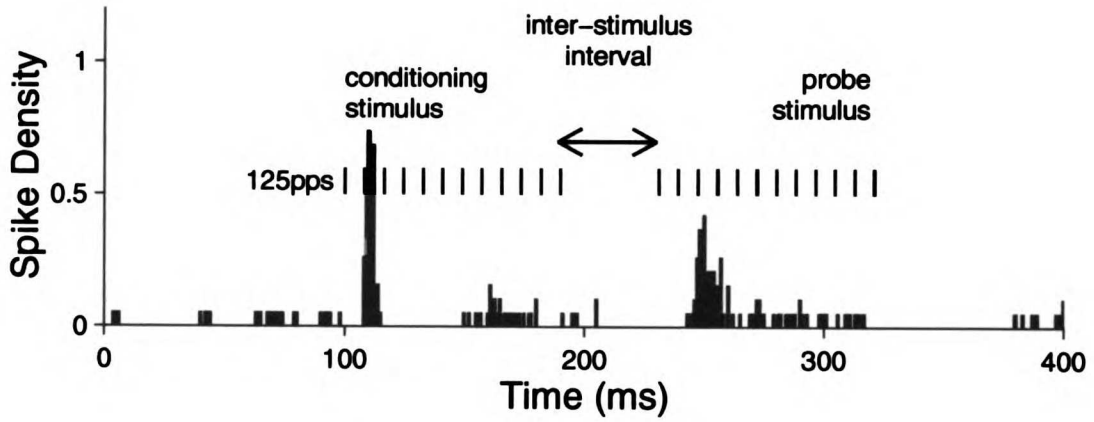
inter–stimulus
interval
conditioning
stimulus
probe
stimulus
125pps
Spike Density
1
0.5
0
0
100
200
300
400
Time (ms)

Figure 3: The time course of recovery of excitability following a click train. A: An example amplitude recovery function. Response amplitude is total number of spikes measured over a 3 ms window normalized to the number of trial repetitions. Response to probe stimulus in isolation is indicated by the horizontal line. Recovery time as measured by amplitude is defined as the ISI at which the probe evokes 50% of the response of the probe in isolation. B: An example latency recovery function. Latency is to the peak of the response. Latency to probe stimulus in isolation is indicated by the horizontal line. Recovery time as measured by latency is defined as the ISI at which the latency to the probe is twice the latency of the response to the probe in isolation.

A

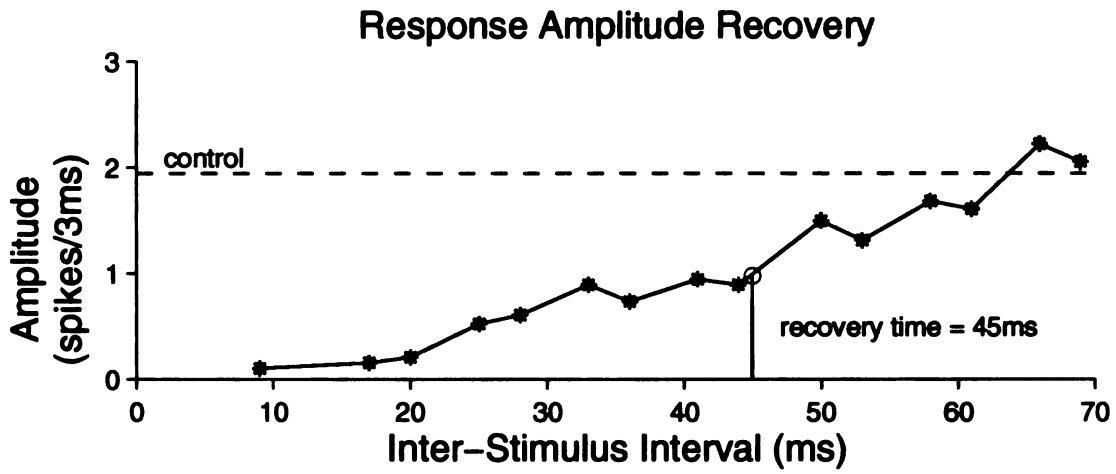
Response Amplitude Recovery
Amplitude (spikes/3ms)
control
recovery time = 45ms
Inter–Stimulus Interval (ms)

B

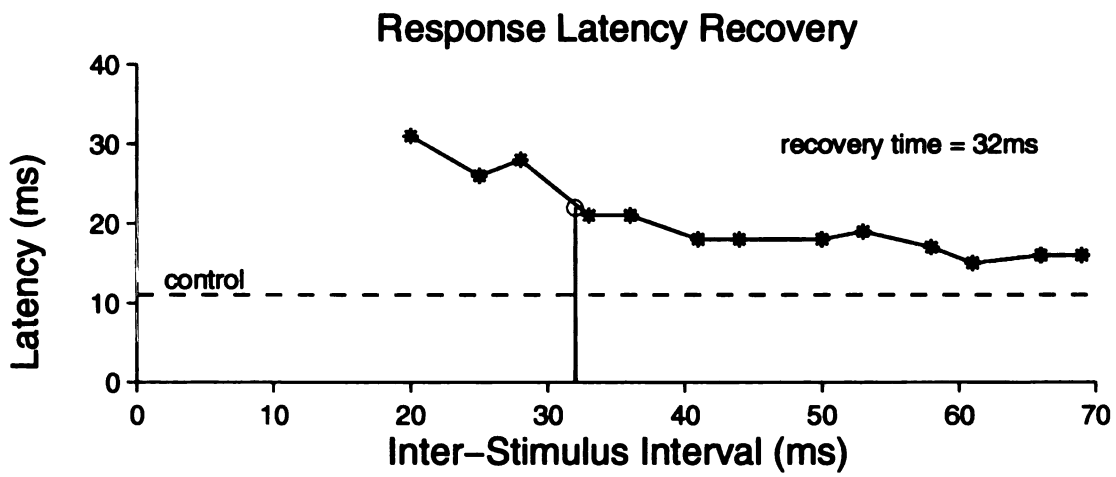
Response Latency Recovery
Latency (ms)
recovery time = 32ms
control
Inter–Stimulus Interval (ms)

Figure 4: Distribution of recovery times. A: Recovery times measured by amplitude were collected from 96 recording sites. Approximately 25% of sites did not exhibit a 50% recovery of excitability at the longest ISI tested and were discarded from this and subsequent analyses. Mean is 48±13 (s.d.). B: Recovery times measured by latency were collected from 117 recording sites. Sites that did not exhibit recovery of excitability at the longest ISI tested were discarded. Mean is 39±12 (s.d.)

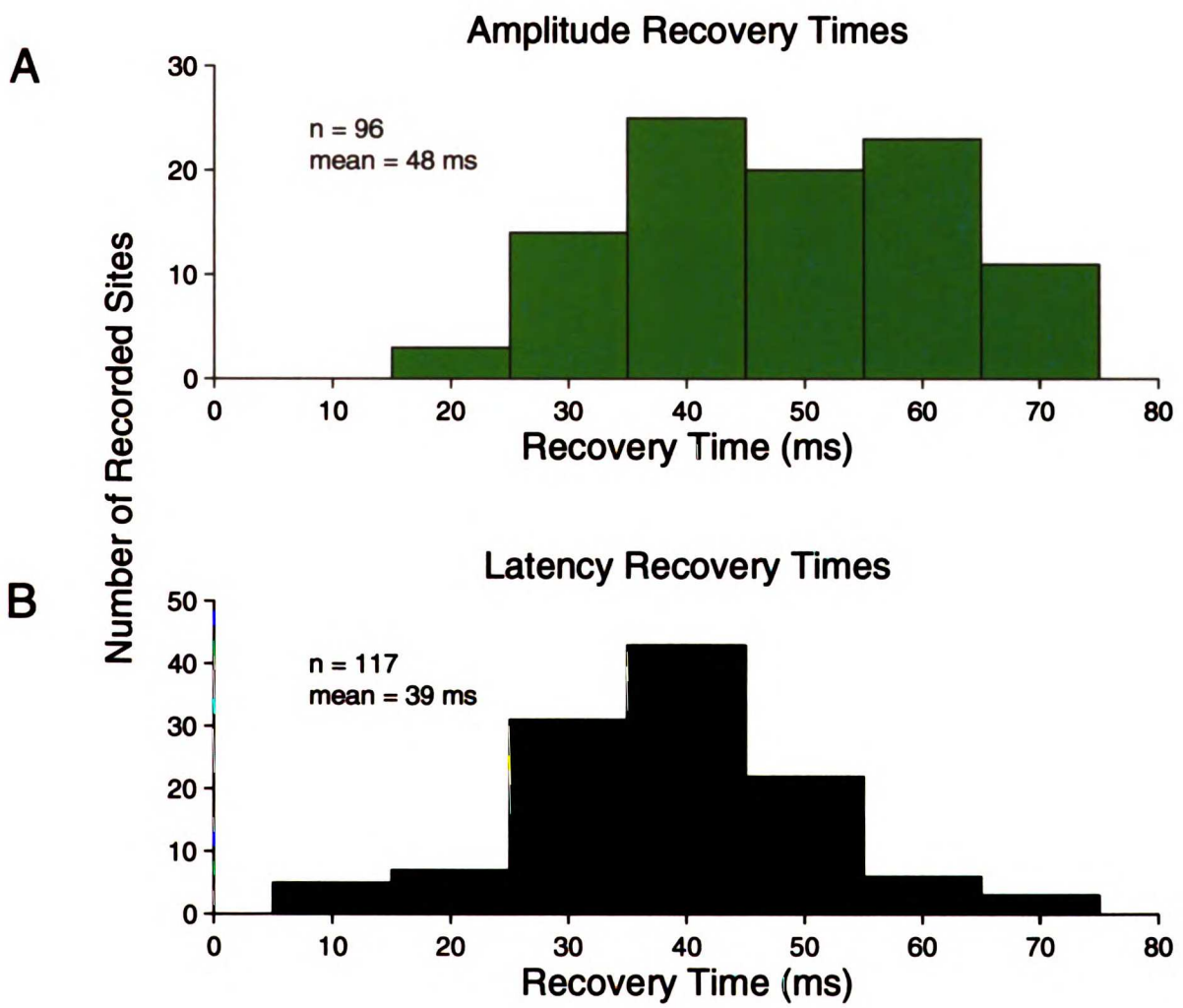
A
Amplitude Recovery Times
n = 96
mean = 48 ms
Number of Recorded Sites
Recovery Time (ms)
B
Latency Recovery Times
n = 117
mean = 39 ms
Number of Recorded Sites
Recovery Time (ms)

Figure 5: The effect of the rate of the conditioning stimulus on recovery time. A: A diagram of the standard stimulus configuration and an example PSTH for 125 pps conditioning stimulus and 41 ms ISI. B: A diagram of the stimulus configuration used in these experiments and an example PSTH for 250 pps conditioning stimulus and 42 ms ISI.

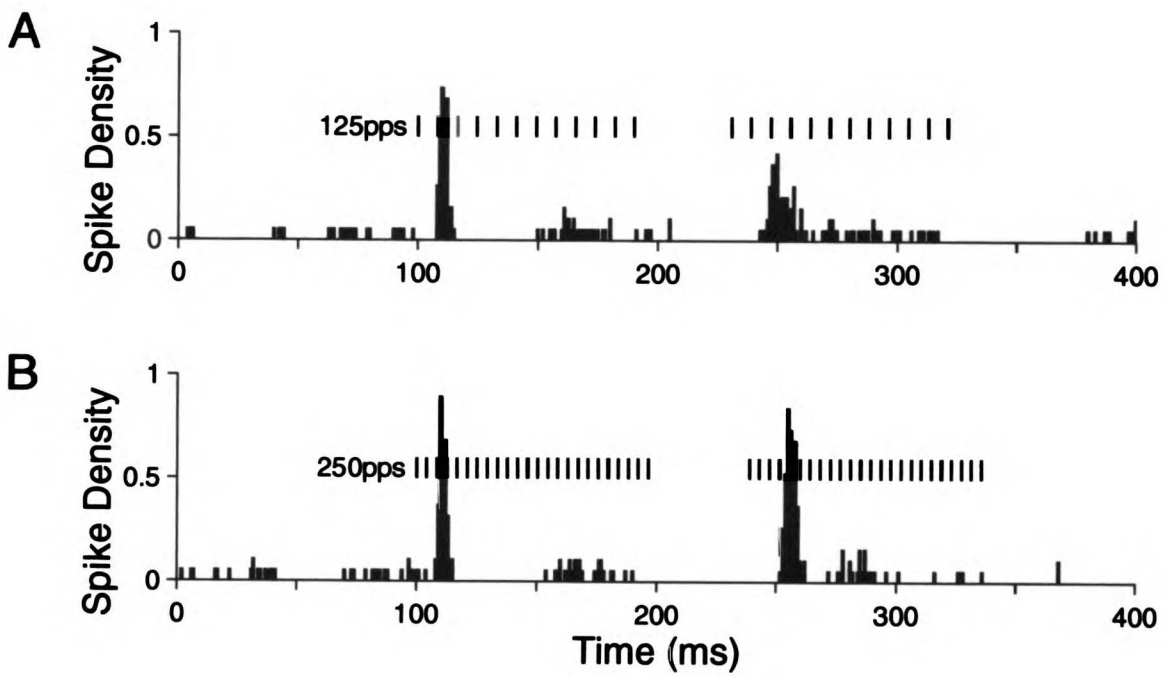
A
Spike Density
1
0.5
0
125pps
0
100
200
300
400
B
Spike Density
1
0.5
0
250pps
0
100
200
300
400
Time (ms)

Figure 6: The effect of the rate of the conditioning stimulus on recovery time. A: Example amplitude recovery functions. (') 250 pps conditioning stimulus. (*) 125 pps conditioning stimulus. B: Example latency recovery functions. (') 250 pps conditioning stimulus. (*) 125 pps conditioning stimulus.

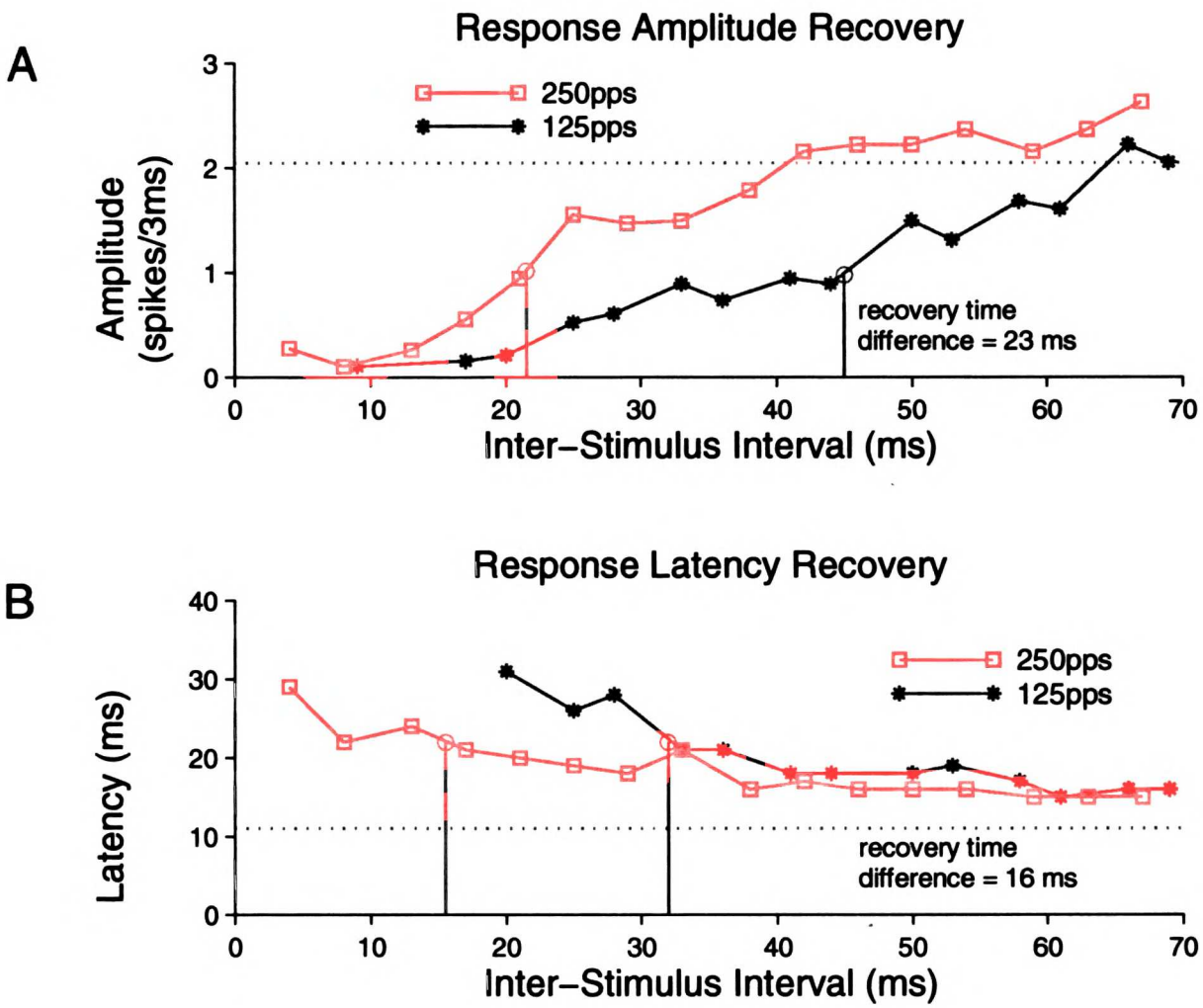
A
Response Amplitude Recovery
250pps
125pps
Amplitude (spikes/3ms)
recovery time
difference = 23 ms
Inter–Stimulus Interval (ms)
B
Response Latency Recovery
250pps
125pps
Latency (ms)
recovery time
difference = 16 ms
Inter–Stimulus Interval (ms)

Figure 7: Relationship between conditioning train rate and recovery time. A: Amplitude recovery times are subtractively normalized on a site by site basis to the 125 pps standard stimulus. Values greater than zero represent rates that recovered more slowly than the standard. Values less than zero represent rates that recovered more quickly than the standard. Error bars are s.e. Data at the standard rate have no error by definition. Dashed line is the least squares fit to the data, excluding the 500 pps point. The slope is significantly different than zero (two-tailed t test, $p < 0.0001$, d.o.f = 82, $t = -13.06$). B: Latency recovery times are subtractively normalized on a site by site basis to the 125 pps standard stimulus. Dashed line is the least squares fit to the data, excluding the 500 pps point. The slope is significantly different than zero (two-tailed t test, $p < 0.0001$, d.o.f = 98, $t = -7.27$).

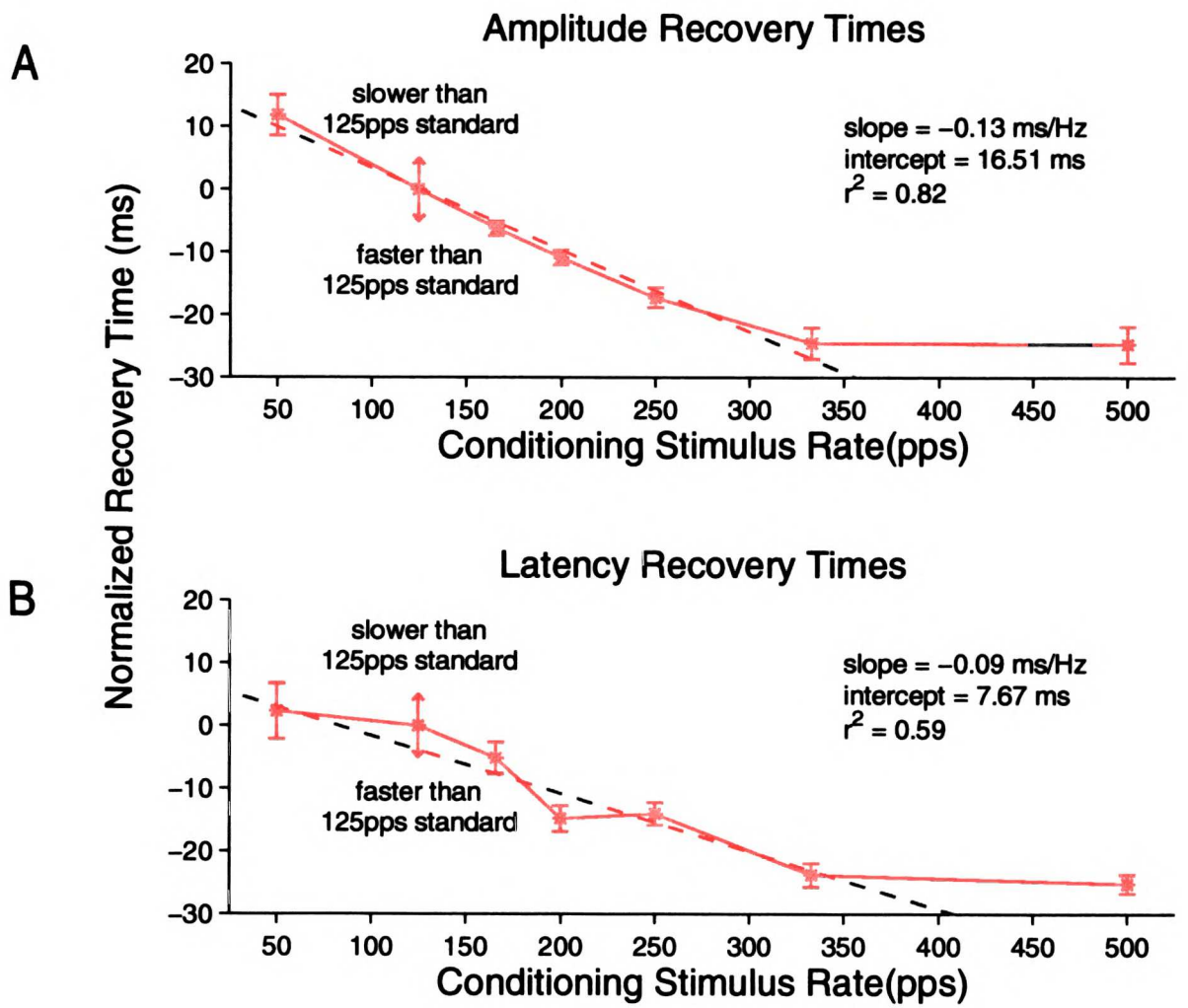
A
Amplitude Recovery Times
slower than
125pps standard
faster than
125pps standard
slope = –0.13 ms/Hz
intercept = 16.51 ms
r2 = 0.82
Normalized Recovery Time (ms)
Conditioning Stimulus Rate(pps)
B
Latency Recovery Times
slower than
125pps standard
faster than
125pps standard
slope = –0.09 ms/Hz
intercept = 7.67 ms
r2 = 0.59
Conditioning Stimulus Rate(pps)

Figure 8: Comparison of click trains and single clicks as probe stimuli. A: Average response of a site to a single click delivered at t = 0 ms. B: Average response of the same site to a 250 pps click train starting at t = 0 ms. Bins are 1 ms in size. No statistically significant relationship between click train rate and response amplitude or latency exists. C: Recovery times following a 250 pps click train as measured with 250 pps probe click trains are shown as gray bars, n = 44, mean 31±10 (s.d.). Recovery times following a 250 pps click train as measured with single clicks are shown as black bars, n = 10, mean 32±8 (s.d.). Bin size is 5 ms. The distributions are not statistically different (Mann-Whitney test, $p > 0.3$, d.o.f. = 9, $z = 0.568$) These two stimuli sets were not presented to the same site but are comparisons of different recording sites.

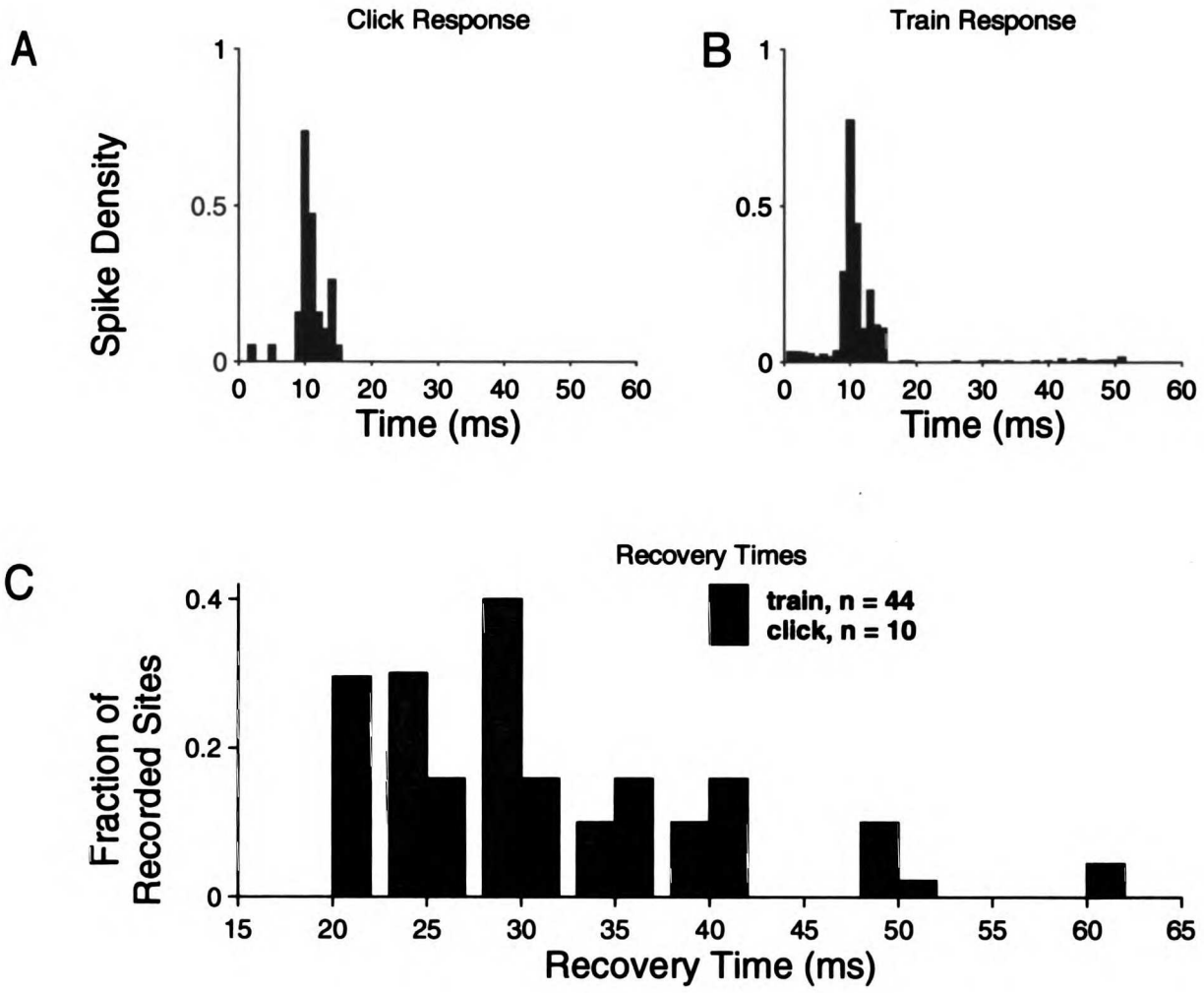
A
Click Response
Spike Density
1
0.5
0
0 10 20 30 40 50 60
Time (ms)
B
Train Response
1
0.5
0
0 10 20 30 40 50 60
Time (ms)
C
Recovery Times
train, n = 44
click, n = 10
Fraction of Recorded Sites
0.4
0.2
0
15 20 25 30 35 40 45 50 55 60 65
Recovery Time (ms)

Figure 9: Comparison of long and short conditioning click trains. Recovery times following a 100 ms duration, 250 pps click train are shown as black bars, n = 10, mean 32±8 (s.d.). Recovery times following 200 ms duration 250 pps click train are shown as gray bars, n = 10, 31±10 (s.d.). Bin size is 10 ms. The distributions are not statistically different (Wilcoxon test, $p > 0.25$, d.o.f. = 9, $z = 0.739$) These two stimuli sets were presented interleaved to the same recording sites.

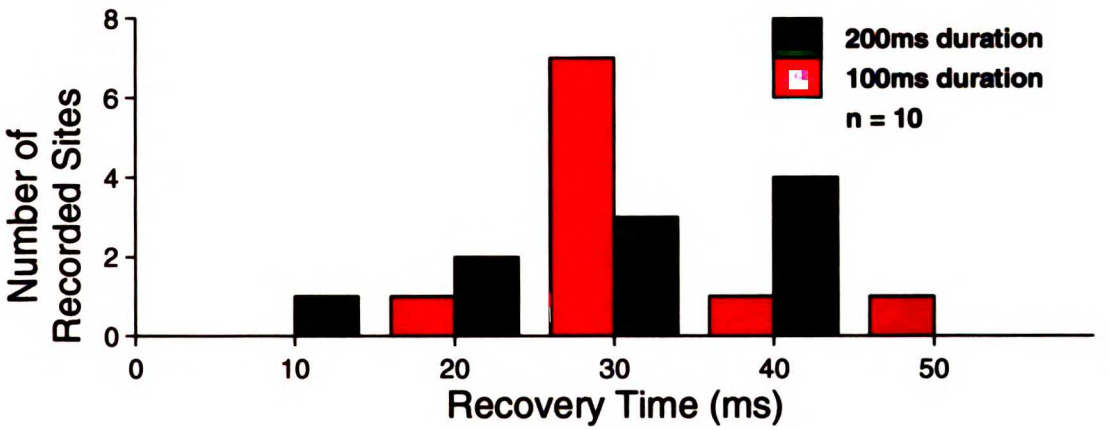
Number of Recorded Sites
8
6
4
2
0
0
10
20
30
40
50
Recovery Time (ms)
200ms duration
100ms duration
n = 10

Figure 10: Recovery functions following a single click over long intervals. A single clicks is the probe stimulus. A: Diagram of the stimulus configuration used in these experiments and an example PSTH for the click conditioning stimulus at 41 ms ISI. B: Example recovery function following click conditioning stimulus. Horizontal bar marks the period of the recovery function, measured between peaks.

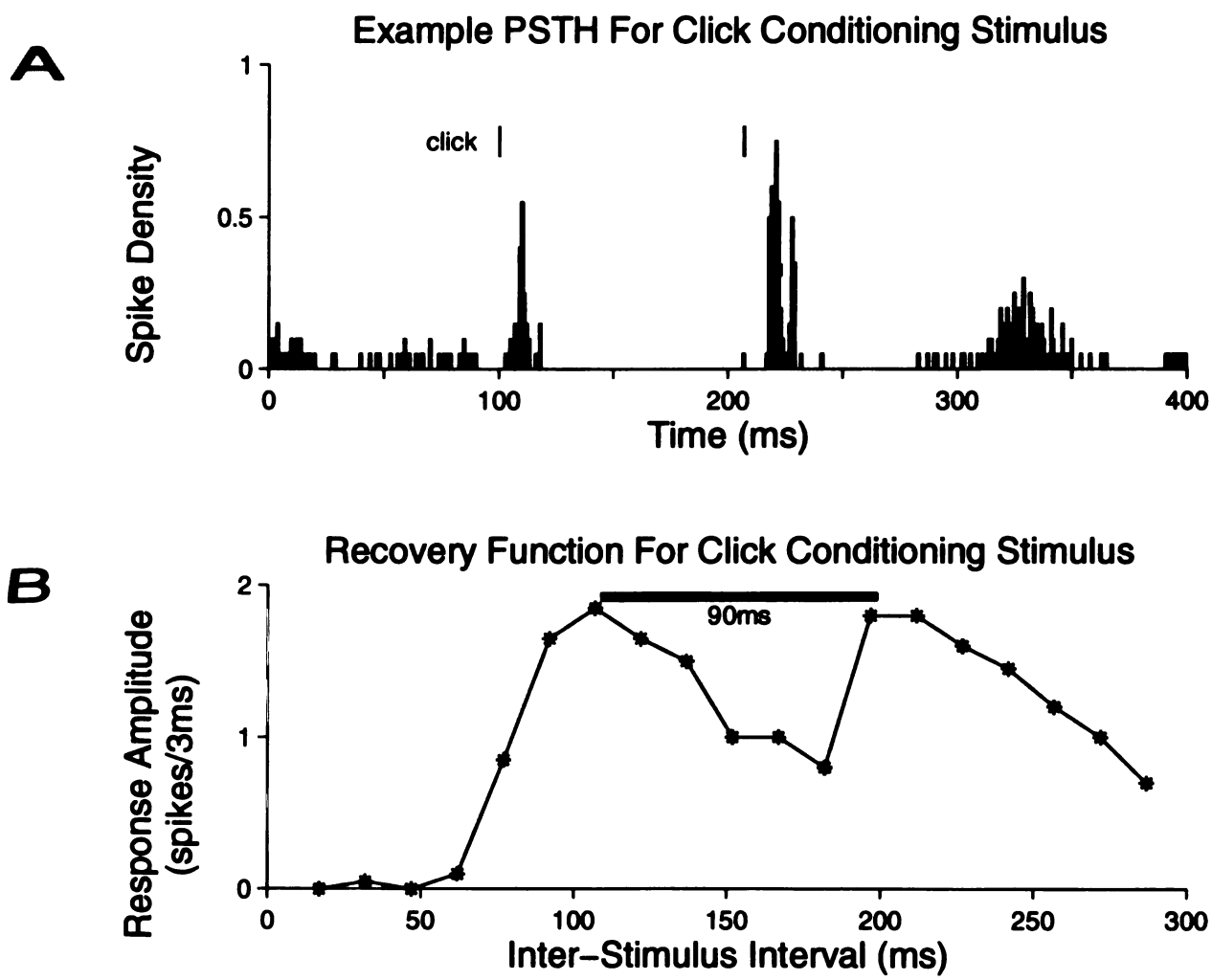
A
Example PSTH For Click Conditioning Stimulus
Spike Density
1
0.5
0
click
0
100
200
300
400
Time (ms)
B
Recovery Function For Click Conditioning Stimulus
Response Amplitude
(spikes/3ms)
2
1
0
90ms
0
50
100
150
200
250
300
Inter-Stimulus Interval (ms)

Figure 11: Recovery functions following a 250 pps click train over long intervals. A single clicks is the probe stimulus. A: Diagram of the stimulus configuration used in these experiments and an example PSTH for 250 pps click train conditioning stimulus at 41 ms ISI. B: Example recovery function following click train conditioning stimulus. Horizontal bars marks periods of the recovery function, measured between peaks.

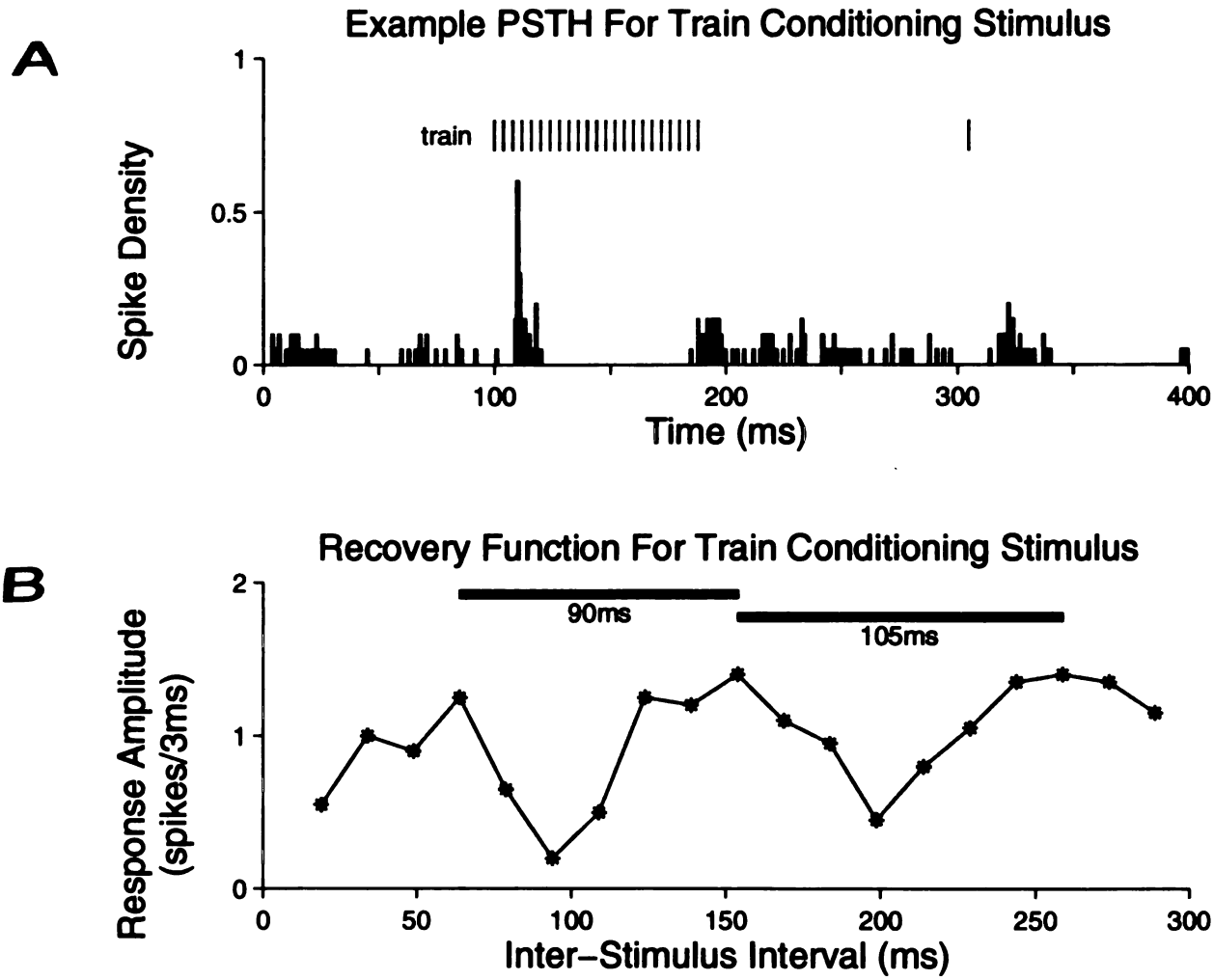
A
Example PSTH For Train Conditioning Stimulus
train
Spike Density
1
0.5
0
0
100
200
300
400
Time (ms)
B
Recovery Function For Train Conditioning Stimulus
90ms
105ms
Response Amplitude
(spikes/3ms)
2
1
0
0
50
100
150
200
250
300
Inter-Stimulus Interval (ms)

Figure 12: Oscillatory period of recovery function following a single click and a 250 pps click train over long intervals. Periods following click conditioning stimuli are shown as black bars, n = 29, mean 105±14 (s.d.). Periods following 250 pps click train conditioning stimuli are shown as gray bars, n = 29, mean 102±18 (s.d.). Bin size is 20 ms. The period for a given site is the mean of all observed full periods. The distributions are not statistically different (Wilcoxon test, $p > 0.2$, d.o.f. = 28, $z = 1.09$) These two stimuli sets were presented interleaved to the same recording sites.

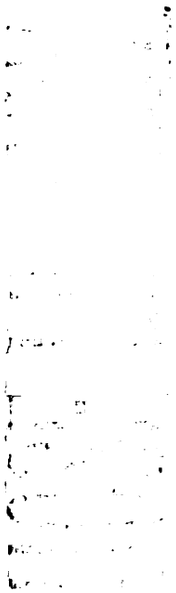

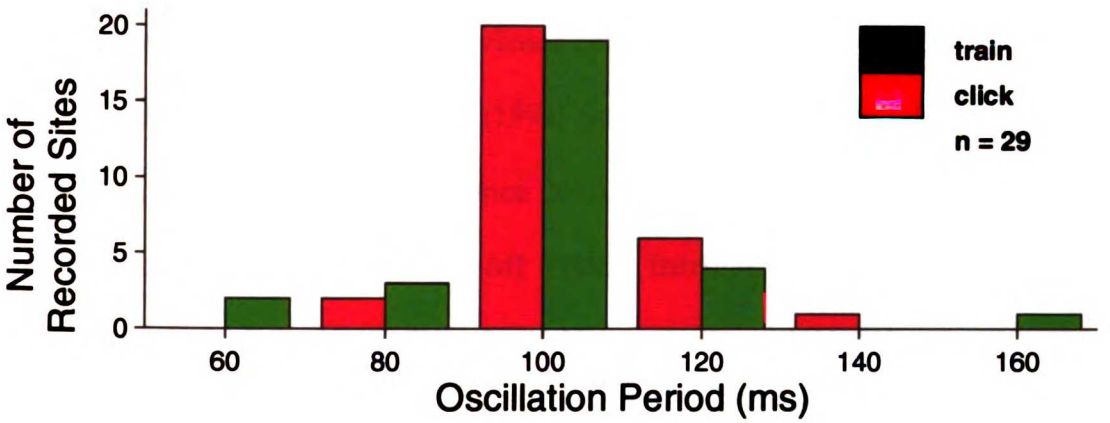
Number of Recorded Sites
20
15
10
5
0
60
80
100
120
140
160
Oscillation Period (ms)
train
click
n = 29

References:

Abbott LF, Varela JA, Sen K, and Nelson SB (1997) Synaptic depression and cortical gain control. Science 275:220-224.

Buell TN and Hafter ER (1991) Combination of binaural information across frequency bands. Journal of the Acoustical Society of America 90:1894-1900.

Carandini M and Ferster D (1997) A tonic hyperpolarization underlying contrast adaptation in cat visual cortex. Science 276:949-952.

Carandini M and Heeger DJ (1994) Summation and division by neurons in primate visual cortex. Science 264:1333-1336.

Connors BW and Gutnick MJ (1990) Intrinsic firing patterns of diverse neocortical neurons. Trends in Neuroscience 13:99-104.

Creutzfeldt O, Hellweg FC, and Schreiner C (1980) Thalamocortical transformation of responses to complex auditory stimuli. Experimental Brain Research 39:87-104.

Eggermont JJ (1992) Stimulus induced and spontaneous rhythmic firing of single units in cat primary auditory cortex. Hearing Research 61:1-11.

Eggermont JJ (1994) Temporal modulation transfer functions for AM and FM stimuli in cat auditory cortex. Effects of carrier type, modulating waveform and intensity. Hearing Research 74:51-66.

Finlayson PG and Cynader MS (1995) Synaptic depression in visual cortex tissue slices: an in vitro model for cortical neuron adaptation. Experimental Brain Research 106:145-155.

Gray CM and McCormick DA (1996) Chattering cells: superficial pyramidal neurons contributing to the generation of synchronous oscillations in the visual cortex. Science 274:109-113.

Hafter ER and Dye RH, Jr. (1983) Detection of interaural differences of time in trains of high-frequency clicks as a function of interclick interval and number. Journal of the Acoustical Society of America 73:644-651.

Hafter ER, Dye RH, Jr., and Wenzel E (1983) Detection of interaural differences of intensity in trains of high-frequency clicks as a function of interclick interval and number. Journal of the Acoustical Society of America 73:1708-1713.

Heeger DJ (1992) Normalization of cell responses in cat striate cortex. Visual Neuroscience 9:181-197.

Kenmochi M and Eggermont JJ (1997) Autonomous cortical rhythms affect temporal modulation transfer functions. Neuroreport 8:1589-1593.

Kopecz K, Schoner G, Spengler F, and Dinse HR (1993) Dynamic properties of cortical evoked (10 Hz) oscillations: theory and experiment. Biological Cybernetics 69:463-473.

Langner G and Schreiner CE (1988) Periodicity coding in the inferior colliculus of the cat. I. Neuronal mechanisms. Journal of Neurophysiology 60:1799-1822.

Lisman JE (1997) Bursts as a unit of neural information: making unreliable synapses reliable. Trends in Neuroscience 20:38-43.

McCormick DA, Wang Z, and Huguenard J (1993) Neurotransmitter control of neocortical neuronal activity and excitability. Cerebral Cortex 3:387-398.

Nakayama K (1985) Biological image motion processing: a review. Vision Research 25:625-660.

Ohzawa I, Sclar G, and Freeman RD (1982) Contrast gain control in the cat visual cortex. Nature 298:266-268.

Ohzawa I, Sclar G, and Freeman RD (1985) Contrast gain control in the cat's visual system. Journal of Neurophysiology 54:651-667.

Petersen SE, Baker JF, and Allman JM (1985) Direction-specific adaptation in area MT of the owl monkey. Brain Research 346:146-150.

Poeppel D, Nagarajan SS, Mahncke HW, Roberts TPL, Rowley HA, and Merzenich MM (1996) Stimulus evoked low frequency magnetic field oscillations in somatosensory cortex of awake humans. Society for Neuroscience.

Roger M and Arnault P (1989) Anatomical study of the connections of the primary auditory area in the rat. Journal of Comparative Neurology 287:339-356.

Sally SL and Kelly JB (1988) Organization of auditory cortex in the albino rat: sound frequency. Journal of Neurophysiology 59:1627-1638.

Schoner G, Kopecz K, Spengler F, and Dinse HR (1992) Evoked oscillatory cortical responses are dynamically coupled to peripheral stimuli. Neuroreport 3:579-582.

Schreiner CE and Sutter ML (1992) Topography of excitatory bandwidth in cat primary auditory cortex: single-neuron versus multiple-neuron recordings. Journal of Neurophysiology 68:1487-1502.

Schreiner CE and Urbas JV (1988) Representation of amplitude modulation in the auditory cortex of the cat. II. Comparison between cortical fields. Hearing Research 32:49-63.

Singer W (1993) Synchronization of cortical activity and its putative role in information processing and learning. Annual Review of Physiology 55:349-374.

South DA and Weinberger NM (1995) A comparison of tone-evoked response properties of 'cluster' recordings and their constituent single cells in the auditory cortex. Brain Research 704:275-288.

Steriade M, McCormick DA, and Sejnowski TJ (1993) Thalamocortical oscillations in the sleeping and aroused brain. Science 262:679-685.

Stratford KJ, Tarczy-Hornoch K, Martin KA, Bannister NJ, and Jack JJ (1996) Excitatory synaptic inputs to spiny stellate cells in cat visual cortex. Nature 382:258-261.

Tsodyks MV and Markram H (1997) The neural code between neocortical pyramidal neurons depends on neurotransmitter release probability. Proceedings of the National Academy of Science (USA) 94:719-723.

Zwicker E (1965) Temporal Effects in Simultaneous Masking by White-Noise Bursts. Journal of the Acoustical Society of America 37:653-663.

FUTURE DIRECTIONS

Chapter 6

Summary

This work has laid the foundations for the study of the temporal interactions between sensory stimuli. The existence of a sensory evoked alpha-band oscillation in the awake and attending human that alters the response to subsequent stimuli has been documented. This long-lasting temporally structured response, is likely to play an important role in the response to sequential stimuli. The generator of this oscillatory response was demonstrated to lie in cortical layer 5 and is likely to consist of the subcortically projecting pyramidal output cells of the cortex, suggesting that these oscillations are in a position to affect the fundamental input-output processing of the cortex. Finally, the temporal interactions of more complex stimuli were studied and it was shown that the rate of a stimulus governs the integration time following that stimulus.

These results raise many new questions. Two potential lines of future inquiry will be explored here: first, an effort to establish a psychophysical consequence of the alpha rhythm; second, an exploration of the role that these oscillatory and integrative response features play in determining the cortical response to more naturalistic and complex sequential stimuli.

Future directions: psychophysical consequences of the alpha rhythm

Having established the existence of sensory evoked alpha-band oscillations in human subjects performing sensory discriminations, an important goal is to determine the precise role that these oscillations play in perceptual performance. The simplest possible effect that the modulation of the

amplitude of the stimulus response might have is on the perceived amplitude of the stimulus. The effect of the sensory-evoked oscillation on the perceived amplitude of a stimulus could be measured. In these experiments, a large amplitude stimulus would be presented to evoke an oscillation and the subject would perform a detection task upon a subsequent near threshold amplitude stimulus. The interval between the two stimuli would be varied across a several hundred millisecond range, presenting the test stimulus at troughs, peaks, and slopes of the evoked oscillation. The detection threshold would be measured as a function of the phase of the spontaneous alpha rhythm. Finding that this threshold varied systematically with the phase of the evoked oscillation would establish that the evoked alpha rhythm governs perceptual thresholds.

This type of experiment could also be conducted with reference to the spontaneous alpha rhythm. In these experiments, a single near threshold stimulus would be presented while spontaneous brain activity was monitored. The detection threshold would be measured as a function of the phase of the spontaneous alpha rhythm. Since performance at threshold is variable by definition, it is likely that internal neural fluctuations govern whether a given stimulus is perceived. This methodology would quantify the contribution of structured variations in psychophysical threshold caused by the alpha rhythm to the fluctuations in perceptual performance previously ascribed to chance. Understanding the neural basis of perceptual thresholds has been a long-standing goal of neuroscience. Quantifying the role that

structured changes in excitability, whether stimulus-evoked or spontaneous, would be an important step towards this goal.

A different approach to the effect of alpha-band oscillations on amplitude perception would be to study amplitude discrimination. In these experiments, the subject would compare the amplitude of two large amplitude stimuli. The first stimulus would evoke an alpha-band oscillation that would alter the response to the second stimulus. The interval between the two stimuli would be varied across a several hundred millisecond range, again presenting the test stimulus at troughs, peaks, and slopes of the evoked oscillation. The amplitude at which the stimuli are perceived as identical in amplitude would be measured as a function of the phase of the oscillation evoked by the first stimulus. Finding that equivalence point varied systematically with the phase of the evoked oscillation would establish that the evoked alpha rhythm governs perceptual magnitude.

An important control for all of the above experiments would be to measure the relationship between the amplitude of a stimulus and the magnitude of the evoked response. This measure would predict the changes in the perceived amplitude of a given stimulus that should result from changes in the response to that stimulus caused by its presentation at different phases of an alpha-band oscillation. The extent to which changes in perceived amplitude match changes in actual amplitude as the strength of the evoked response is manipulated will quantify the extent to which the physiological response measure is correlated with perception.

A second line of experiments should be to examine the effects that the alpha-band response imposes on the perceived temporal structure of sensory stimuli. It has previously been suggested that the visual alpha rhythm governs temporal integration by controlling the likelihood that sequentially presented stimuli will be perceived as simultaneous or ordered(Varela et al. 1981; Gho and Varela 1988). It would be interesting to perform similar experiments in the auditory system, where disorders of temporal abilities are known to be related to learning disabilities (Merzenich et al. 1996; Tallal et al. 1996). If the alpha rhythm over auditory cortex governed temporal binding, experiments could be performed in subjects with learning disabilities to determine if abnormalities in the alpha rhythm could contribute to the spectrum of their behavioral impairments.

Future experiments, physiological role of the alpha rhythm

The stimuli used to characterize the cortical basis of the alpha rhythm in vivo were simple clicks in these studies. The anesthetized rat preparation lends itself to the study of several aspects of this phenomenon that can not be adequately characterized in awake humans, namely the spatial distribution of activity across the cortex in response to combinations of stimuli. The click stimuli used in the current experiments are broad-band stimuli that are likely to activate large regions of the auditory cortex synchronously. It would be interesting to use band-limited stimuli such as tone pips to study the spatiotemporal pattern of activation that this stimulus generates across the cortex. In particular, it would be interesting to know if the evoked oscillation

spread across the cortex to activate areas that were not activated by the onset response to the stimulus and to determine the rate of this spread. These studies would lead naturally to the search for combination sensitive neurons, which respond preferentially to a particular combination of stimuli at a particular temporal interval (Margoliash and Fortune 1992). The interactions between sensory-evoked oscillations from sequentially presented stimuli could conceivably create a spectrum of delay tuned combination sensitive neurons in sensory cortex. The appearance of PSTH's of combination sensitive neurons from primate auditory cortex suggest the involvement of alpha-band oscillations.

Future experiments, temporal integration

The experiments on temporal integration and segregation in this work open the door to a series of studies on this topic. Physiological experiments designed to further the understanding of this phenomenon would benefit from being designed to study the responses to psychophysically defined stimuli. The best-studied phenomenon of perceptual integration and segregation is temporal streaming (Bregman 1994). In these experiments, subjects are presented with a sequence of tones alternating between two different frequencies. Depending on the temporal interval and frequency separation between the tones, the subject either perceives the stimulus as a single "stream" alternating between two tones or as two streams of different tones intermingled together. It would be interesting to study the physiological responses to these stimuli. Both the evoked alpha rhythm and the rate

sensitivity of temporal integration could play a role in shaping the neural response to these types of stimuli. The presentation rate in psychophysical studies of streaming is typically in the 10 Hz range, with stimulus onset asynchronies ranging from 60 ms to 150 ms. These parameters suggest that these stimuli may entrain an alpha rhythm. As the rate of presentation of the stimuli is increased, the frequency difference required for the perception of two streams shrinks, suggesting that at higher rates, a stimulus of one frequency is less able to capture to subsequent stimulus of the other frequency. This suggests that the integration time is rate sensitive, analogous to data derived from very different stimuli in the current work. The study of temporal streaming could provide a framework for uniting these two mechanisms by which stimuli interact across time.

References:

Bregman AS (1994) Auditory Scene Analysis: The Perceptual Organization Of Sound. Cambridge:MIT Press. Pages pp.

Gho M and Varela FJ (1988) A quantitative assessment of the dependency of the visual temporal frame upon the cortical rhythm. Journal of Physiology (Paris) 83:95-101.

Margoliash D and Fortune ES (1992) Temporal and harmonic combination-sensitive neurons in the zebra finch's HVc. Journal of Neuroscience 12:4309-4326.

Merzenich MM, Jenkins WM, Johnston P, Schreiner C, Miller SL, and Tallal P (1996) Temporal processing deficits of language-learning impaired children ameliorated by training. Science 271:77-81.

Tallal P, Miller SL, Bedi G, Byma G, Wang X, Nagarajan SS, Schreiner C, Jenkins WM, and Merzenich MM (1996) Language comprehension in language-learning impaired children improved with acoustically modified speech. Science 271:81-84.

Varela FJ, Toro A, John ER, and Schwartz EL (1981) Perceptual framing and cortical alpha rhythm. Neuropsychologia 19:675-686.

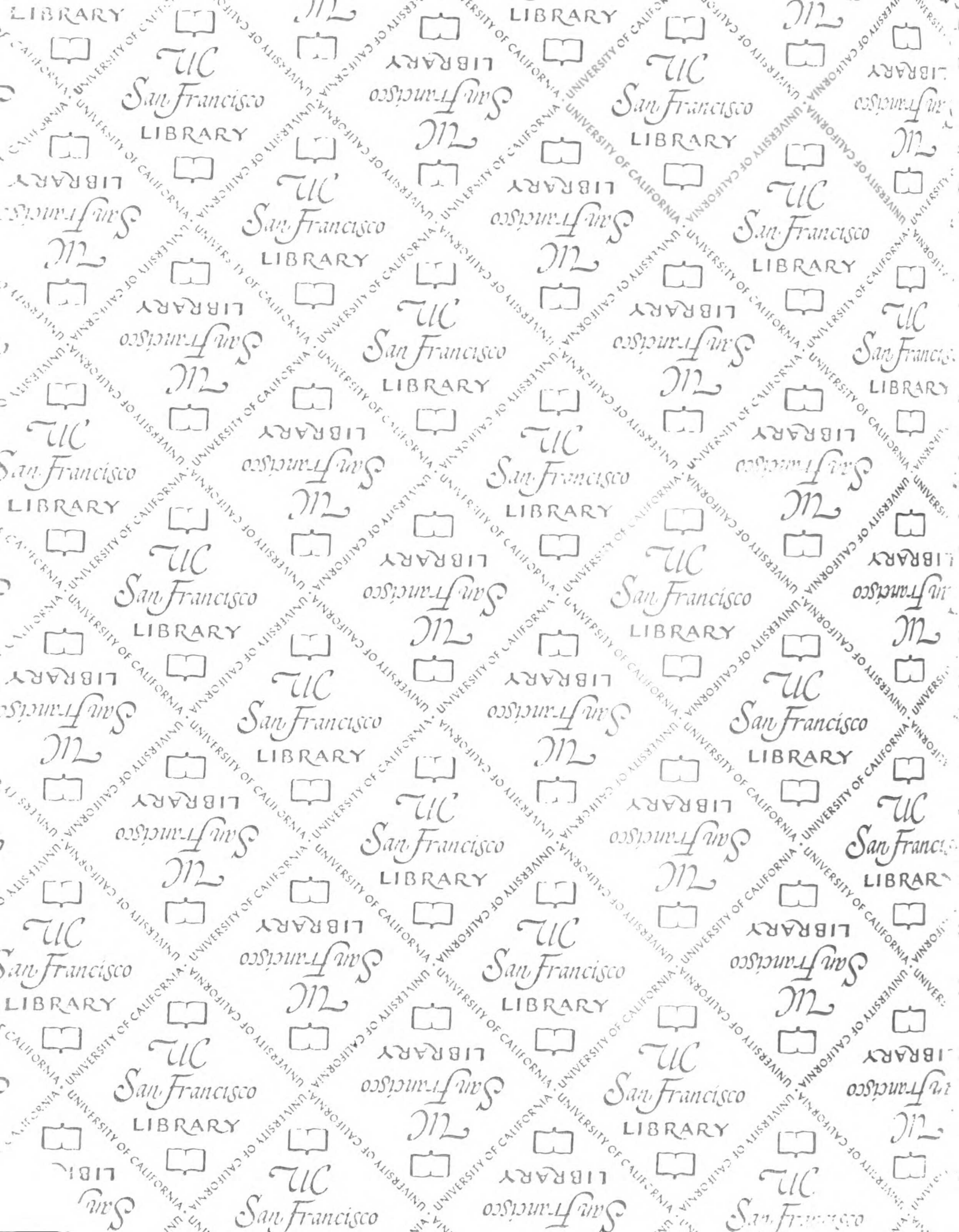
UC
San Francisco
LIBRARY
UNIVERSITY OF CALIFORNIA · UNIVERSITY OF CALIFORNIA